

PREFACE

We would like to offer the readers the scientific activity report of the Frank Laboratory of Neutron Physics for 2016. The first part of the report presents a brief review of the experimental and theoretical results achieved in the main scientific directions – condensed matter physics, neutron nuclear physics, applied research and development and creation of elements of neutron spectrometers for condensed matter investigations. The second part includes the reports on the operation of the modernized IBR-2 pulsed reactor, the development of the IREN neutron source and researches carried out on EG-5 facility. A list of publications for 2016, the information regarding the seminars and conferences organized in FLNP and a statistical view on the FLNP personnel structure are presented as well.

In 2016 the main achievements of the Laboratory were:

- successful fulfillment of the user program at the IBR-2 spectrometers;
- development of spectrometer complex at the IBR-2 reactor;
- development of IREN facility.

In 2016 the IBR-2 reactor operated for physical experiments for 2477 hours, the IREN facility 265 hours and EG - 620 hours.

FLNP has cooperation agreements in the field of neutron investigations with almost 200 scientific institutes and universities from more than 40 countries from all over the world. A significant contribution to this cooperation is made by the JINR Member States.

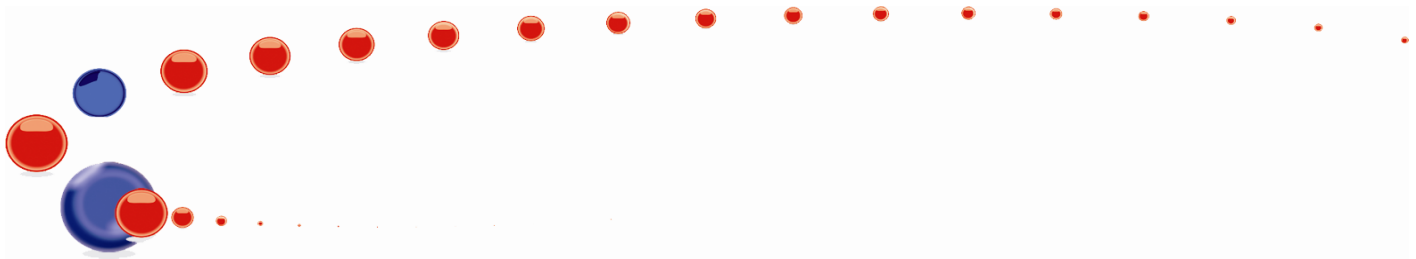
The FLNP staff consists of more than 500 employees in this about 170 less than 35 years of age. The scientific staff includes 93 Ph.D. and 19 D.Sc. researchers and 90 researchers and specialists from 16 of the JINR Member States (besides the Russian Federation) and associated members.

The organization of annual conferences and schools covering all FLNP research fields helps to recruit young specialists — one of the top priority tasks of the FLNP Directorate.

All these facts confirm that the Laboratory continues to develop successfully and dynamically, carrying out investigations in the interests of the JINR Member States.



V.N. Shvetsov
Director



Members of the Directorate of the Frank Laboratory of Neutron Physics:

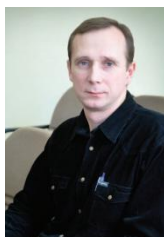


SHVETSOV
Valeryi
Nikolaevich
Director
since 2013

Deputy Directors for Science



CULICOV
Otilia
Ana
since 2013



LYCHAGIN
Egor
Valerievich
since 2013



KUČERKA
Norbert
since 2014



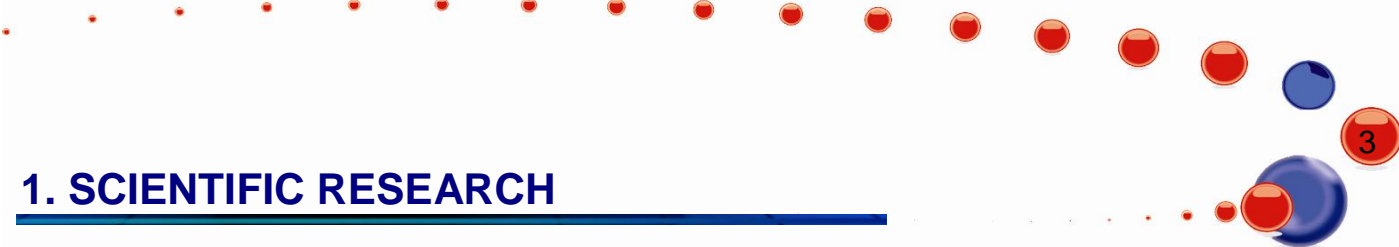
KOZENKOV
Sergey
Vyacheslavovich
Deputy Director
for General Issues
since 1989



VINOGRADOV
Alexander
Vital'evich
Chief Engineer
since 2007



CHUDOBA
Dorota
Marta
Scientific secretary
since 2013



1. SCIENTIFIC RESEARCH

I. CONDENSED MATTER PHYSICS

The main objectives of research in the framework of the theme involved the application of neutron scattering techniques and complementary methods to investigate the structure, dynamics and microscopic properties of nanosystems and novel materials, which are of great importance for the development of nanotechnologies in the fields of electronics, pharmacology, medicine, chemistry, modern condensed matter physics and interdisciplinary sciences.

In 2016, the greater part of experimental research was carried out on the spectrometers of the modernized IBR-2 reactor in accordance with the Topical Plan for JINR Research and International Cooperation and FLNP User Program. A number of scientific experiments were performed in neutron and synchrotron centers in Russia and abroad under the existing cooperation agreements and accepted beam time application proposals. Also, the activities on the modernization of the available spectrometers and the development of new instruments were carried out in accordance with the development program plan for the IBR-2 spectrometers. Most attention was given to the realization of the top-priority projects (creation of the final configuration of a new DN-6 diffractometer for studying microsamples and a multipurpose GRAINS reflectometer, neutron radiography and tomography facility, upgrade of the HRFD diffractometer and REFLEX reflectometer).

Within the framework of investigations under the theme the employees of the FLNP Department of Neutron Investigations of Condensed Matter (NICM) maintained broad cooperation with many scientific organizations in Russia and abroad. The cooperation, as a rule, was documented by joint protocols or agreements. In Russia, especially active collaboration was with the thematically-close organizations, such as RRC KI, PNPI, MSU, IMP UB RAS, IC RAS, INR RAS and others.

A list of the main scientific topics studied by the employees of the NICM Department includes:

- Investigation of the structure and properties of novel functional materials;
- Investigation of the structure and properties of materials under extreme conditions;
- Investigation of fundamental regularities of real-time processes in condensed matter;
- Investigation of atomic dynamics of materials for nuclear power engineering;
- Computer simulation of physical and chemical properties of novel crystalline and nanostructured materials;
- Investigation of magnetic properties of layered nanostructures;
- Investigation of structural characteristics of carbon- and silicon-containing nanomaterials;
- Investigation of molecular dynamics of nanomaterials;
- Investigation of magnetic colloidal systems in bulk and at interfaces;
- Structural analysis of polymer nanodispersed materials;
- Investigation of supramolecular structure and functional characteristics of biological materials;
- Investigation of structure and properties of lipid membranes and lipid complexes;
- Investigation of texture and physical properties of Earth's rocks, minerals and engineering materials;
- Non-destructive control of internal stresses in industrial products and engineering materials;
- Introscopy of internal structure and processes in industrial products, rocks and natural heritage objects.

1. Scientific results

1.1. Structure investigations of novel oxide, intermetallic and nanostructured materials

Iron oxides play an important role in the formation of magnetic and other physical properties of the Earth, and find a wide range of technological applications. Recently, a new iron oxide, Fe_4O_5 , which can presumably exist in the layers of the Earth's upper mantle, has been synthesized under the combined effect of high pressures and temperatures. A comprehensive study of its physical properties, as well as atomic and magnetic structure using neutron diffraction techniques at the IBR-2 reactor, has revealed a new type of the charge-ordering state with the formation of dimeric and trimeric electronic states in this compound. The phase transition into this state is accompanied by a sharp increase in the electrical resistance and a subsequent change in the symmetry of the magnetic order, namely from a collinear antiferromagnetic (AFM) order to a canting AFM order with a ferromagnetic (FM) component, as well as by a change in the nature of the modulation of the atomic structure, **Fig. 1-I-1** [1].

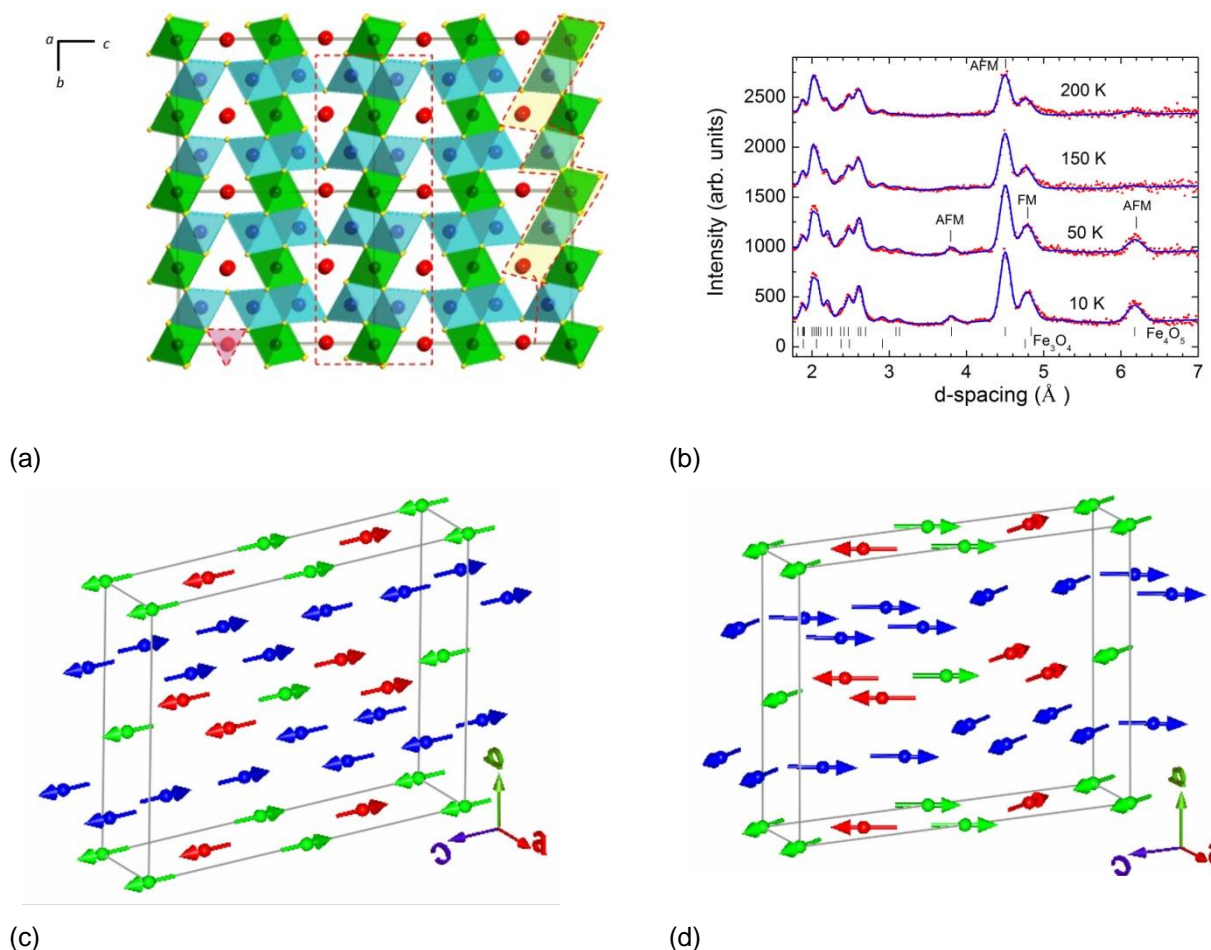


Fig. 1-I-1. Crystal structure of Fe_4O_5 (a), neutron diffraction spectra obtained at different temperatures and treated by the Rietveld method (b), the magnetic structure at $T = 150$ K (c) and $T = 10$ K (d).

The search for new multiferroics and magnetoelectrics is of current interest in modern condensed matter physics and materials science. A promising system is $\text{BaMn}_{1-x}\text{Ti}_x\text{O}_3$ whose end members are a classical ferroelectric BaTiO_3 with a high Curie temperature ($T_C = 395$ K) and

1. SCIENTIFIC RESEARCH

BaMnO_3 – a compound exhibiting a giant magnetoelectric effect and having a relatively high temperature of magnetic ordering ($T_N = 230$ K). The studies of $\text{BaMn}_{1-x}\text{Ti}_x\text{O}_3$ over the entire concentration range $0 < x < 1$ have revealed a very rich structural polymorphism. An increase in the titanium concentration was followed by a sequence of phase transitions between different rhombohedral and hexagonal phases differing by the ratio of oxygen octahedra connected through the corners and edges, 15R - 8H - 9R - 10H - 12R, **Fig. 1-I-2**. [2,3]. It has been found that the formation of a long-range magnetic order is possible only in structures: 9R, 8H, 15R and at concentrations of Ti $x < 0.25$, and the Neel temperature has a very sharp concentration dependence and drops from 230 to 100 K in the given x -range.

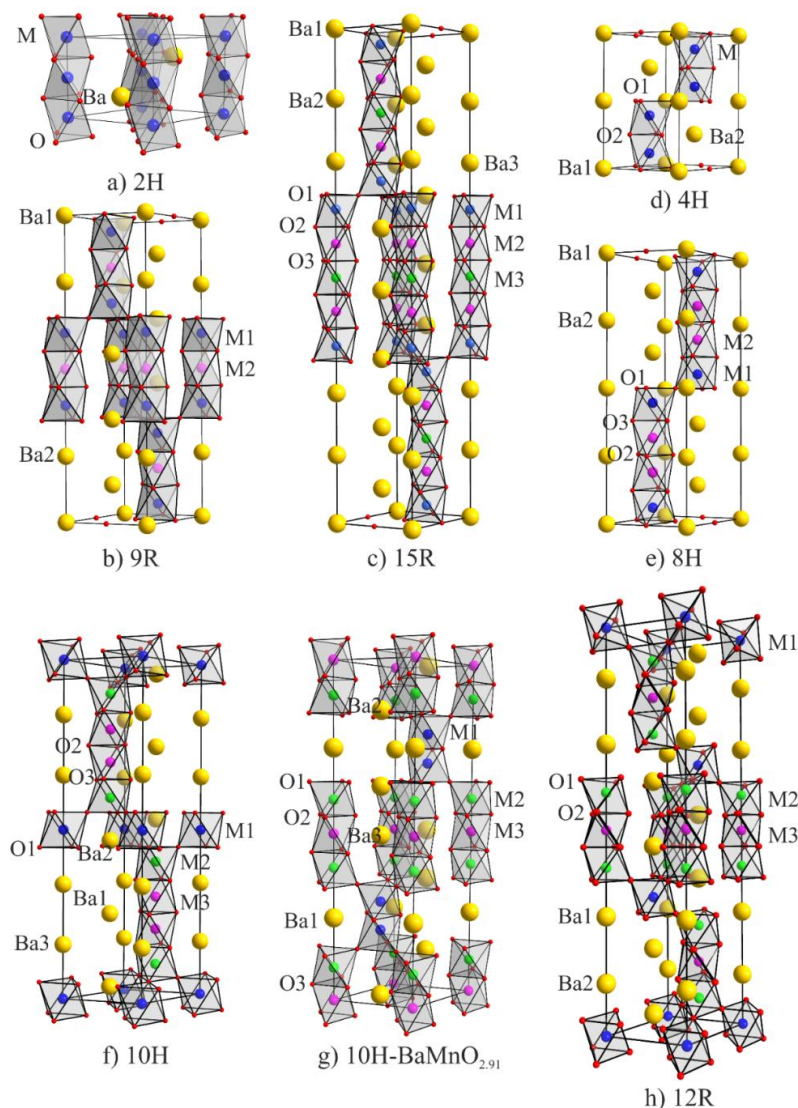
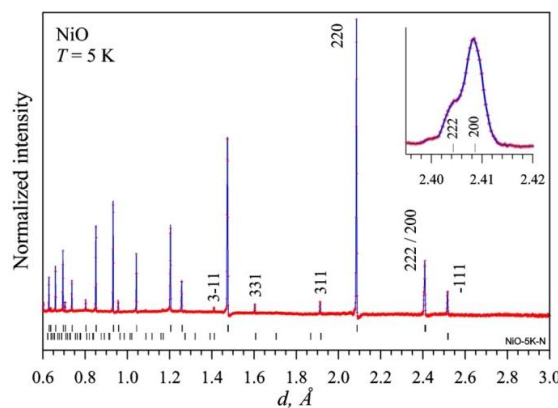
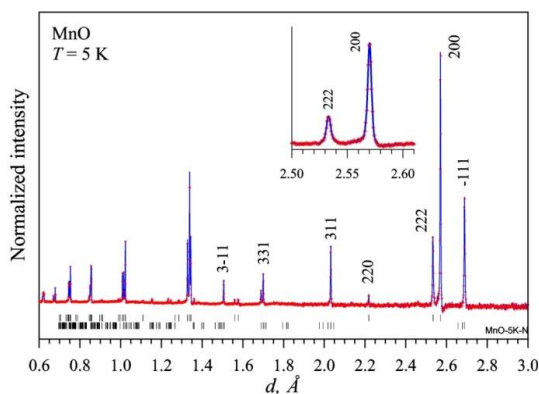


Fig. 1-I-2. Structure of polymorphic phases in the system $\text{BaMn}_{1-x}\text{Ti}_x\text{O}_3$.

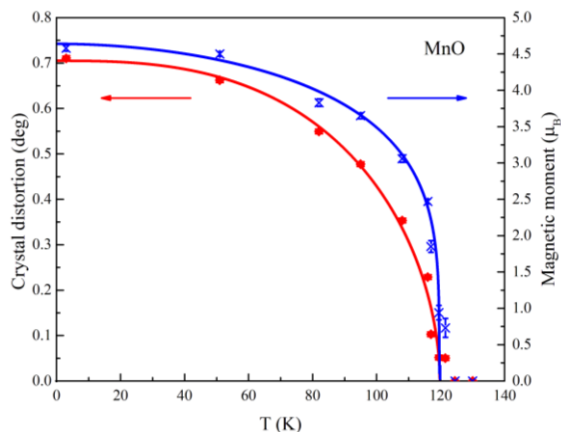
Using high-resolution neutron diffraction the structural (from the cubic phase to the rhombohedral phase) and magnetic (from the paramagnetic phase to the antiferromagnetic phase) phase transitions in NiO and MnO have been studied, **Fig. 1-I-3**, [4]. Despite the already long history of the study of phase transitions in simple antiferromagnets of NiO type by various experimental methods, the literature data about them are quite contradictory. It has been shown

1. SCIENTIFIC RESEARCH

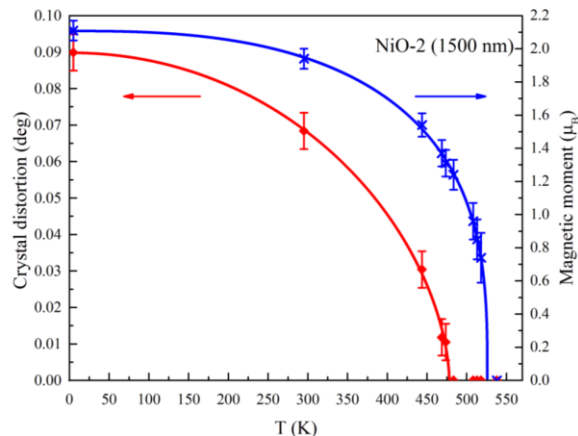
that in MnO the structural and magnetic transitions occur simultaneously, their temperatures are the same within the experimental error: $T_{\text{str}} \approx T_{\text{mag}} \approx (119 \pm 1)$ K. For NiO the measurements were performed on powders with different mean crystallite sizes (~ 1500 nm and ~ 138 nm), and in both cases it has been found that the transition temperatures differ by ~ 50 K: $T_{\text{str}} = (471 \pm 3)$ K, $T_{\text{mag}} = (523 \pm 2)$ K.



(a)



(b)



(c)

(d)

Fig. 1-I-3. Neutron diffraction spectra of high resolution at $T = 5$ K for MnO (a) and NiO (b) obtained at HRFD. Dashes indicate the positions of crystal (top row) and magnetic (bottom row) diffraction peaks. Miller indices (for a large R-lattice) are shown for several magnetic and first crystalline diffraction peaks. The inset shows the splitting of the peaks (200) and (222) due to the rhombohedral distortion. The dependence of the angle of rhombohedral distortion (left scale, red points) and magnetic moment (right scale, blue points) on temperature for MnO (c) and NiO-2 sample with the mean crystallite size of 138 nm (d).

$\text{La}_{1-x}\text{Sr}_x\text{Fe}_{2/3}\text{Mo}_{1/3}\text{O}_3$ ($0 \leq x \leq 1$) perovskites allow exceptionally wide variation of the Mo charge state from +3 ($x = 0$) to +6 ($x = 1$) while the charge state of Fe^{3+} remains virtually unchanged. The end members of this series show antiferromagnetic ordering in $\text{LaFe}_{2/3}\text{Mo}_{1/3}\text{O}_3$ at $T_N = 520$ K and ferrimagnetic ordering in $\text{SrFe}_{2/3}\text{Mo}_{1/3}\text{O}_3$ at $T_C = 420$ K. In both cases, the magnetic structure is dictated by antiferromagnetic superexchange between localized magnetic moments. At intermediate compositions, an interplay of antiferromagnetic-superexchange and double-exchange interactions results in nonmonotonous variations of both the magnetic-ordering temperature and saturation magnetization. To determine the magnetic phase diagram (**Fig. 1-I-4**) and the cation charge states, neutron diffraction spectra were measured, and XANES data and data on magnetic

1. SCIENTIFIC RESEARCH

susceptibility and magnetization were obtained. Also, the magnetic moment per formula unit was determined (**Fig. 1-I-4**). On the basis of all experimental data, a detailed analysis of the emerging interactions was carried out [5].

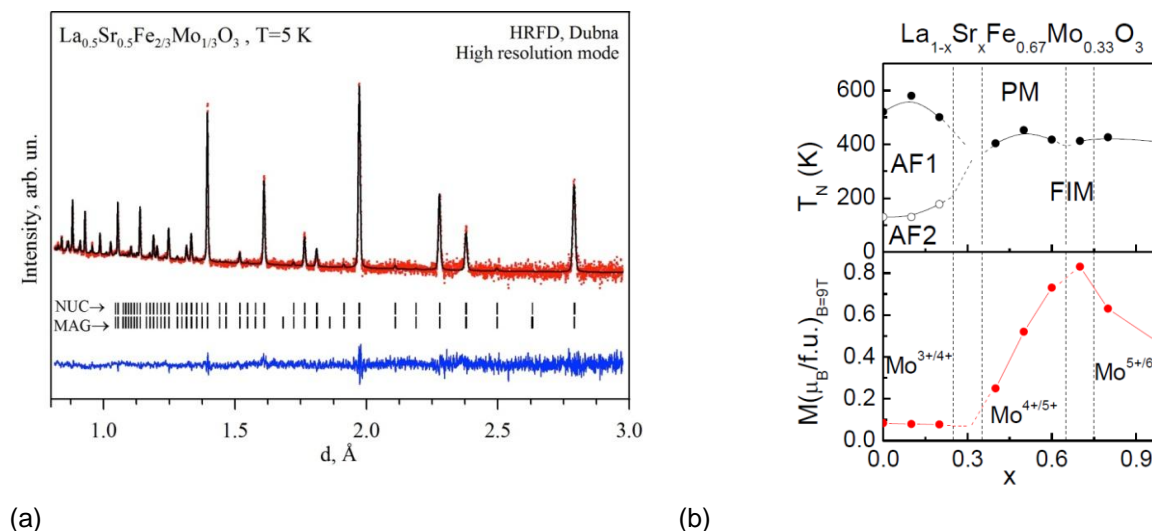


Fig. 1-I-4. Neutron diffraction spectrum from $\text{La}_{0.5}\text{Sr}_{0.5}\text{Fe}_{2/3}\text{Mo}_{1/3}\text{O}_3$ treated by the Rietveld method (a). Experimental points, calculated function and difference curve are shown. Dashes show the calculated positions of the nuclear (top row) and magnetic (bottom row) diffraction peaks. The magnetic phase diagram (top) and the magnetic moment value measured at 2 K in a field of 9 T for the $\text{La}_{1-x}\text{Sr}_x\text{Fe}_{2/3}\text{Mo}_{1/3}\text{O}_3$ series (b). Vertical lines separate the regions with different charge states of molybdenum.

Neutron diffraction studies of the $\text{Fe}_{0.735}\text{Al}_{0.265}$ compound were carried out in a wide temperature range (20-900°C) to determine its structural states and atomic ordering mechanism [6], **Fig. 1-I-5**.

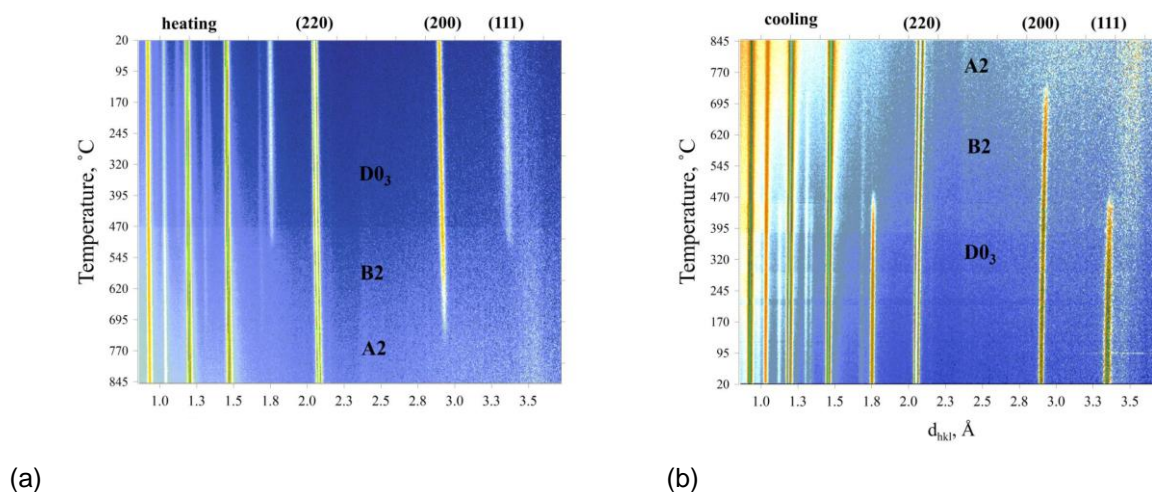


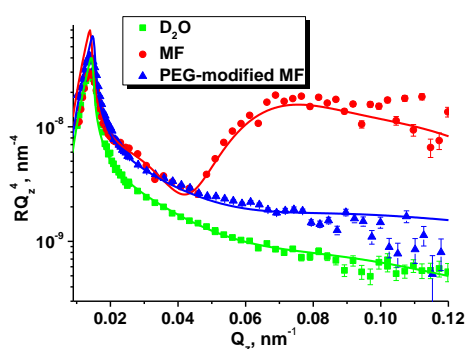
Fig. 1-I-5. 2D representation of structural transitions in Fe-27Al under heating (a) and cooling (b). The initial (before heating) and final (after cooling) conditions – D0_3 phase characterized by the presence of peaks (111) and (200). In the B2 phase the peak (111) is absent, while the peak (200) remains. In the A2 phase both of these peaks are absent. The rates of heating and cooling were ± 2 °C/min, the measurement time of one spectrum – 1 min, i.e. each picture contains about 400 spectra.

The combination of high-resolution diffraction and real-time diffraction made it possible to establish that, in contrast to traditional approaches, the structure of this compound at room temperature is a phase with only partially ordered arrangement (B2) of Fe and Al in a unit cell. A completely ordered phase (Fe_3Al - D0_3 type) is present as clusters of mesoscopic size (~ 200 Å) coherently incorporated into the matrix of the main phase. After the transition to a disordered state ($T > 740^\circ\text{C}$) and slow cooling to room temperature, the dimensions of the structurally ordered clusters increased to ~ 900 Å.

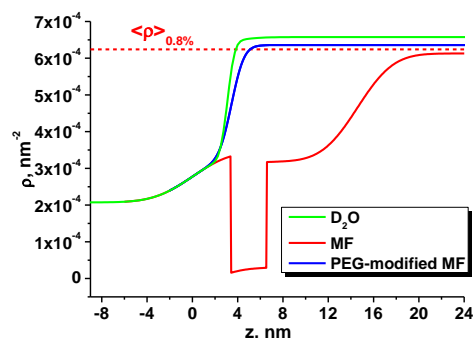
A high contrast between the coherent neutron scattering lengths of iron and aluminum made it possible to determine with a good accuracy the temperature dependence of the occupancy factors of sites by Fe and Al atoms up to a phase transition to the disordered state. The obtained results call for further analysis of the equilibrium phase diagram for the Fe-Al system.

1.2. Investigations of magnetic fluids and nanoparticles

A number of experiments on small-angle neutron scattering (SANS) and neutron reflectometry with a horizontal sample plane for the interface of magnetic fluids with silicon (GRAINS) have been carried out in the framework of investigations of the structure and stability of magnetic nanoparticles in bulk and at interfaces, **Fig. 1-I-6** [7]. It has been found that in the bulk of aqueous ferrofluids stabilized by sodium oleate there are comparatively small (size ~ 30 nm) and compact aggregates of magnetic particles. When magnetic fluids are modified by biocompatible polymer polyethylene glycol (PEG), cluster reorganization in the bulk of magnetic fluids is observed, namely large and branched clusters (size > 130 nm, fractal dimension of 2.7) appear. The observed in-bulk reorganization of the magnetic fluids is correlated with the neutron reflectometry data, which is indicative of the formation of a single adsorption layer of magnetic particles on the surface of oxidized silicon in the initial magnetic fluid and the absence of any layer at the ferrofluid/silicon interface after the polymer modification. The study has been performed in collaboration with the Institute of Experimental Physics, Slovak Academy of Sciences (Kosice, Slovakia); the Faculty of Physics of the Taras Shevchenko Kyiv National University (Kiev, Ukraine); the National Institute of Physics and Nuclear Engineering (Bucharest, Romania); Timisoara Branch of the Romanian Academy of Sciences (Timisoara, Romania) and the Max-Planck Institute for Solid State Physics (Stuttgart, Germany).



(a)



(b)

Fig. 1-I-6. (a) Experimental reflectivity curves for heavy water and magnetic fluids; (b) resulting scattering length density profiles.

In order to improve the synthesis procedure for biocompatible magnetic fluids, SANS (YuMO) and SAXS experiments have been carried out for magnetic fluids prepared using three

1. SCIENTIFIC RESEARCH

different methods (Fig. 1-I-7). An important feature of the ferrofluids under study was the addition of a specific component (polysaccharide agarose) to the water-based carrier, which complemented the stabilization effect and also provided biocompatibility of the initial fluids. It has been demonstrated that all investigated magnetic fluids have a complicated and highly aggregated structure, but nevertheless are stable in time. The structures of the magnetic fluids obtained by two methods of synthesis are similar to each other and different from that synthesized using the third method. In the last case two power-law type scattering levels corresponding to mass and surface fractals were observed along with an increase in the characteristic size of magnetic particles. The study [8] has been performed in collaboration with the V.I.Vernadsky Institute of General and Inorganic Chemistry (Kiev, Ukraine) and the Department of Physics of the Taras Shevchenko Kyiv National University (Kiev, Ukraine).

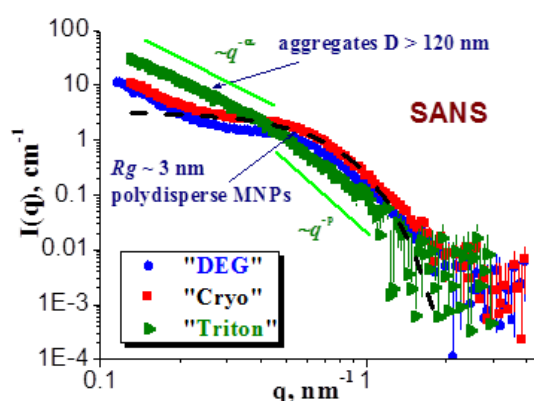


Fig. 1-I-7. SANS curves for magnetic fluids with agarose synthesized by three different methods. The concentration of magnetite is ~8.8. %; agarose – 0.1 vol. %.

As a part of a comprehensive study of the interaction of magnetic nanoparticles with amyloid protein formations, the experiments on small-angle scattering of synchrotron radiation, transmission electron microscopy, atomic force microscopy and magneto-optical methods have been carried out for the mixtures of fibril amyloid aggregates of protein lysozyme (egg white) with magnetite nanoparticles in the concentration range of 0.01-0.1 vol. % [9, 10]. The analysis of the complementary data has revealed that the magnetic nanoparticles are adsorbed onto the surface of amyloids, and the adsorption mode depends on the concentration ratio between the magnetic particles and the protein in solution. Thus, with increasing concentration of magnetic nanoparticles in solution there appear particle aggregates repeating a cylindrical shape of the amyloids. The observed effect has been considered in connection with the formation of an amyloid liquid crystal phase under an external magnetic field which can be used in practice. The study has been performed in collaboration with the Institute of Experimental Physics, Slovak Academy of Sciences (Kosice, Slovakia), Department of Physics, Taras Shevchenko National University of Kyiv (Kiev, Ukraine) and Helmholtz Centre Geesthacht (Geesthacht, Germany).

In the framework of the investigation of factors affecting the stability of magnetic fluids, studies of the effect of the surfactant excess on the stability of ferrofluids have been continued [11]. In particular, using SANS the structure of magnetic fluids based on non-polar solvent decalin and stabilized by saturated monocarboxylic acids of different alkyl chain lengths (C16, palmitic acid; C12, lauric acid), with an excess of acid molecules has been studied. It has been shown that the addition of the acid to the initial stable system with an optimum composition results in structural changes associated with the more significant aggregation than that previously observed for this class of magnetic fluids. By comparing the impact of mono-carboxylic acids on the stability of non-

polar ferrofluids, one can conclude that the aggregation growth is substantially more evident in excess of palmitic acid. This confirms the findings of the previous studies that an increase in the length of saturated acids reduces their stabilization efficiency in respect to magnetic fluids. The study has been carried out in collaboration with the Department of Physics, Taras Shevchenko National University of Kyiv (Kiev, Ukraine) and the Wigner Research Centre of the Hungarian Academy of Sciences (Budapest, Hungary).

1.3. Investigations of carbon nanomaterials

The biophysical research of fullerene solutions, in particular aqueous solutions of C₆₀ and C₇₀, has been continued. They included the analysis of the cluster structure when placing fullerenes in physiological environment and the study of the interaction of C₆₀ fullerene with antitumor antibiotics, **Fig. 1-I-8** [12, 13]. Using SANS and tests on mutagenic activity of Doxorubicin and C₆₀ admixture with Doxorubicin on Salmonella Typhimurium TA98 cells it has been shown that fullerene C₆₀ can act as an interceptor of the antitumor antibiotic Doxorubicin and form hetero-complexes with this drug.

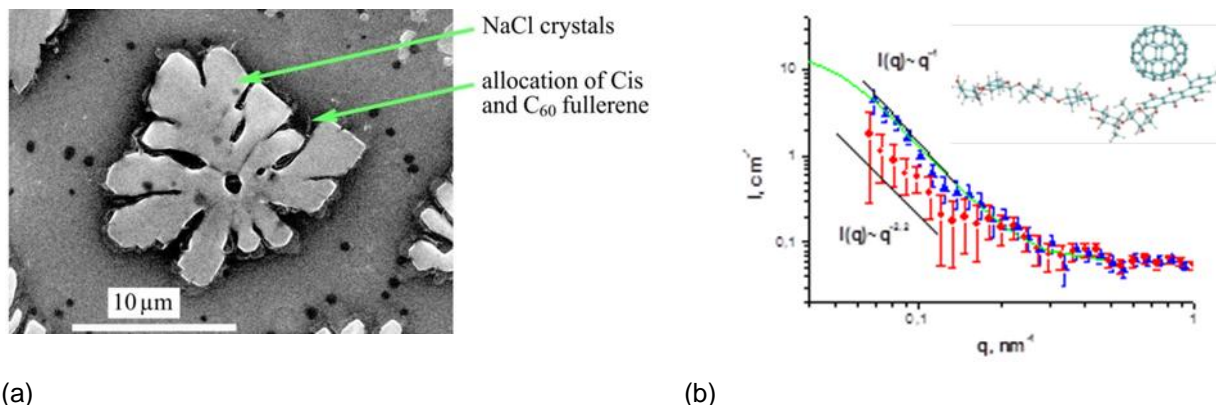


Fig. 1-I-8. SEM data for C₆₀/Cisplatin solution (a). SANS for aqueous C₆₀ solution (blue triangles) and mixture of C₆₀ with Landomycin A (red circles). The green line corresponds to the model curve obtained from the inverse Fourier transform. Insert: estimated structure of C₆₀ + Landomycin A complex (b).

The research on the interaction of C₆₀ with Doxorubicin, including SANS, scanning electron (SEM) and atomic force (AFM) microscopy, calorimetry, dynamic light scattering (DLS) and UV-Vis spectroscopy, has been extended to include other aromatic drugs with a similar to Doxorubicin spatial structure such as Landomycin and Cisplatin. New effects of the biological interaction of fullerene C₆₀ in combination with various anticancer drugs have been discovered and described. The work was carried out in collaboration with the Departments of Biology and Physics, Taras Shevchenko National University of Kyiv (Kiev, Ukraine).

The investigations related to the structural characterization of aqueous dispersions of detonation nanodiamonds (DND) have been continued [14]. In particular, the structures of DND hydrogels with a positive ζ -potential have been studied. The results of the SANS contrast variation have been compared with the data of the previous similar experiments for DND suspensions with a negative ζ -potential. No principal differences from a structural viewpoint between $\zeta+$ and $\zeta-$ stabilizations of aqueous DND suspensions have been found. The identity of the structure on the size scale up to 100 nm has been proved with respect to the developed clusters characterized by similar values of fractal dimensions, as well as to the DND particles characterized by polydispersity (above 30%) and diffuse surface. This demonstrates the existence of a common mechanism for

1. SCIENTIFIC RESEARCH

DND cluster formation and growth in suspensions, regardless of the method of stabilization. It has been assumed that nanosystems are stabilized by the formation of a charged interface around the whole clusters rather than around individual particles in them. The study has been carried out in collaboration with the Ioffe Physical-Technical Institute RAS (Saint-Petersburg, Russia) and the Department of Physics, Taras Shevchenko National University of Kyiv (Kiev, Ukraine).

1.4. Investigation of layered nanostructures

In the framework of the studies on improving the performance of lithium batteries, a series of experiments on neutron reflectometry (GRAINS reflectometer) to study electrochemical interfaces of liquid electrolyte/solid electrode have been carried out (Fig. 1-I-9). From the specular reflectivity analysis, the formation of a solid-electrolyte interphase (SEI) on the surface of the electrode (Cu) has been concluded, as well as the lithium electrodeposition and growth of parasitic dendritic structures during the operation of an electrochemical cell have been tracked.

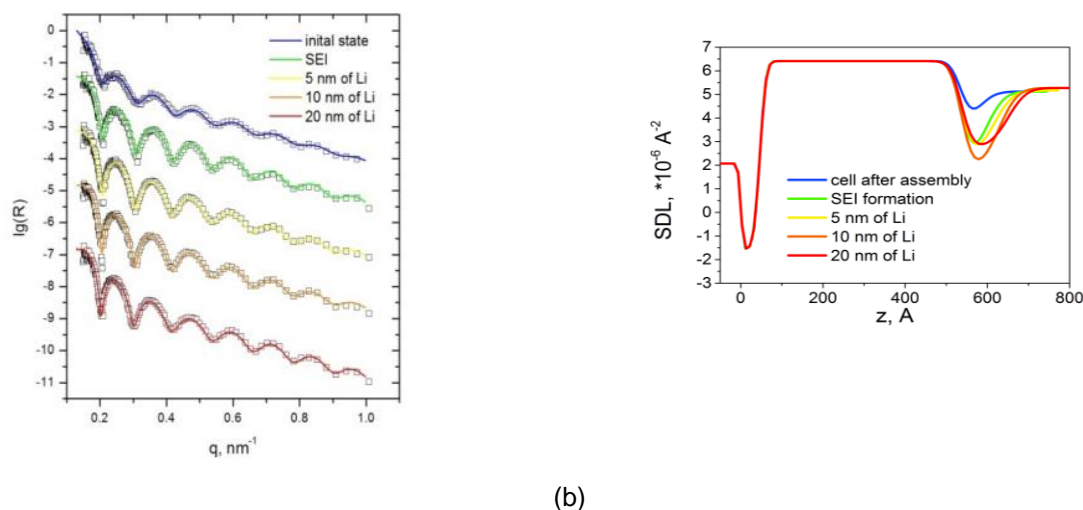
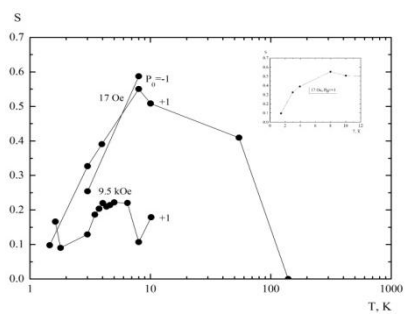


Fig. 1-I-9. (a) Experimental neutron specular reflectivity curves (points) for a copper electrode at the interface with the electrolyte at different current and voltage supply modes. (b) Resulting scattering length density profiles for different modes presented in (a) with indicated characteristic thicknesses of deposited lithium.

The obtained profiles of the scattering length density perpendicular to the electrode surface have made it possible to analyze different modes of SEI formation, as well as the formation and growth of nanometer lithium layers of different roughness on the initially formed SEI. It has been shown that neutron reflectometry can be effectively used for *in situ* characterization of lithium plating on metal electrodes [15]. The study has been performed in collaboration with the Department of Chemistry, Moscow State University (Moscow, Russia).

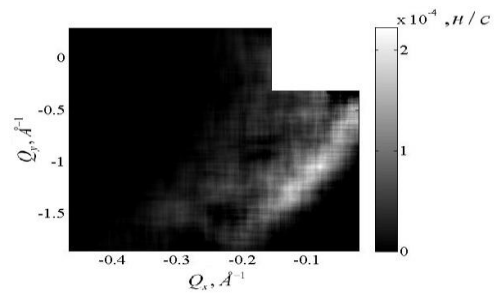
In layered structures S1/FM/S2 consisting of ferromagnetic and superconducting layers, the effect of superconductivity on ferromagnetism has been studied by using reflectivity and scattering of polarized neutrons. It has been shown experimentally that at low temperatures magnetic structures with linear dimensions in the range from 5 nm to 30 μm are formed. At temperatures below the superconducting transition, the magnetization of the magnetic structures in the vanadium and niobium layers is suppressed by superconductivity. **Figure 1-I-10** demonstrates for different structures that the neutron scattering diminishes as the temperature decreases from 8 to 1.5 K.

Also, **Fig. 1-I-10** shows how the structure of the cluster system at 8K is transformed into the structure at 1.5 K.

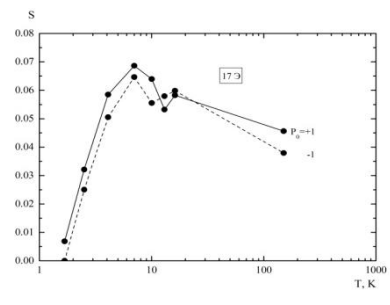


(a)

T=10.04 K, H=25 Oe

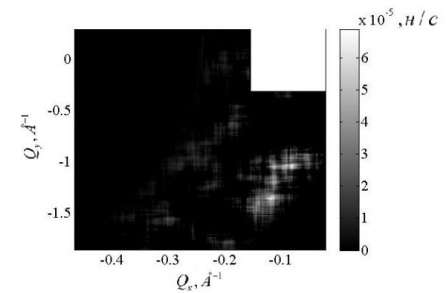


(c)

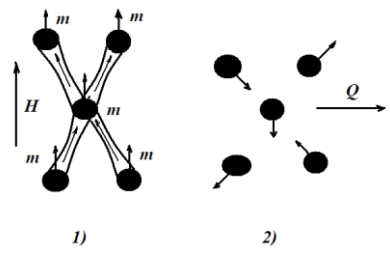


(b)

T=1.35 K, H=25 Oe



(d)



(e)

Fig. 1-I-10. Dependence of the neutron scattering coefficient $S(T)$ for the structure

$V(150\text{nm})/(FM(7\%)+V(50\%)+Nb(43\%)(25\text{ nm}))/Nb(150\text{ nm})$ at $H = 17\text{ Oe}$ and 9.5 kOe (a). The dependence of the neutron scattering coefficient $S(T)$ for the structure $V(150\text{nm})/(FM(7\%)+V(43\%)+Nb(43\%)+Cr(7\%))(25\text{ nm}))/Nb(150\text{ nm})$ at $H = 17\text{ Oe}$ (b). The contours of the neutron scattering intensity on the plane of transfer wave vectors Q_y - Q_x at $H = 25\text{ Oe}$ and $T = 10.04\text{ K}$ (c) and 1.35 K (d). The structure of the cluster system at 8 K (1) and 1.5 K (2) (e).

Using the *in situ* reflectometry of polarized neutrons the magnetic state of a superconducting-ferromagnetic layered structure Ta/V/FM/Nb/Si has been studied. The relaxation of a non-uniform magnetic state of the structure with a characteristic time of a few hours was observed at temperatures both above and below the superconducting transition points in the structure layers. The character of the time dependence of the neutron scattering depends on the magnitude of the magnetic field H , temperature and neutron polarization. **Figure 1-I-11** shows the time dependence for the coefficient of neutron scattering. The dependence on polarization due to the scattering from magnetic clusters can be seen. The moments of the clusters are reoriented from the initial direction along the field to the direction against the field. There is also a scattering contribution which is independent of polarization and caused by the formation of a domain structure with time.

1. SCIENTIFIC RESEARCH

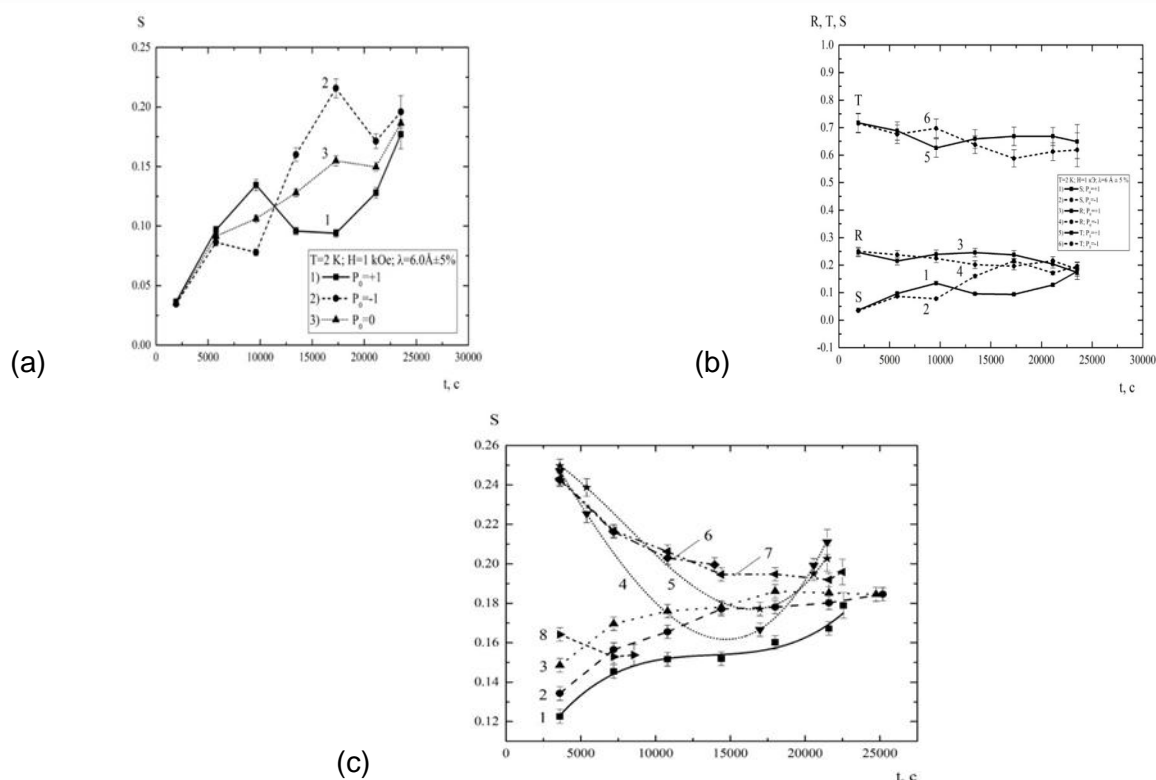


Fig. 1-I-11. Dependence $S(t)$ in magnetic field of 1 kOe at temperature of 2 K for $\lambda = 6 \text{ \AA}$ and $P_0 = +1, -1$ and 0 (a). Time dependences for coefficients of transmission T , reflection R and scattering S (b). Dependence $S(t)$ at $T = 3$ K: $P_0 = +1$ at H -values: 17 Oe (1), 1 kOe (2), 2 kOe (3), 4 kOe (4), 6 kOe (6), 7 kOe (7) and 8 kOe (8); $P_0 = -1$ and $H = 4$ kOe (5) (c).

At a large field of 4 kOe (curves 4 and 5, **Fig. 1-I-11(c)**), in early stages there is a depinning of superconducting vortices in the mixed state of superconducting layers of vanadium and niobium, which is changed to the motion of cluster moments.

Thus, apparently it was for the first time when neutron reflectometry (coherent propagation - reflection and transmission, as well as GISANS) was used to study the relaxation of the magnetic state and observe relaxation in a hybrid structure consisting of ferromagnetic and superconducting layers. In this case, the characteristic time of the change in the magnetic state of the systems of clusters, domains and vortices was a few hours with a several percent accuracy in the time dependence measurement. The measurement of the time dependences for the coefficients of scattering, reflection and transmission occurring under changes in the average and local potentials of the interaction of neutrons with the medium, was an effective method for identifying types of magnetic systems in the layered structures. In principle, a potential increase in the intensity of the neutron beam at the REMUR spectrometer used in the present study could allow one to achieve time resolution of a few minutes in studies of irreversible processes.

1.5. Investigation of biological nanosystems, lipid membranes and lipid complexes

It is well known that fermentative systems of oxidative phosphorylation in mitochondria can operate in two states - in a state of supercomplex and in a dissociated state. The comprehensive studies have shown that heart mitochondria operate in the state of supercomplex in a wide range of tonicities of incubation media. This result has been obtained by the polarographic method using

the double inhibitor technique by Baum. The investigation of mitochondrial ultrastructure by the methods of electron microscopy (EM) and small-angle neutron scattering (SANS) under conditions of normal tonicity (300 mOsm - isotonia) and low-amplitude swelling (120 mOsm - hypotonia) has proved the existence of two types of mitochondrial ultrastructure. Using EM, it has been found that the mitochondrial cristae in hypotonic and isotonic conditions have different shape and thickness. The tomography method has demonstrated a folded configuration of the cristae. The studies of the ultrastructure of heart mitochondria by methods of EM and inhibition analysis have been carried out on intact functioning mitochondria in the presence of respiratory substrates. Using the SANS method it has been shown that in hypotonic and isotonic media highly-organized lipid-protein lamellar structures are formed in mitochondria. The formation of lipid structures has been demonstrated by using the contrast variation technique (variation of the fraction of heavy water in a solution). Also, it has been shown that the thickness of the mitochondrial cristae depends on the medium tonicity. Thus, the data obtained from the investigation of the functioning and structure of mitochondria suggest the existence of two states for the system of oxidative phosphorylation, which forms cristae with different structural parameters [16].

The passive transport of particles through lipid membranes in different lipid phase states has been investigated by inelastic X-ray scattering. It is known that the passive transport of molecules through a cell membrane depends on thermal motions of lipids. However, the nature of transmembrane transport and its precise mechanism are not fully understood. The phonon excitations in a lipid bilayer of 1,2-dipalmitoyl-*sn*-glycero-3-phosphocholine above and below the main phase transition temperature have been measured. In the gel phase, for the first time the presence of transverse high-frequency modes has been shown. The modes are terminated when the lipids change into the liquid phase. This termination is apparently due to the formation of short-lived nanometer lipid clusters and transient pores which facilitate the passive molecular transport through the lipid bilayer. The obtained data suggest that the phononic motion of the lipid hydrocarbon tails provides an effective mechanism of passive transport [17].

The investigations (diffraction and small-angle scattering of neutrons and synchrotron radiation) of lipid membranes and nanoparticles on their basis have been continued in collaboration with the University of Messina, Italy, and NRC "Kurchatov Institute". The structural organization of vesicular drug carriers, including a vesicular transport system Phospholipovit, has been studied (Fig. 1-I-12) [18].

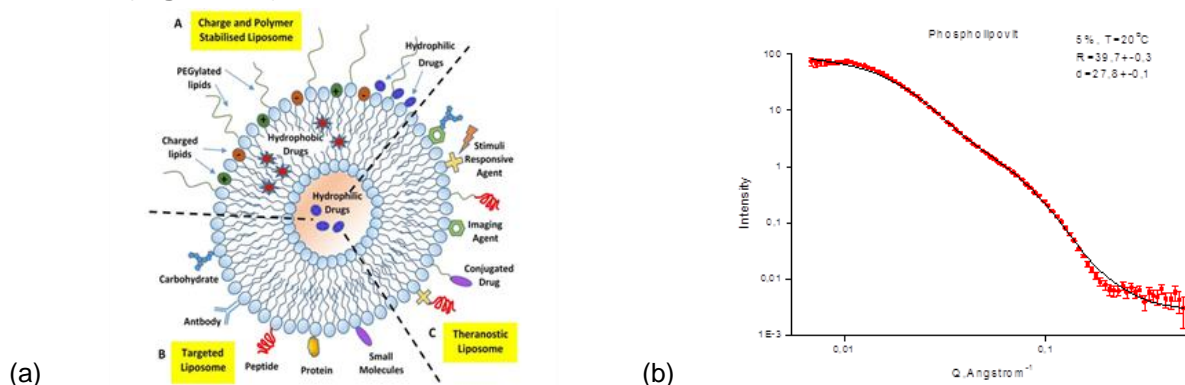


Fig. 1-I-12. Schematic representation of vesicular transport systems of various types for drug delivery (a). Experimental and calculated curves of small-angle neutron scattering (YuMO) for vesicular transport system Phospholipovit (b).

Particular attention has been given to the processes of interaction and aggregation of vesicles. The general principles of the organization of vesicular drug carriers have been formulated.

1. SCIENTIFIC RESEARCH

In the framework of the study of the structure and properties of membranes the experiments on molecular dynamics simulation (MD) and SANS for Ca^{2+} and Zn^{2+} cations with the gel phase of a model lipid membrane of dipalmitoylphosphatidylcholine (DPPC) have been carried out. As a result, the formation of oriented multilamellar membranes has been studied. An increase in the bilayer thickness has been revealed for both considered cations at a molar ratio of divalent metal ion to lipid ($\text{Me}^{2+}:\text{DPPC}$) of $\sim 1:7$. The MD simulations have made it possible to reveal a slight difference in the effect of the cations on the gel-phase of membranes. The study [19] has been performed in collaboration with the Comenius University (Bratislava, Slovakia), a number of research laboratories in the USA and LRB JINR.

Comprehensive studies of the phase transitions, morphology and internal structure of an organogel of 4-heptyloxyphenylolithocholic acid (7OPHOLCA) – a derivative of lithocholic acid (LCA) have been carried out. The obtaining of stable organogels with specified chemical and physical properties is a challenging direction regarding the potential applications in optoelectronics, drug delivery in medicine, regeneration of damaged tissues, etc. The samples of 7OPHOLCA in DMSO- d_6 with various concentrations have been studied by the SANS method, as well as temperature ranges for the sol-gel transition have been determined, **Fig. 1-I-13** [20].

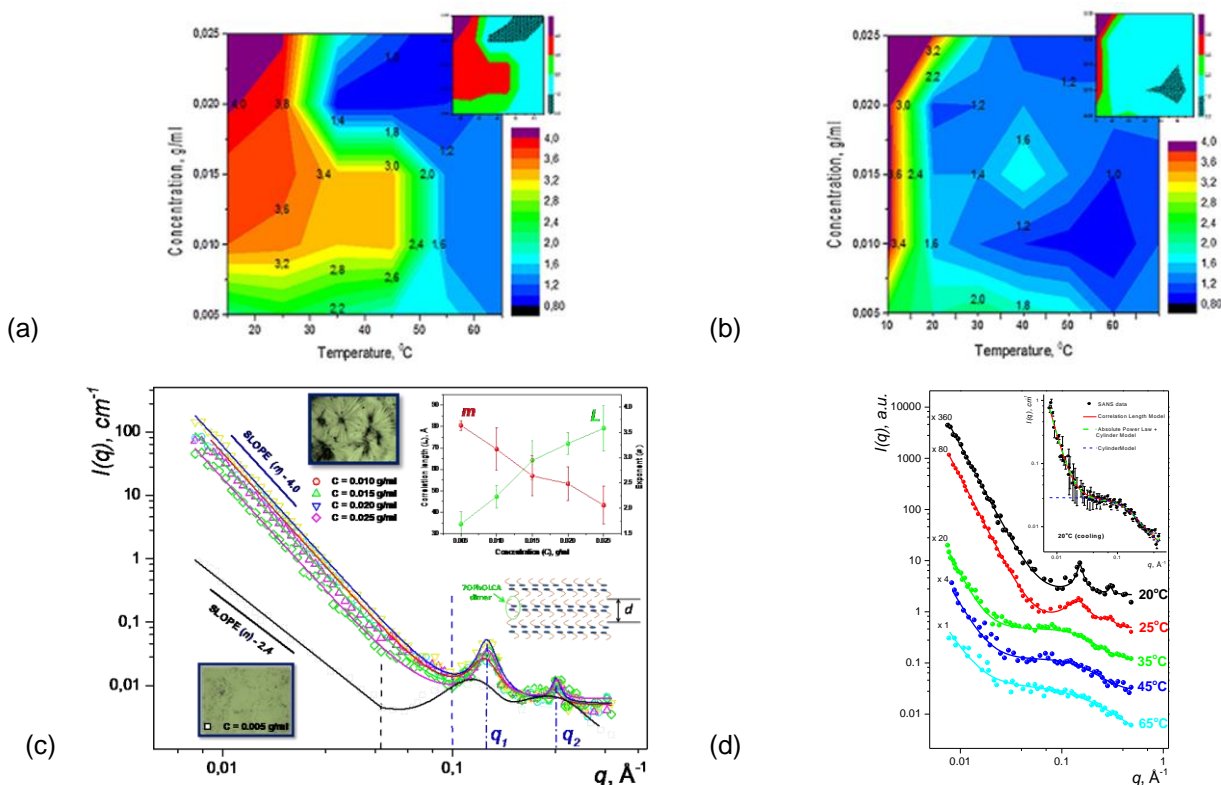
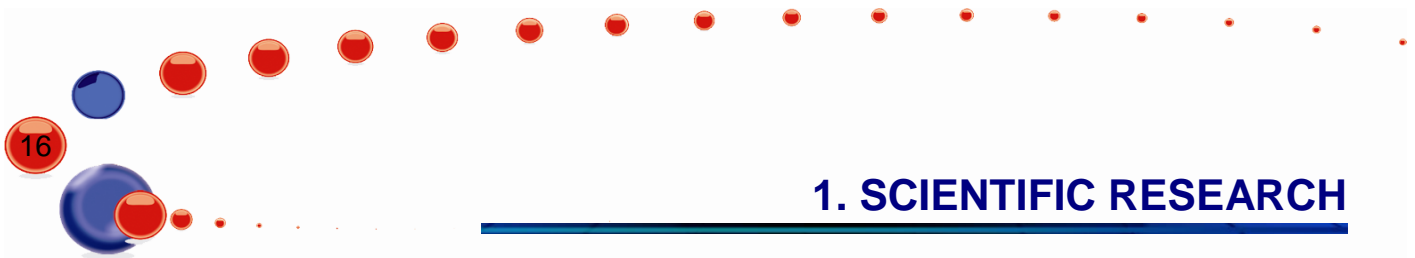


Fig. 1-I-13. Sol-gel transition for heating (a) and cooling (b). SANS curves (symbols) with fits (lines) for 7OPHOLCA in DMSO- d_6 at concentration $C = 0,005, 0,010, 0,015, 0,020,$ and 0.025 g/ml at $T = 10^{\circ}\text{C}$ after a single heating-cooling cycle (c). Dashed vertical lines divide the ranges of small and large q -values; q_1 and q_2 correspond to the maximum intensity of Bragg peaks. Optical microscopy images were obtained for samples stabilized for 12 hours in quartz cells at $T = 10^{\circ}\text{C}$. Insert: change in the correlation length, L , and the exponent, m , as a function of concentration of 7OPHOLCA. Changes in the SANS curves with increasing temperature for 7OPHOLCA in DMSO- d_6 at $C = 0.015$ g/ml (d). Insert: SANS curves (circles) at $T = 20^{\circ}\text{C}$ during cooling.



1. SCIENTIFIC RESEARCH

It has been shown that the transition temperature decreases with increasing concentration of organogel when heated. The reason for the changes in the internal structure around the sol-gel transition is the destruction of hydrogen bonds, as shown by IR spectroscopy. Furthermore, the analysis of small-angle scattering curves has revealed morphological changes of the studied samples in the gel phase, which had not been initially detected by DSC because of low enthalpy (compared to the phase transitions). In particular, at temperatures above 25°C the lamellar organization of dimers is destroyed.

At the same time, no reorganization of hydroxyl groups is observed (IR spectroscopy). In the analysis of the SANS data three models have been proposed. The time stability of organogels has also been studied. It has been found that all the phases observed are reversible and the structure of the studied samples exhibits a memory effect.

1.6. Polymeric materials

Small-angle neutron scattering has been used to study the structural peculiarities of perfluorinated proton conducting polymer samples containing sulfonic groups of Aquivion. A fine structure of polymeric membranes based on a system of proton conducting channels in a perfluorinated polymer matrix has been revealed. The way this fine structure changes has been determined as a function of the equivalent weight of the membrane, and the relation of these changes with the proton conductivity value has also been established. The contrast variation technique has made it possible to study the effect of orientational stretching on the fine structure. It has been found that the stretching is accompanied by an increase in the proton conductivity due to changes in the fine structure of the channel system. Our investigations confirm that a reduction of the side chain length affects the fine structure of the perfluorinated proton conducting membranes. This is accompanied by an improvement in their performance in hydrogen fuel cells [21].

Silver sols synthesized in polymer matrices have been investigated by small-angle X-ray scattering (SAXS) in combination with ultraviolet-visible (UV-VIS) spectroscopy and quasielastic light scattering (QELS). The characteristics of the particle size distribution obtained by each of the methods are in good agreement. It has also been found that there are deviations of the experimentally measured characteristics from the existing theoretical models. The most likely reason for this is that the nanoparticle clusters have a non-spherical shape [22].

The modeling of the glass transition kinetics for polystyrene has been continued. Using different theoretical methods currently applied to polymer systems, a single measurement of the temperature dependence for the heat capacity under heating and cooling has been modeled. It has been shown that for single curves good agreement is achieved, however the resulting model parameters do not allow one to describe correctly the dependence of the glass transition temperature on the cooling rate. In the opposite case, if the dependence $T_g(q)$ is fitted the agreement with a single measurement is of poor quality. Thus, it has been clearly shown that the modeling of glass transition in terms of the general parameters depending on the cooling rate simultaneously with the transition kinetics is impossible within the framework of the existing models [23]. The study has been performed in collaboration with the University of Rostock (Rostock, Germany).

1.7. Atomic and molecular dynamics

Inhibitors of 3-hydroxy-3-methylglutaryl coenzyme A (HMG-CoA) reductase are among the most effective and widely used drugs for lowering the cholesterol level, known as statins. Statin monotherapy is generally well tolerated and has minimal side effects. The first HMG-CoA inhibitor approved by FDA (Food and Drug Administration, USA) – lovastatin (MEVACOR®; ALTOCOR® &

1. SCIENTIFIC RESEARCH

ALTOPREV®, below referred to as LOV was mainly used to control hypercholesterolemia (**Fig. 1-I-14**).

In the LOV molecule three main parts can be distinguished – lactone ring (lct), naphthalene fragment (nph) and methylbutanoate chain (mbt). The molecules are linked by hydrogen bonds $O\cdots HO$ (**Fig. 1-I-14**). Hydrogen bonds bind lactone rings (methyl group) with methylbutanoate chains (carbonyl group). The second carbonyl group of lactone rings is unbound.

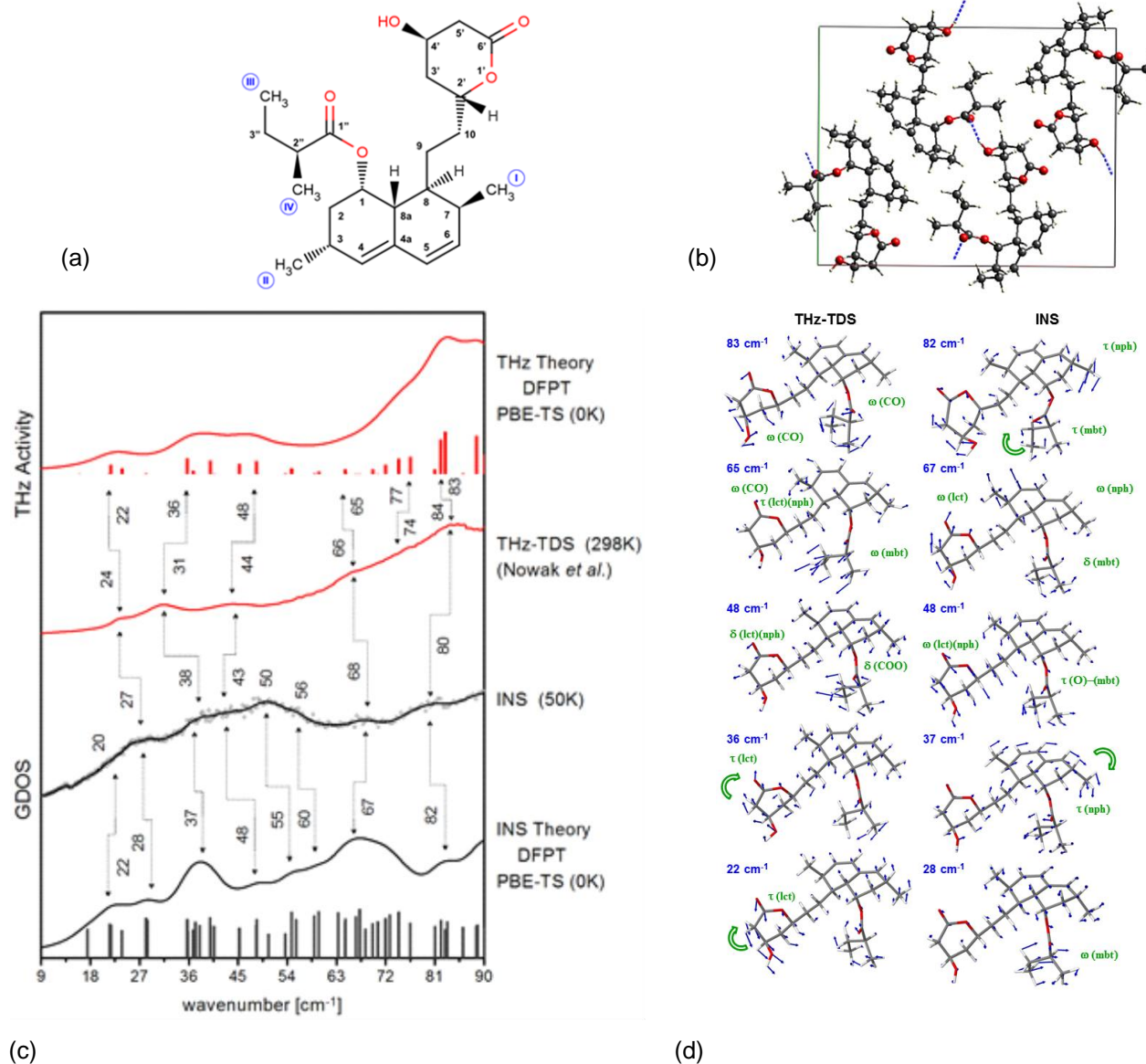


Fig.1-I-14. Molecular formula of lovastatin (LOV; (1*S*,3*R*,7*S*,8*S*,8*aR*)-8-{2-[(2*R*,4*R*)-4-Hydroxy-6-oxooxan-2-yl]ethyl}-3,7-dimethyl-1,2,3,7,8,8*a*-hexahydronaphthalen-1-yl (2*S*)-2-methylbutanoate) with marked methyl groups (I-IV) (a). Crystal structure of lovastatin (space group $P2_12_12_1$) optimized using PW - DFT (PBE-TS) (b). Comparison of theoretically calculated (harmonic approximation DFPT PBE-TS) and experimental vibrational spectra of lovastatin according to the data of neutron (IINS) and optical terahertz spectroscopy (data by Nowak et al. *Acta Poloniae Pharmaceutica in Drug Research*, Vol. 72 No. 5 (2015) pp. 851-866) (c). The most important vibrational modes of lovastatin contributing to the INS and THz-TDS spectra. The eigenvectors obtained from the harmonic PBE-TS calculations are shown in the projection of one molecule(d).

1. SCIENTIFIC RESEARCH

In collaboration with the Adam Mickiewicz University (Poznan, Poland), atomic and molecular dynamics of lovastatin has been studied by ^1H NMR and inelastic neutron scattering complemented by theoretical ab-initio calculations using the PW-DFT method. A consistent molecular dynamics model has been obtained, which can be later used to describe the dynamics of other alternative drug forms and tendencies to amorphization. It has been found that the molecular dynamics of lovastatin is determined by the motions of methyl groups and the conformational disorder in the methylbutanoate fragment. The vibrational dynamics of lovastatin was analyzed focusing on the energy transfer range with low wave numbers, which was experimentally studied by neutron (INS) and terahertz (THz-TDS) spectroscopy. The theoretical calculations made it possible for the first time to describe with a high accuracy the phonon spectrum of lovastatin in this region (**Fig. 1-I-14**).

It should be noted that the main contribution to the inelastic neutron scattering spectra is from vibrations of hydrogen-containing molecular groups, which are the most mobile ones for the movable mbt fragment contributing to the most intense vibrational mode. At the same time, the primary contribution to the terahertz spectra is from the most polar molecular groups containing oxygen and included in the lct fragment. The corresponding normal vibrational modes are shown in **Fig. 1-I-14**. The most intensive spectral features for THz-TDS are due to the modes related to the vibrations of hydrogen bridges $\text{O}\cdots\text{O}$ in a range of above 65 cm^{-1} , while the modes in a range of below 65 cm^{-1} are determined by the vibrations of the whole lct fragment. This set of modes is of a general nature without intending to be bound to a particular LOV compound and can be used in further studies of statins.

The experimental and theoretical investigations of the dynamics of a nitrated derivative of ortho-hydroxy acetophenone have been carried out. To estimate the barriers of the conformational changes and folding, the potential barriers for the nitro group rotation and hydroxyl group isomerization were calculated. Two polymorphic forms of this compound were obtained by slow and rapid evaporation of the polar and nonpolar solutions, respectively. Both polymorphs were investigated by means of infrared, Raman and neutron spectroscopy (**Fig. I-15**), nuclear quadrupole resonance, differential scanning calorimetry, and theoretical calculations using the DFT method were performed as well. In one of the polymorphs phase transitions were detected.

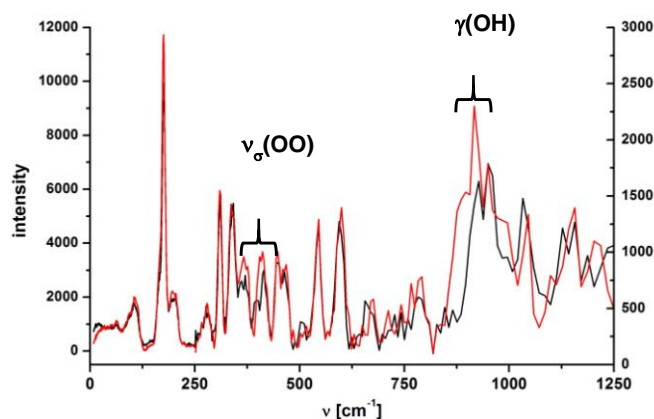


Fig. 1-I-15. Spectra of inelastic scattering (NERA, IBR-2, JINR) from polymorphic forms of *o*-hydroxyacetophenone (red line) and its mono-deuterated analogue. The left and right Y-scales correspond to the spectral ranges of $0\text{-}250\text{ cm}^{-1}$ and $250\text{-}1250\text{ cm}^{-1}$.

The position of the nitro group and its influence on the crystal structure were analyzed by X-ray diffraction. A full spectrum analysis of the vibrational spectra for the interpretation of the two

1. SCIENTIFIC RESEARCH

conformations was performed. On the basis of the obtained data the nature of the phase transition has been explained [24].

1.8. Applied research

On FSD, the experiments to study the distribution of residual stresses in welds after using various welding methods have been continued. The work has been carried out in collaboration with the Institute of Electronics, BAS (Sofia, Bulgaria) and the Brandenburg University of Technology (Germany). In 2016, residual stresses were measured in a massive (thickness ~ 20 mm) sample from structural steel S355J2+N welded with combined multipass welding: 1st pass – metal welding in shielding gases (MSG-welding), 2nd and 3rd passes – submerged arc welding (SAW-welding), **Fig. 1-I-16**.

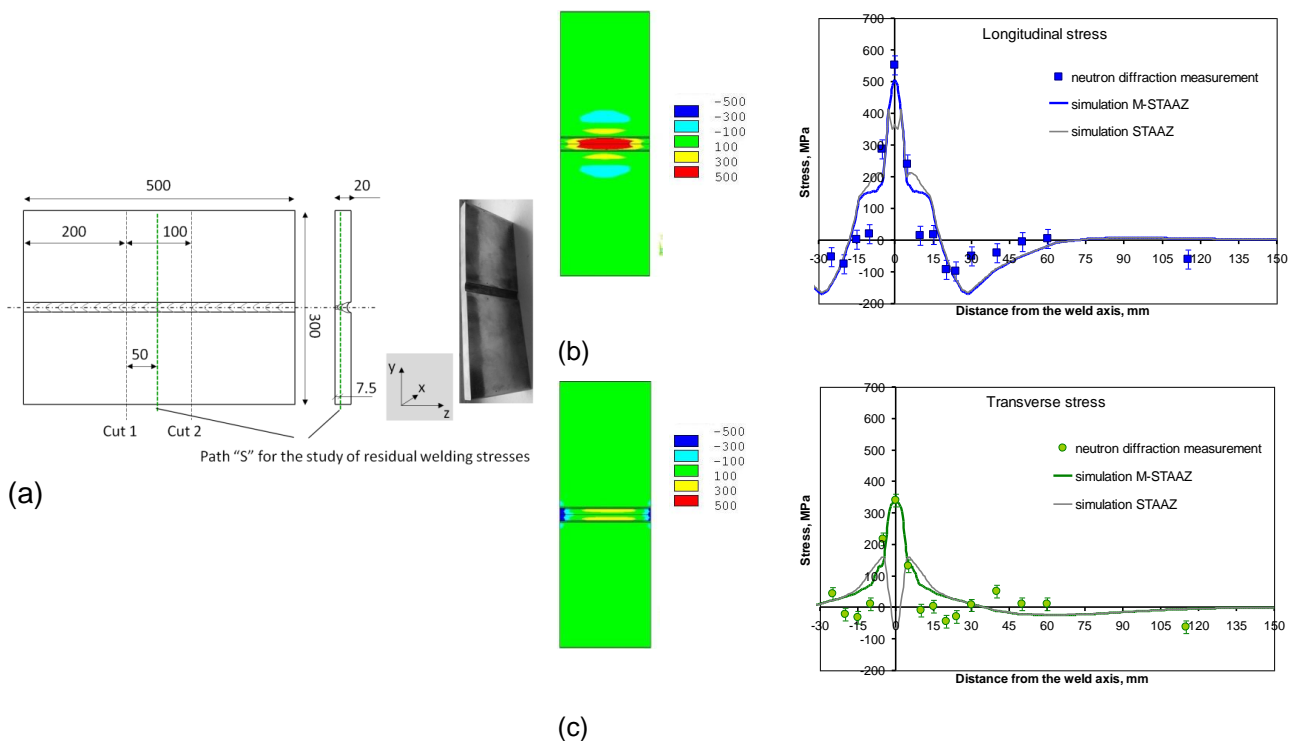


Fig. 1-I-16. Sample cut from a thick (~ 20 mm) plate welded with multi-pass submerged arc welding (SAW-welding). "S" is a scan-line in neutron measurements. Arrows indicate the strain tensor components (X, Y, Z) (a). Full map of distribution of the longitudinal component (σ_x) in the tensor of residual stresses calculated by the finite element method (FEM) and the comparison of the experimentally measured σ_x -values along the scan-line "S" with the results of numerical modeling by FEM (solid line) (b). Full map of distribution of the transverse component (σ_y) in the tensor of residual stresses calculated by FEM and the comparison of the experimentally measured σ_y -values along the scan-line "S" with the results of the numerical modeling by FEM (solid line) (c).

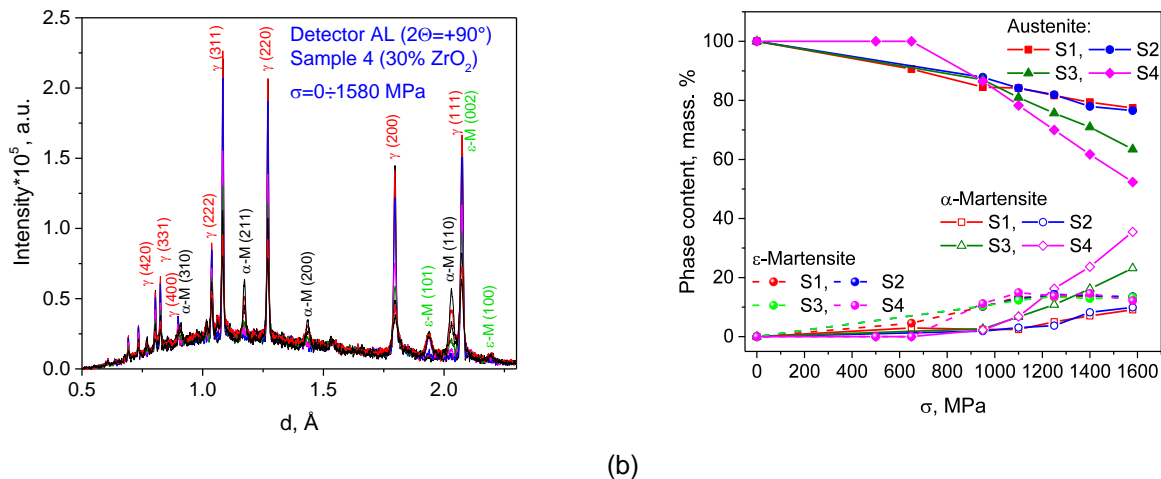
In neutron experiments with new radial collimators in the middle part of the sample the residual stress tensor components were measured in a wide X-range across the weld, which were further used to determine the residual stress values (**Fig. 1-I-16**). The maximum component is the longitudinal stress tensor component σ_x (~ 550 MPa) directed along the weld which is of the stretching character in the center of the weld. The level of the transverse component of the stress

1. SCIENTIFIC RESEARCH

tensor σ_y is significantly lower (~ 350 MPa), and the level of the normal component σ_z does not exceed 180 MPa.

In addition to the experiments on neutron diffraction, numerical calculations by the STAAZ method have been performed in the framework of the existing cooperation with the research group of Prof. V. Mikhailov (Brandenburg University of Technology, Germany). The comparison of the neutron data and FEM calculations has shown good agreement, indicating the reliability of the developed theoretical model for the multi-pass welding process. This information can serve as a basis for the development of specific technical recommendations to achieve the desired level and profile of residual stresses.

On FSD, a series of TRIP-composites with austenitic matrix and different content of reinforcing ceramic phase of zirconium dioxide ZrO_2 partially stabilized by magnesium (Mg-PSZ) have been investigated at various degrees of plastic deformation (uniaxial compressive load), Fig. 1-I-17.



(a)

(b)

Fig. 1-I-17. The change in the diffraction spectra of the TRIP-composites as a function of plastic deformation (a). The change in the phase mass content in the TRIP composites depending on the degree of plastic deformation (b).

The study has been done in collaboration with the Freiberg University of Mining and Technology (Freiberg, Germany). At the load values above 650 MPa, the formation of two phases in the austenitic matrix was observed: cubic α' -martensite and hexagonal ϵ -martensite. The content of ϵ -martensite reached $\sim 15\%$ for all samples under deformation up to $\sigma = 1100$ MPa and then remained almost unchanged until the maximum load values of $\sigma = 1580$ MPa. In contrast, the α' -martensite phase exhibited a monotonic increase in the load range from 950 to 1580 MPa. In the ceramic sample of pure zirconium dioxide (100% ZrO_2) two phases were observed: cubic ($f \approx 55\%$) and tetragonal ($f \approx 45\%$). The residual deformation of the crystal lattice of the austenitic matrix is of compressive character and increases up to $\sim 10^{-3}$. In this case, the crystal lattice deformation in α' - and ϵ -martensites is more complex and reflects the redistribution of the load between the phases. Furthermore, under the deformation in the range from 650 to 1580 MPa a noticeable broadening of the diffraction peaks with increasing plastic deformation was observed, which was caused by the variation in the contrast factor of dislocations. For the austenitic matrix the dislocation densities were evaluated from the peak broadening. They reached the values in the range of $12 \pm 20 \cdot 10^{14} \text{ m}^{-2}$ depending on the content of zirconium dioxide in the composite.

1. SCIENTIFIC RESEARCH

The texture and microstructure of the pristine and retrogressed samples of eclogite and surrounding metasediments have been investigated to gain insights into the deformation processes in the palaeo-subduction channel of the Tauern region (Austria), **Fig. 1-I-18** [25]. The texture features and deformation processes in omphacite and glaucophane have been analyzed. The presence of a plastic deformation cycle in the metamorphism of eclogite and blueschist facies associated with the subduction and exhumation of rocks has been established.

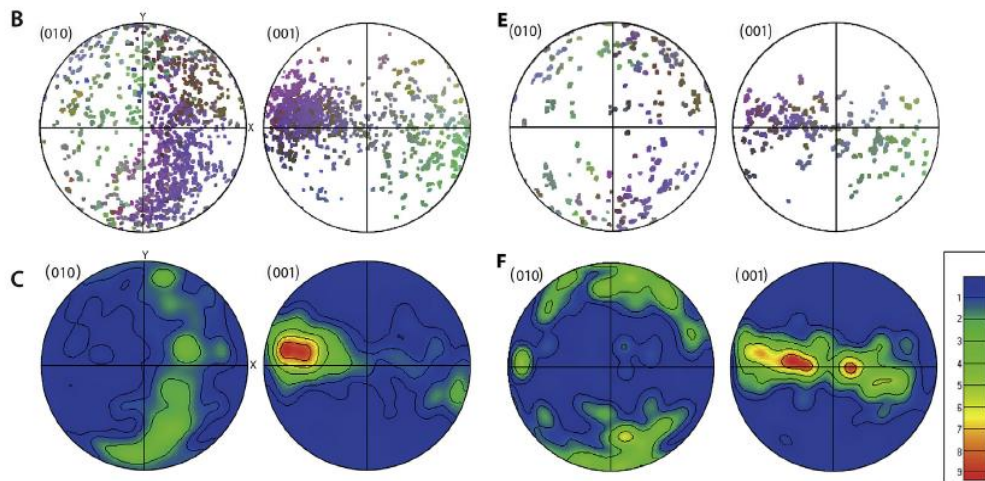


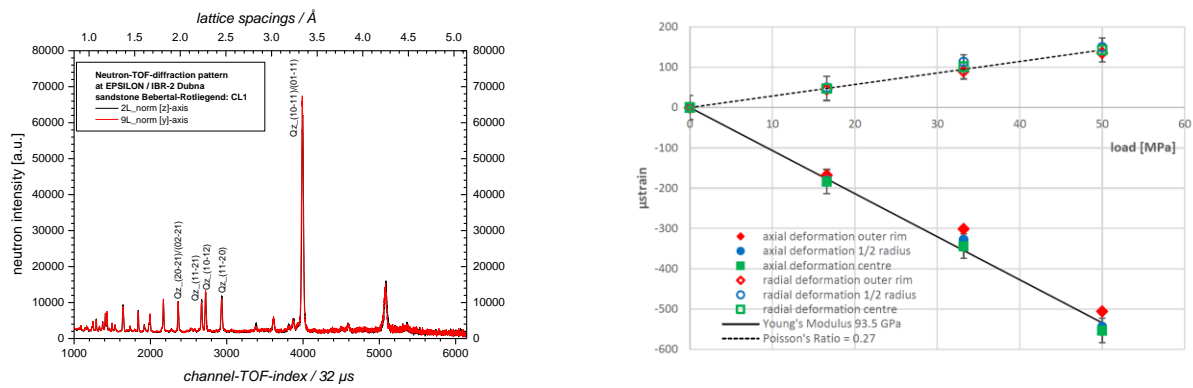
Fig. 1-I-18. Pole figures for eclogite rocks obtained with the SKAT diffractometer.

A new approach has been developed for a quantitative comparison of pole figures with the same crystallographic indexes, but measured for different samples. The approach is based on the consideration of the measured pole figures as specific implementations of a certain orientation distribution, i.e., as samples from a general ensemble of orientations. Thus, for the first time in the texture analysis a statistically valid measure for the quantitative comparison of pole figures has been introduced. This measure is the probability that the samples belong to the same orientation distribution and follows the statistics calculated within the Kolmogorov-Smirnov statistical test. The application of the introduced measure has been demonstrated on numerical examples for materials with cubic and hexagonal symmetry, as well as for real experimental data (pole figures of wheel steel). Also, using numerical examples, the peculiarities of the new approach have been demonstrated in comparison with the traditional calculation of the RP value when comparing pole figures [26].

The work has been done on the development of the methodology for evaluating the amount of residual austenite in high strength steels using the neutron diffraction method. The neutron diffraction spectra were measured on the texture instrument SKAT at FLNP JINR in order to eliminate the influence of the texture on the results. The measurements of calibration samples with the known austenite content were made. Using the results from the measurements of these samples, the calibration lines were obtained and applied to determine the fraction of residual austenite in the samples of medium-carbon steels (0.3 to 0.4%) with a tensile strength of 1500 MPa and 1700 MPa at different annealing temperatures (150 to 400°C) following the hardening treatment [27].

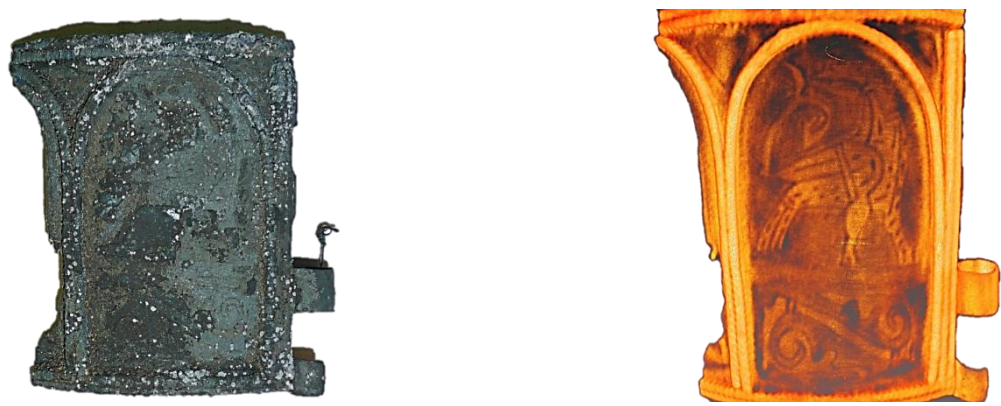
On the EPSILON diffractometer, *in-situ* experiments to study the dependence of deformation on the load on a cylindrical sample of sandstone have been carried out (**Fig. 1-I-19**). A load of up to 56.33 MPa was applied during 9 stages to determine the Young's modulus for the crystallographic planes of quartz (01-11), (10-11), (11-20), (01-12)/(10-12). These results are

consistent with the Hooke's law [28]. Instead of traditional fitting of diffraction data using the Rietveld method, an elastomechanical model has been developed to describe the stress-strain behavior, taking into account the changes in the pore space as a result of compaction of sediments associated with the change in the shape of quartz grains. This model was used to calculate the displacement of the diffraction peaks in the Voigt or Reuss approximations and their combinations. It has been established that the developed model can simulate with a high accuracy the diffraction data under load using the data measured without load including both the displacement of peaks and their half-width changes [29].



(a) (b)
Fig. 1-I-19. Neutron diffraction spectra of sandstone measured on the EPSILON diffractometer (a). Dependence of microstresses on the load at various deformation types (b).

In collaboration with the Institute of archaeology, RAS, the internal organization of a series of objects of cultural heritage (antique coins, bracelets, crosses, etc.) has been studied at the facility of neutron radiography and tomography. As an example, **Fig. 1-I-20** illustrates the results of the study of an ancient bracelet, XIV century AD, from a recently discovered treasure in the city of Tver. A corrosion-coated part of the bracelet was investigated. Neutron tomography revealed the bracelet decor items made by gold-on-copper plating. The differences in the interaction of neutrons with gold and copper made it possible to reveal a decorative pattern on the bracelet hidden under corrosion.

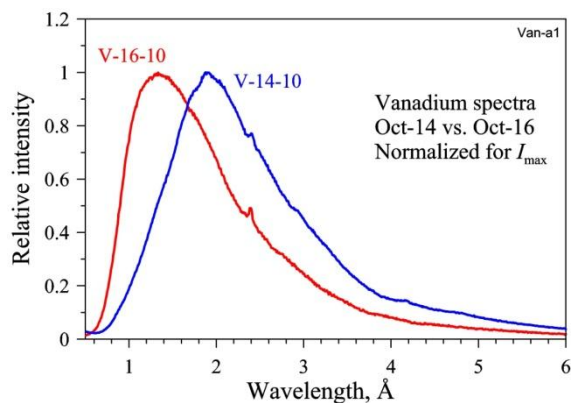


(a) (b)
Fig. 1-I-20. Photo of a fragment of the ancient bracelet from the treasure found in the city of Tver (a) and its 3D image reconstruction from neutron tomography data (b).

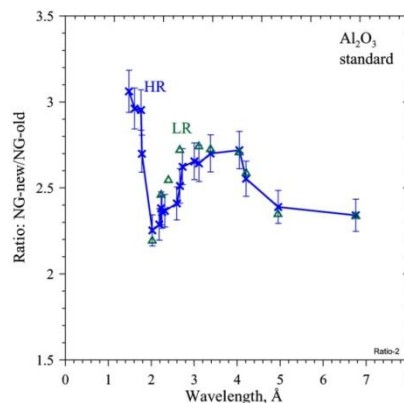
1. SCIENTIFIC RESEARCH

2. Methodological results

A new mirror neutron guide (designed and manufactured by SwissNeutronics, Switzerland) has been installed on the HRFD diffractometer. New mirror sections have been mounted in the available vacuum housing with the entrance (behind Fourier chopper) and exit (in front of sample position) points remaining unchanged (total length of 18.8 m). The neutron guide has been designed to be plane-parallel in the horizontal plane (window width 15 mm) and have a parabolic convergence in the vertical plane (heights of the entrance and exit windows are 200 mm and 100 mm, respectively). The Ni/Ti supermirror glass coating has a critical index $m = 1.75$. The qualitative comparison of the effective scattering spectra from vanadium for the old and new neutron guides has shown that the overall spectrum shape has changed insignificantly, but a considerable shift towards shorter wavelengths by $\approx 0.6 \text{ \AA}$ has occurred (**Fig. 1-I-21**). The gain factor for the neutron flux was determined from the ratio of the intensities of the diffraction peaks from a standard sample of Al_2O_3 (**Fig. 1-I-21**). It can be seen that in the wavelength range from 2 to 7 \AA its value varies from 2.2 to 2.7. At lower wavelengths, the new neutron guide gives even greater increase in the flux.



(a)



(b)

Fig. 1-I-21. Qualitative comparison of effective spectra for old (V-14-10) and new (V-16-10) neutron guides using scattering from vanadium (a). Gain factor for the flux for the new neutron guide determined by comparing intensities of diffraction peaks from a standard Al_2O_3 sample as a function of wavelength (b). Points measured from spectra of high (HR) and low (LR) resolution, i.e. using correlation analysis and without it, respectively.

On HRFD, the operation of a new Fourier chopper (**Fig. 1-I-22**) installed in August of 2016 to replace the old chopper has been started.

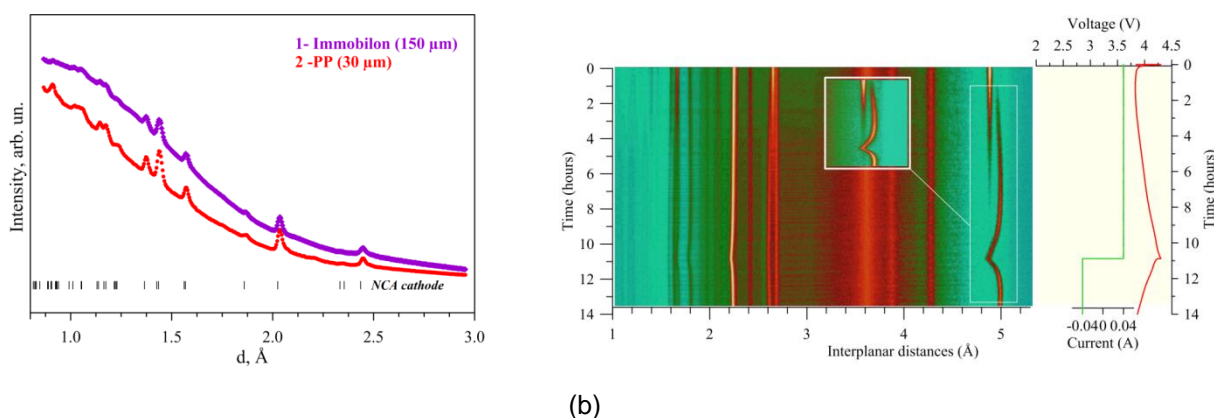


Fig. 1-I-22. New Fourier chopper in the working position.

1. SCIENTIFIC RESEARCH

The Fourier chopper has been mounted on a movable platform to move/remove the chopper into/from the beam. This option is required in *in-situ* experiments performed on the HRFD diffractometer and provides an additional double increase in the flux for the high intensity mode.

A series of *in-situ* and *in-operando* neutron diffraction experiments using specially designed electrochemical cells have been carried out to determine optimal (from the viewpoint of neutron scattering) auxiliary materials for model current sources. Basic requirements to the materials are minimum incoherent scattering, minimum neutron absorption, ease of use in the assembly of the cell, in-store availability. An optimal separator, electrolyte and anode material have been selected (**Fig. 1-I-23**). The paper on the results of the work is under preparation. The demand for this work is testified by an increasing number of applications for experiments at the RTD and HRFD instruments with the use of the developed electrochemical cells.



(a)

(b)

Fig. 1-I-23. Comparison of neutron scattering from electrochemical cells with PVDF Immobilon and usual polypropylene separators (a). Immobilon (despite partial replacement of hydrogen with fluorine) is worse than normal separator because of a larger amount of absorbed electrolyte and resulting incoherent scattering. The evolution of the diffraction spectra obtained with the electrochemical cell with conventional electrolyte and separator during the first "forming" cycle (b). As a cathode, $\text{Li}(\text{Ni}, \text{Co}, \text{Al})\text{O}_2$ was used, as an anode – lithium-7 isotope. The marked region of diffraction peak 003 from the cathode clearly illustrates the cathode activation process over the entire electrode volume: intensity of gradually disappearing peak (top down) is directly proportional to the amount of inactive cathode material. After cell (battery) charging the entire volume of the cathode material is electrochemically active.

In 2016, special cells for *in-operando* reflectometry experiments with electrochemical interfaces and a thermostatic cell with a temperature of up to 150°C were designed and successfully tested on the GRAINS instrument (**Fig. 1-I-24**).



(a)

(b)

(c)

Fig. 1-I-24. Special three-electrode electrochemical cell (a) and thermostatic (up to 150°C) cell (b) for neutron reflectometry; automatic mobile platform with polarizer (c).

1. SCIENTIFIC RESEARCH

An automatic mobile platform for the polarizer has been successfully put into operation at the GRAINS instrument for experiments with polarized neutrons.

Two new wide-aperture radial collimators (by JJ X-Ray, Denmark) have been installed at the FSD diffractometer, **Fig. 1-I-25**. To position the collimators, special tables that allow one to adjust the collimators in the scattered beam and to move/remove them into/from the beam if necessary, have been designed. The new radial collimators cover the entire angle range of $\pm 20^\circ$ in the scattering plane, thus allowing the use of all available elements of ASTRA detectors, which makes it possible to significantly increase the luminosity of experiments and perform measurements with thick samples.



(a)

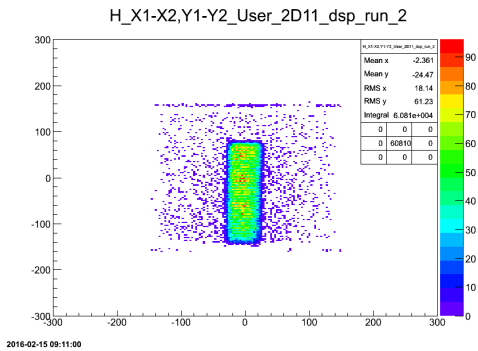
(b)

Fig. 1-I-25. New wide-aperture radial collimators for the FSD Fourier diffractometer, beamline 11A of the IBR-2 reactor (a). Bulk sample under study on the HUBER goniometer at FSD. Small scattering volume (gauge volume) within a sample is cut by the radial collimators mounted on special adjusting frames (b).

On FSD, work to improve algorithms on obtaining diffraction spectra from "raw" data has been continued. In the list mode, a program has been developed to filter detection events and provide the same method of pulse duration discrimination as that implemented in the electronics of the ASTRA detectors at FSD. In addition, two new experimental operation modes of the Fourier chopper at FSD (Dirichlet and Blackman frequency windows) have been introduced, which will allow one to explore different dynamic aspects in the operation of the Fourier chopper and improve its control system.

On beamline 13 of IBR-2, the activities on the creation of the FSS Fourier diffractometer have been continued in collaboration with the SC department (**Fig. 1-I-26**). In 2016, the components of the Ost and West detectors were delivered to the beamline. Modules of a Huber goniometer were mounted and adapted to the table of FSS. A Fourier-chopper was installed on a platform and underwent idle testing. Crates with the detector and acquisition electronics were put in place. The state of the mirror coating in a section of the FSS neutron guide was studied with the GRAINS reflectometer, which revealed a significant damage of the mirror coating and the necessity to replace the sections of the neutron guide in the immediate future. The calculations of the new geometry for the Ost detector, as well as the detector assembly and connection were performed. First test measurements with the Ost detector in the TOF-mode have been carried out and demonstrated the performance capability of all detector elements and the need for its further adjustment (selection of operating voltage, detection thresholds, etc.).

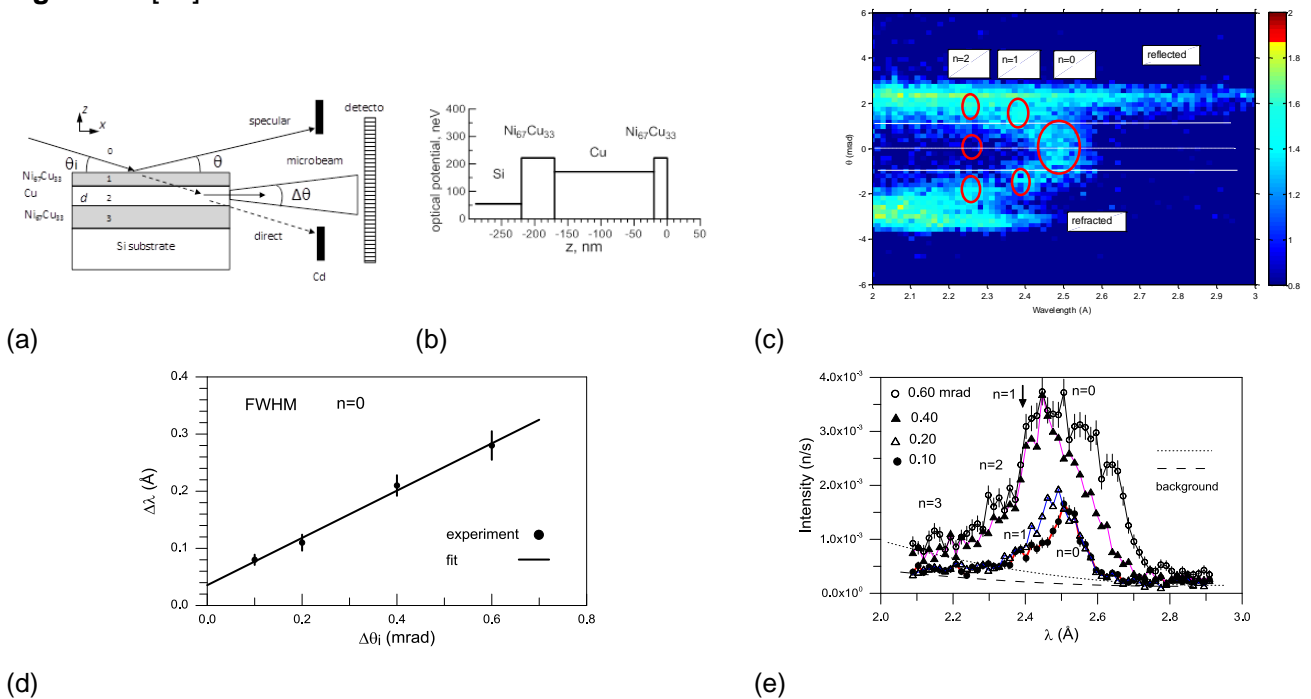
1. SCIENTIFIC RESEARCH



(a) (b)

Fig. 1-I-26. Neutron intensity distribution at the exit of the FSS mirror neutron guide measured by PSD detector (a). Detector Ost (without shielding) after installation and alignment of 12 PMTs with glued ^6Li glasses. At the sample position, modules of the HUBER goniometer are installed and adapted to the FSS table (b).

On the REMUR reflectometer, a spectral width of the microbeam emitted from the end of a flat waveguide has been investigated as a function of the angular divergence of the incident beam, **Fig. 1-I-27** [30].



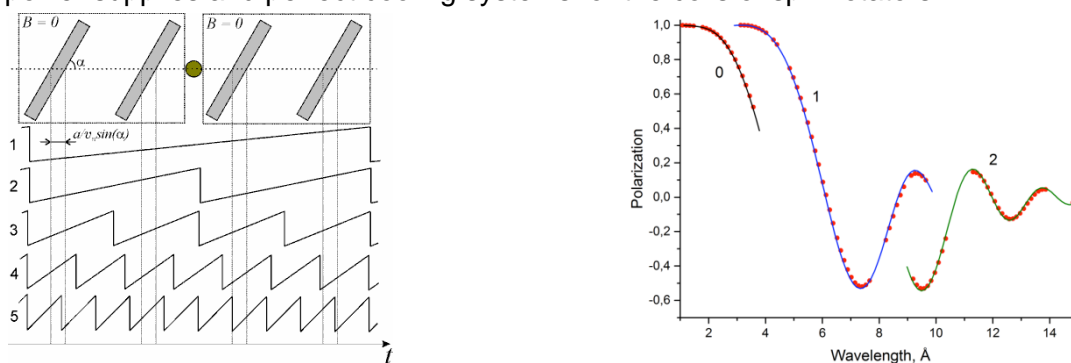
(a) (b) (c) (d) (e)

Fig. 1-I-27. Scheme of experiment (a). Neutron optical potential of sample depending on z-coordinate perpendicular to sample layers (b). 2D-dimensional neutron counting map depending on wavelength and scattering angle at fixed grazing angle of incident beam of 3.69 mrad. Ellipses show the maxima of transmitted microbeams for resonances of orders $n = 0, 1, 2$ (one, two and three maxima over scattering angle, respectively) (c). Microbeam wavelength resolution for resonance order $n = 0$ and its dependence on angular divergence of incident beam (points - experiment, vertical dashes - experimental errors). Solid line shows linear fit (d). Integral microbeam intensity around sample horizon depending on neutron wavelength at different angular divergence of incident beam: 0.60, 0.40, 0.20 and 0.10 mrad. Marked peaks correspond to resonance orders $n = 0, 1, 2, 3$ (e).

1. SCIENTIFIC RESEARCH

It has been shown that the spectral width of the microbeam decreases with diminishing angular divergence of the incident beam. By extrapolating the linear dependence in the zero divergence point of the initial beam and subtracting the reactor pulse duration, the spectral width of the resonance has been experimentally evaluated. The agreement of this value with the theoretical estimate testifies that the description of the resonance properties of the waveguide system is correct. The knowledge of the spectral width of the microbeam makes it possible to evaluate the wavelength resolution limit by probe microscopy. This method uses the Larmor precession of the spin of neutrons in the microbeam passing through the sample and scanning it with a high spatial resolution.

The study of the operating modes of the spin-echo small-angle (SESANS) spectrometer with linearly increasing magnetic fields which is under construction at beamline 9 of IBR-2, has been continued using Monte Carlo simulations (VITESS software package) with the parameters: distance between spin rotators in each arm – 60 cm, thickness of spin rotators $a = 2$ cm, period of sawtooth pulses $T = 1$ ms, pulse amplitude $B = 500$ Oe, inclination of spin rotators relative to the instrument axis $\alpha = 60^\circ$. The TOF spectrum had the wavelength range of 1-15 Å, and the polarization of the beam before entering the first arm of the setup was directed along the Z-axis and was 100% in the entire wavelength range. The scattering object was a set of homogeneous monodisperse spheres. To determine the working intervals in the spectrum $\Delta\lambda$ meeting the necessary criteria, the simulation of the polarization as a function of neutron wavelength $P_z(\lambda)$ was carried out in the absence of the sample. The working plateaus with the length $\Delta\lambda$ covering about 10 time-of-flight channels with 64 ms width are narrow but sufficient for measurements. To simulate the scattering curves, neutrons with wavelengths from the plateaus were used. Neutrons from different working intervals form different scattering curves corresponding to different operation modes of the instrument n (Fig. 1-I-28). The results of the simulation of the SESANS experiment in the VITESS package fully coincide with the analytical calculations, which confirms the correctness of the virtual instrument. This result means that the obtaining of data on the object under study in the considered method is related to the necessity to separately consider different parts of the scattering curves obtained in one measurement. Further technical development of the technique based on the possibility of the broadening of the field pulses under a constant time gradient can reduce the number of modes to two or even one. It is clear that this development will require more powerful power supplies and perfect cooling systems for the coils of spin rotators.



(a)

(b)

Fig. 1-I-28. Time diagram for neutrons of different velocities: one sawtooth field pulse covers neutron time of flight through all four spin rotators (1); only two spin rotators (2); only one spin rotator (3); only one spin rotator and few pulses for time of flight between rotators (4); neutron hits a jump in magnetic field as it passes through at least one spin rotator (a). SESANS signal obtained for scattering from spheres with radius of 100 Å. Scattering curves clearly show formation of three different dependences corresponding to different modes of setup operation. Solid lines – analytical calculations (b).

1. SCIENTIFIC RESEARCH

On the neutron radiography facility, a new two-mirror optical system of the detector has been designed to increase its radiation resistance (**Fig.1-I-29**). It has made it possible to reduce by several times the rate of radiation damages of the matrix in the CCD detector camera.

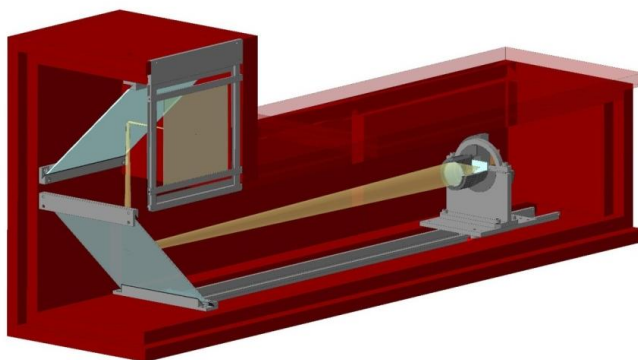


Fig. 1-I-29. Scheme of two-mirror optical system of the detector at the neutron radiography and tomography facility.

On the YuMO instrument, a new unit for thermostating samples has been installed and tested. It has been shown that the use of the new unit increased the sample temperature range up to 120°C. It has been found that the temperature gradients are lower than expected. The number of simultaneously loaded samples has been extended to 25 samples.

References

- [1] S.V.Ovsyannikov, M.Bykov, E.Bykova, D.P.Kozlenko, A.A.Tsirlin, A.E.Karkin, V.V.Shchennikov, S.E.Kichanov, H.Gou, A.M. Abakumov, R.Egoavil, J.Verbeeck, C.McCammon, V.Dyadkin, D.Chernyshov, S. van Smaalen, and L.S. Dubrovinsky "Charge ordering transition in iron oxide Fe_4O_5 , involving competing dimer and trimer formation", *Nature Chemistry*, v. 8, p. 501 (2016).
- [2] N.T.Dang, D.P.Kozlenko, T.L.Phan, S.E.Kichanov, L.H.Khiem, S.H.Jabarov, T.A.Tran, N.V.Dang, T.D.Thanh, D.B.Vo, B.N.Savenko "Structural Polymorphism of Mn-Doped BaTiO_3 " *Journal of Electronic Materials*, 45, 2477-2483 (2016).
- [3] D.P.Kozlenko, N.T.Dang, T.L.Phan, S.E.Kichanov, N.V.Dang, T.D.Thanh, L.H.Khiem, S.H.Jabarov, T.A.Tran, T.V.Manh, A.T.Le, B.N.Savenko "The Structural, Magnetic and Vibrational Properties of Ti-doped BaMnO_3 " *Journal of Alloys and Compounds*, accepted (2016).
- [4] A.M.Balagurov, I.A.Bobrikov, S.V.Sumnikov, V.Yu.Yushankhai, N.Mironova-Ulmane, Magnetostructural phase transitions in NiO and MnO: Neutron diffraction data, *JETP Lett.* 104 (2016) 88 - 93
- [5] S.Ya.Istomin, V.V.Chernova, E.V.Antipov, M.V.Lobanov, I.A.Bobrikov, V.Yu.Yushankhai, A.M.Balagurov, K.Y.Hsu, J.-Y.Lin, J.M.Chen, J.F.Lee, O.S.Volkova, A.N.Vasiliev "Wide range tuning of Mo oxidation state in $\text{La}_{1-x}\text{Sr}_x\text{Fe}_{2/3}\text{Mo}_{1/3}\text{O}_3$ perovskites" *European Journal of Inorganic Chemistry*, v. 2016 (18), pp. 2942–2951 (2016).
- [6] A.M.Balagurov, I.A.Bobrikov, B.Mukhametuly, S.V.Sumnikov, I.S.Golovin, Coherent cluster atomic ordering in the Fe-27Al intermetallic compound, *JETP Lett.* 104 (2016) 539–545.
- [7] M.Kubovcikova, Gapon I.V., Zavisova V., Koneracka M., Petrenko V.I., Soltwedel O., Almasy L., Avdeev M.V., Kopcansky P. On the adsorption properties of magnetic fluids: impact of bulk structure. *JMMM*, 2016, in press.
- [8] A.V.Nagorny, Petrenko V.I., Avdeev M.V., Yelenich O.V., Solopan S.O., Belous A.G., Gruzinov A.Yu., Ivankov O.I., Bulavin L.A. Structural aspects of magnetic fluid stabilization in aqueous agarose solutions. *JMMM*, 2016, in press.
- [9] J.Majorosova, V.I.Petrenko, Siposova K., Timko M., Tomasovicova N., Garamus V.M., Koralewski M., Avdeev M.V., Leszczynski B., Jurga S., Gazova Z., Hayryan Sh., Hu Chin-Kun, Kopcansky P. On the adsorption of magnetite nanoparticles on lysozyme amyloid fibrils. *Colloids Surf. B*, 2016, V. 146, pp. 794–800.
- [10] V.Gdovinova, Tomasovicova N., Batko I., Batkova M., Balejcikova L., Garamus V.M., Petrenko V.I.,

1. SCIENTIFIC RESEARCH

Avdeev M.V., Kopcansky P. Interaction of magnetic nanoparticles with lysozyme amyloid fibrils. JMMM, 2016, in press.

[11] Petrenko V.I., Avdeev M.V., Bulavin L.A., Almasy L., Grigoryeva N.A., Aksenov V.L. Effect of surfactants excess on the stability of low-polarity ferrofluids probed by small-angle neutron scattering. Crystallography reports, 2016, V. 61, Issue 1, pp. 121-125

[12] Yu.I.Prylutsky, Cherepanov V.V., Kostjukov V.V., Evstigneev M.P., Kyzyma O.A., Bulavin L.A., Ivankov O., Davidenko N.A. and Ritter U. Study of the complexation between Landomycin A and C60 fullerene in aqueous solution. RSC Adv., 2016, V. 6, pp. 81231-81236.

[13] S.Prylutska, Panchuk R., Gołuński G., Skivka L., Prylutsky Yu., Hurmach V., Skorokhyd N., Borowik A., Woziwodzka A., Piosik J., Kyzyma O., Haramus V., Bulavin L., Evstigneev M., Buchelnikov A., Stoika R., Berger W., Ritter U., Scharff P. C60 fullerene enhances cisplatin anticancer activity and overcomes tumor cells drug resistance. Nano Res., 2016, accepted.

[14] M.V.Avdeev, Tomchuk O.V., Ivankov O.I., Alexenskii A.E., Dideikin A.T., Vul' A.Ya. On the structure of concentrated detonation nanodiamond hydrosols with a positive ζ potential: analysis of small-angle neutron scattering. Chemical Physics Letters, 2016, V. 658, P. 58-62.

[15] M.V.Avdeev, Rulev A.A., Bodnarchuk V.I., Ushakova E.E., Petrenko V.I., Gapon I.V., Tomchuk O.V., Matveev V.A., Pleshanov N.K., Kataev E.Yu., Yashina L.V., Itkis D.M. Monitoring of Lithium Plating by Neutron Reflectometry. Applied Surface Science, 2016, accepted.

[16] I.M.Byvshev, Vangeli, I. M., Murugova, T. N., Ivankov, O. O., Kuklin, A. I., Popov, V. I., Yaguzhinsky, L. S. On the existence of two states of OXPPOS system supercomplex in heart mitochondria. Biochimica et Biophysica Acta - Bioenergetics, 1857, e35-e36 (2016).

[17] M.Zhernenkov, D.Bolmatov, D.Soloviov, K.Zhernenkov, B.P.Toperverg, A.Cunsolo, A.Bosak & Y.Q.Cai. Revealing the mechanism of passive transport in lipid bilayers via phonon-mediated nanometre-scale density fluctuations. Nature Communications, 7, 1-9 (2016).

[18] D.Lombardo, P.Calandra, D.Barreca, S.Magazu, M.A.Kiselev. Soft Interaction in Liposome Nanocarriers for Therapeutic Drug Delivery. Nanomaterials 6, 125 (2016).

[19] N.Kučerka, Dushanov E., Kholmurodov Kh., Katsaras J., Uhríková D. Cation-containing lipid membranes – experiment and MD simulations. European Pharmaceutical Journal, 2016, accepted.

[20] M.Ordon, Yu.Gorshkova, M.Ossowska-Chruściel. Lithocholic acid derivative in the dimethyl sulfoxide presence: Morphology and phase transitions, Thermochemica Acta 643 (2016) 1–12.

[21] Y.V.Kulvelis, et al., Structure and properties optimization of perfluorinated short side chain membranes for hydrogen fuel cells using orientation stretching. RSC Advances, 6, 108864–108875 (2016).

[22] L.Bulavin, Kutsevol, N., Chumachenko, V., Soloviov, D., Kuklin, A., & Marynin, A. (2016). SAXS Combined with UV-vis Spectroscopy and QELS: Accurate Characterization of Silver Sols Synthesized in Polymer Matrices. Nanoscale research letters, 11(1), 1-8 (2016).

[23] T.V.Tropin, J.W.P.Schmelzer, V.L.Aksenov. Modern aspects of the kinetic theory of glass transition. Physics – Uspekhi, 59 (1) pp.42-66 (2016).

[24] Ł.Hetmańczyk, D.Chudoba, A.Filarowski et al. To the question of conformational equilibrium and polymorph's states in the solid state and under the matrix condition. J. Chem. Phys., submitted (2016).

[25] R.Keppler, Stipp, M., Behrmann, J.H., Ullemeyer, K. & Heidelbach, F. Deformation inside a paleosubduction channel – Insights from microstructures and crystallographic preferred orientations of eclogites and metasediments from the Tauern Window, Austria. J. Struct. Geol. 82, 60-79 (2016).

[26] T.Lychagina, & Nikolayev, D. Quantitative comparison of the measured crystallographic textures. J. Appl. Cryst. 49 (4), 1290-1299 (2016).

[27] D.Nikolayev, & Lychagina, T., Zisman, A.A. & Yashina, E. Directly verifiable neutron diffraction technique to determine retained austenite in steel. Materials Science and Engineering A., submitted (2016).

[28] Ch.Scheffzük, Müller, B.I.R., Breuer, S., Altangerel B. & Schilling, F.R. Applied Strain Investigation on Sandstone Samples Using Neutron Time-of-Flight Diffraction at the Strain Diffractometer EPSILON, IBR-2M Dubna. Mongolian J. Physics, submitted (2016).

[29] S.Breuer, Schilling, F.R., Scheffzük, Ch. & Müller, B.I.R. Forward Modeling Neutron Time-of-Flight Diffraction Data for Uniaxial Load Conditions by Using the Example of Sandstone. J. Appl. Cryst., submitted (2016).

[30] S.V.Kozhevnikov, V.K.Ignatovich, F.Radu, Neutron resonances in planar waveguides, JETP, 123 (6) (2016) 950-956.

II. MULTIMODAL PLATFORM FOR RAMAN AND NONLINEAR OPTICAL MICROSCOPY AND MICROSPECTROSCOPY FOR CONDENSED MATTER STUDIES

In 2016, the research activities of the Raman Spectroscopy Sector were focused mainly on accomplishing the following objectives:

- highly sensitive, contrast, and, most notably, noninvasive imaging of biological samples using Raman scattering microscopy and nonlinear optics methods (CARS, SHG);
- further increase in the concentration sensitivity limit of sample measurements by the SERS method at a level no worse than 10^{-10} M;
- acquisition of new data on photo- and upconversion luminescence in glass-ceramics based on nanosized ZnO crystals doped with rare-earth elements.

In addition, methodological studies aimed at further upgrading and modification of the CARS microscope were carried out during the period under review.

The Sector was also very active within the JINR Educational Programme in engaging students, postgraduates, and young scientists from the JINR Member States in its research for different periods of time.

1. Further modified “CARS” microscope

Figure 1-II-1 shows an optical diagram of the CARS microscope modified in 2016. To allow complementary imaging of the samples under investigation using not only nonlinear CARS microscopy but also the second harmonic generation (SHG), the corresponding narrow-band filters (532 nm Maxline) were added to the optical train, and sample excitation for generation of the second harmonic in it was performed with the Stokes frequency of a picosecond cw laser.

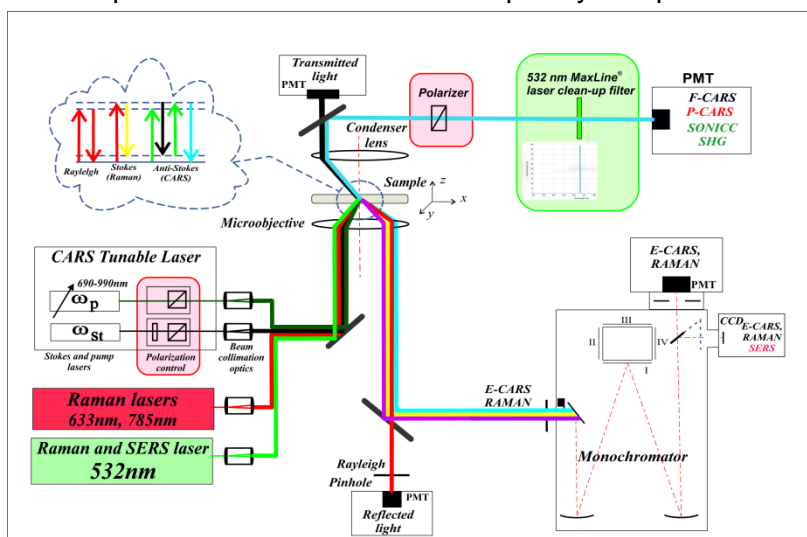


Fig. 1-II-1. Diagram of the modified “CARS” microscope: two new options are introduced.

In addition, an option was developed and installed, which allows the Raman scattering to be measured on samples excited at a wavelength of 785 nm, which is very important when working with samples with high autofluorescence background.

1. SCIENTIFIC RESEARCH

Using this optical platform, samples can be imaged by utilizing vibrational frequencies in the spectral range of $(1000\text{--}3580)\text{ cm}^{-1}$, which covers all most important vibrational modes of biomolecules. Five detection channels allow two forward- and three backward- propagated signals to be recorded. The polarization control is adjustable with a half-wave plate in the Stokes beam.

2. Scientific results

2.1. Highly Sensitive Coherent anti-Stokes Raman Scattering Imaging of Protein Crystals

In the reporting period, the work (started in 2015) on highly sensitive and high-speed visualization of protein crystals using the polarized coherent anti-Stokes Raman scattering (P-CARS) and the second harmonic generation (SHG) was completed.

It is well known that serial crystallography at last generation X-ray synchrotron sources and free electron lasers have enabled data collection with micrometer and even sub-micrometer size crystals resulting in amazing progress in structural biology. However, imaging of small crystals which although is highly demanded remains a challenge, especially in the case of membrane protein crystals.

CARS microscopy provides an advanced nondestructive and label-free technique with high sensitivity and high lateral spatial resolution capable of selective chemical imaging of major types of macromolecules: proteins, lipids, nucleic acids, etc.

Along with the P-CARS modality, in 2016 we developed a nonlinear imaging technique based on SONICC (Second Order Nonlinear Imaging of Chiral Crystals) technology for identifying chiral crystals, which relies on SHG (Second Harmonic Generation) and UV-TPEF (Ultraviolet Two Photon Excited Fluorescence) techniques. SONICC makes it easy to visualize microcrystals, including also optically-obscured crystals buried in meso matrix. Nevertheless, the technique fails when there are salt crystals in the probe and/or protein crystals with high symmetry classes. In the latter case the crystals will generate poorly detectable SHG signal scattering. In addition, at the moment there is no sufficiently cheap option of an SHG device for crystal imaging, therefore a search for new complementary approaches to crystals' studies and imaging might be very important.

The obtained main results are illustrated in **Fig. 1-II-2**.

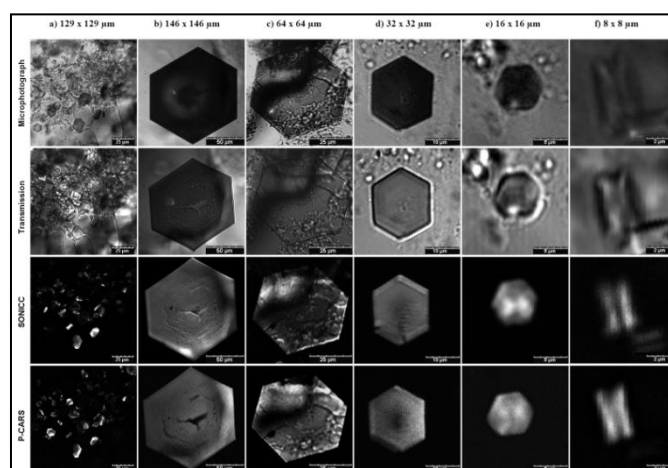


Fig. 1-II-2. Gallery of micrograph, transmission, SHG (SONICC) and P-CARS images of bR crystals acquired in various modes: (a) panoramic picture of a crystallization probe, (b, c) big crystals, (d) intermediate size crystals, (e and f) very small crystals.

Also, we observed that in the case of some crystals (**Fig. 1-II-3**) the shape and/or size of the same crystals imaged by CARS and SHG are different. We suggest that it happens when some parts of the crystals are not well ordered. It is known that an SHG signal is strong only when the crystal is well ordered. It is of interest because a complementary use of both methods can provide information about the level of order in crystal packing and help to select crystals preliminarily for X-ray crystallography. It can be very useful because quite often the crystals may have a perfect shape but do not diffract at all.

Amazing sensitivity of the P-CARS imaging is further demonstrated by the detection and imaging of merohedrally twinned bR crystals (**Fig. 1-II-3**). Merohedral twinning is one of the most common crystal-growth defects. There is neither a fast approach to the detection of twinned crystals nor an efficient method to determine the twinning ratio. Twinned crystals cannot be optically distinguished. The only reliable method to detect crystal twinning is X-ray crystallography, which requires time-consuming X-ray data collection. In our work, we studied the potential of CARS for the detection of such crystals.

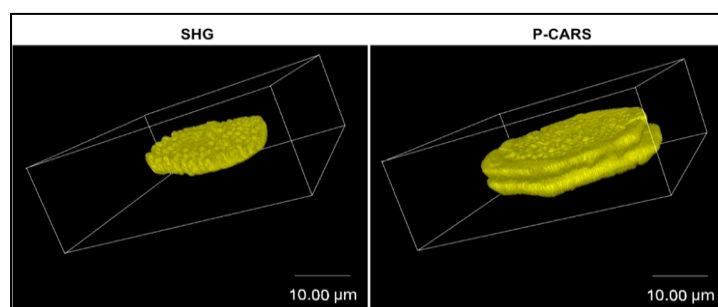


Fig. 1-II-3. 3D SHG and 3D P-CARS images of a twinned bR crystal.
Box size: 48×48×24 μm. Images were obtained with 6 ps laser.

Figure 1-II-3 demonstrates that the twinning of bR can be easily detected even in the case of small crystals with a micrometer size thickness, whereas an SHG signal with 6-ps excitation hardly discriminates the morphology of the twinned crystal if it partly consists of low-ordered segments. In contrast to X-ray crystallography, CARS makes the characterization of their morphology possible and demonstrates that the crystal consists of two nearly equal domains with a thickness of about 2.5 μm.

Thus, CARS, especially P-CARS, can be successfully applied for fast, high-resolution, high-contrast and very informative imaging of protein crystals. The CARS and SHG images are composed of 500 × 500 pixels taken by raster scanning the sample. Signal integration time was 3 μs/pixel.

The research was performed in close cooperation with Russian, French, and Belarusian scientists. All the experimental work on Raman imaging of the samples was done using the CARS microscope.

2.2. Detection of biomolecules by SERS spectroscopy

During the period under review considerable advances have been made in SERS research. In particular, the concentration sensitivity limit at a level of 10^{-10} M has been obtained for DNA molecules. It is 2–3 orders of magnitude better than in 2015.

The research was carried out with SERS-active substrates developed in Belarus on the basis of porous silicon and silver nanoparticles. Porous silicon was fabricated by electrochemical

1. SCIENTIFIC RESEARCH

anodic etching of a highly doped n-type silicon wafer. It has been found that silvered porous silicon is SERS active in relation to herring sperm DNA under the excitation at 473, 633 and 785 nm (**Fig. 1-II-4**). Laser powers were 1.45, 0.68, and 0.86 mW, respectively.

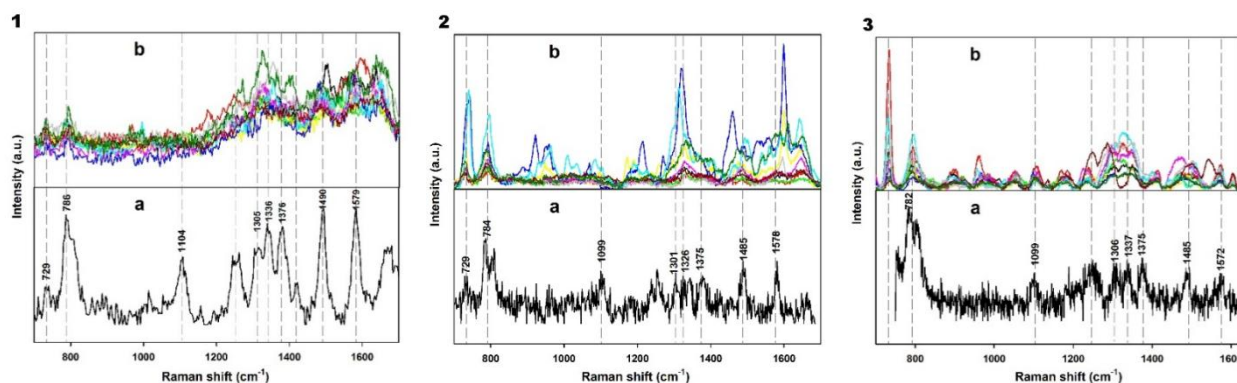


Fig. 1-II-4. Raman (a) and SERS (b) spectra of 10–8-M herring sperm DNA collected at excitation wavelengths of 473 (1), 633 (2) and 785 (3) nm.

The peaks observed in the Raman spectra around 730 cm^{-1} (adenine), 787 cm^{-1} (thymine, cytosine), 1104 cm^{-1} ($\nu(\text{C-O})$, deoxyribose-phosphate), 1242 cm^{-1} (cytosine, adenine), 1381 cm^{-1} (thymine, guanine, гуанин, adenine), 1490 cm^{-1} (guanine, adenine) and 1581 cm^{-1} (guanine, adenine) are the characteristic Raman bands of the herring sperm DNA molecules. SERS spectra were collected in 10 random points of the silvered porous silicon substrate. Remarkably the silvered PS demonstrates SERS activity for all three lasers.

The following SERS mapping of the substrates allowed us to detect identifiable SERS spectra of the herring sperm DNA collected under each laser excitation (**Fig. 1-II-5A**).

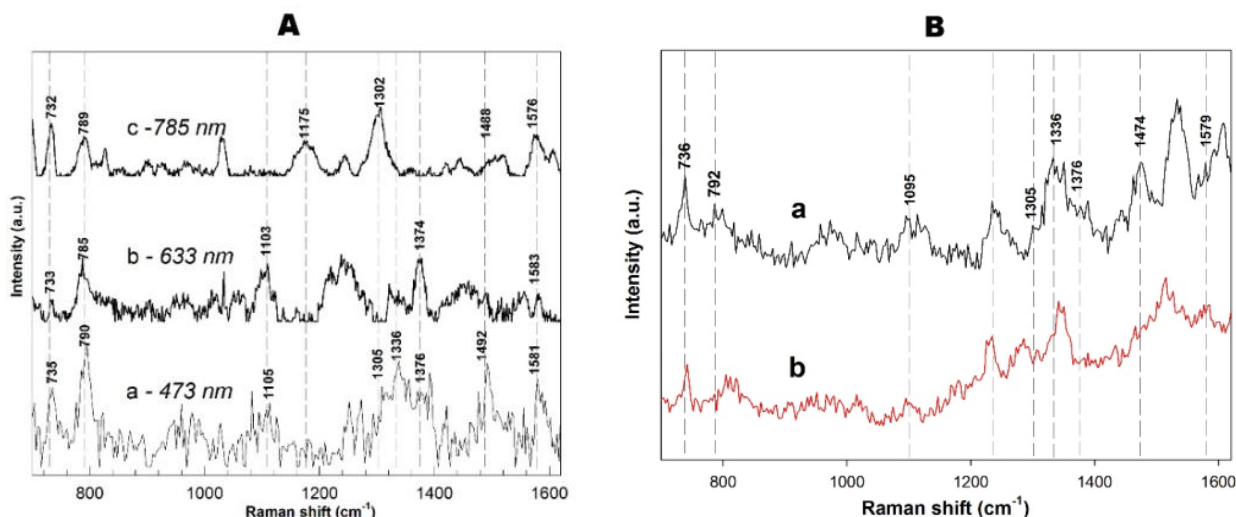


Fig. 1-II-5. (A) SERS spectra of the 10–8M herring sperm DNA adsorbed on the surface of the silvered PS collected at excitation wavelengths of 473, 633 and 785 nm. (B) SERS spectra of the 10–8M (a) and 10–10M (b) herring sperm DNA adsorbed on the surface of the silvered PS. The spectra were collected at an excitation wavelength of 473 nm.

Finally, the SERS mapping was used to detect the herring sperm DNA at an extremely low concentration of 10^{-10} M . In **Fig. 1-II-5B** the comparison of two SERS spectra of the DNA

1. SCIENTIFIC RESEARCH

molecules at different concentrations is presented. The SERS spectra were recorded at an excitation wavelength of 473 nm since both red and near-IR lasers showed no results for the lowest concentration.

The results of these studies suggest that the classical spectra of DNA molecules can be found by the SERS substrate mapping. Moreover, the prospects for the DNA detection by the SERS spectroscopy with lasers of 473, 633, and 785 nm wavelengths are very encouraging. To our knowledge, the detection of such a small amount of DNA has not been reported previously.

2.3. Photo- and upconversion luminescence of transparent glass-ceramics based on ZnO nanocrystals activated with rare earth elements.

In 2016, new impressive results were obtained in the sphere of photo- and upconversion luminescence activities. As phosphor we employed transparent zincite (ZnO) glass-ceramics obtained from the initial glass matrices by secondary heat treatment at 680-860°C. The average crystal size obtained from the X-ray diffraction data was found to be in the range between 14 and 35 nm (Fig. 1-II-6).

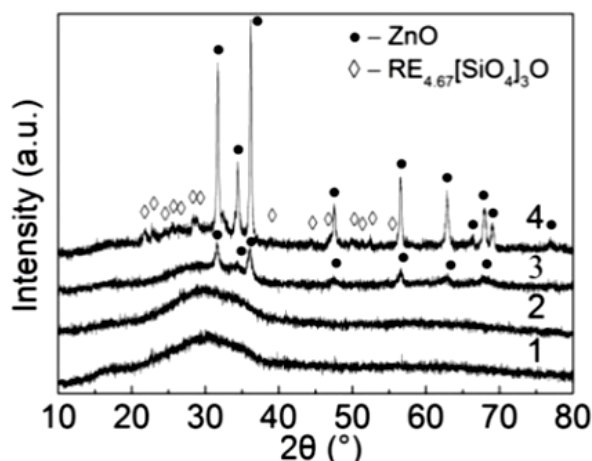


Fig. 1-II-6. XRD patterns of the initial glass co-doped with 1 mol% Eu_2O_3 and 1.5 mol% Yb_2O_3 (1), initial glass co-doped with 1 mol% Eu_2O_3 and 1 mol% Yb_2O_3 (2) and GC doped with 1 mol% Eu_2O_3 and 1 mol% Yb_2O_3 and heat-treated at 680°C for 12 h (3) and at 860°C for 2 h (4).

The luminescence properties of the glass and glass-ceramics were studied by measuring their excitation and emission spectra at 300, 78, and 4.2 K. The results are presented in Fig. 1-II-7 (1,2,3). Strong red emission of Eu^{3+} ions dominated by the $^5\text{D}_0$ - $^7\text{F}_2$ (612 nm) electric dipole transition was detected. Changes in the luminescence properties of the Eu^{3+} -related excitation and emission bands were observed after heat treatment at 680°C and 860°C. The ZnO nanocrystals showed both broad luminescence (400-850 nm) and free-exciton emission near 3.3 eV at room temperature.

1. SCIENTIFIC RESEARCH

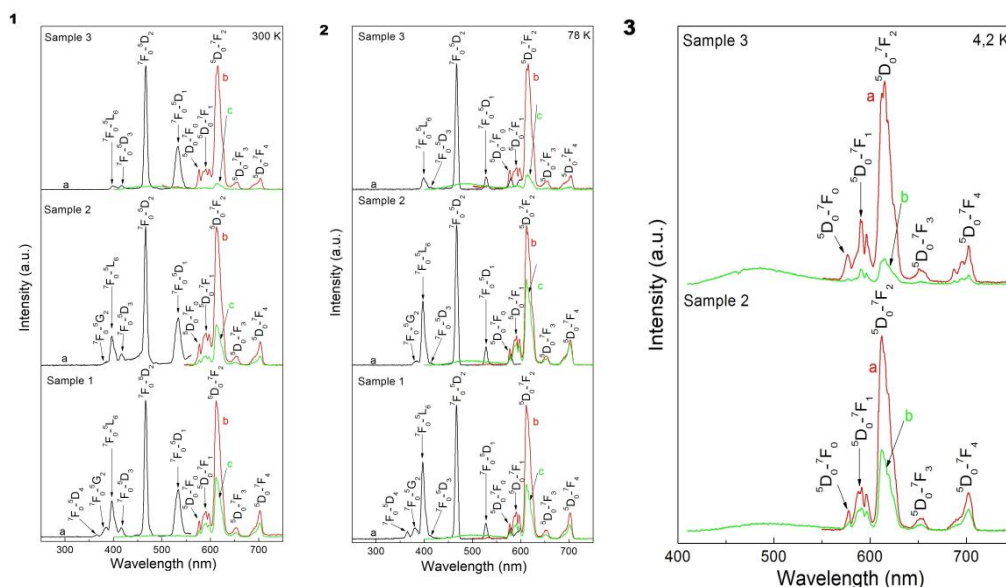


Fig. 1-II-7. (1) Normalized luminescence excitation spectra (a) and luminescence spectra for glass and GC recorded for excitation wavelengths of $\lambda_{ex} \sim 467$ nm (b) and $\lambda_{ex} \sim 397$ nm (c) at room temperature. **(2)** Normalized luminescence excitation spectra (a) and luminescence spectra for glass and GC recorded for excitation wavelengths of $\lambda_{ex} \sim 467$ nm (b) and $\lambda_{ex} \sim 397$ nm (c) at liquid nitrogen temperature. **(3)** Luminescence spectra for GC recorded for excitation wavelengths of $\lambda_{ex} \sim 467$ nm (a) and $\lambda_{ex} \sim 397$ nm (b) at liquid helium temperature.

The upconversion luminescence spectrum of the initial glass was obtained under excitation of a 976-nm laser source. A simplified energy level diagram for $\text{Eu}^{3+}/\text{Yb}^{3+}$ ions and corresponding UCL spectrum are demonstrated in **Fig. 1-II-8 (a,b)**, respectively. The CIE color coordinates corresponding to the UCL of the sample under investigation are estimated to be $(x=0.59, y=0.34)$. They are located in the orange-reddish region (**Fig. 1-II-8 (c)**).

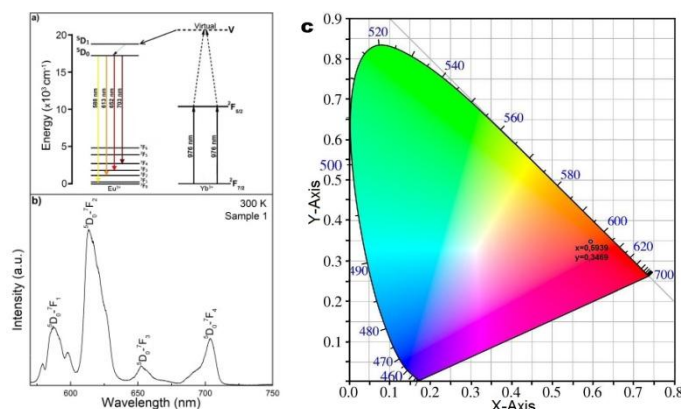
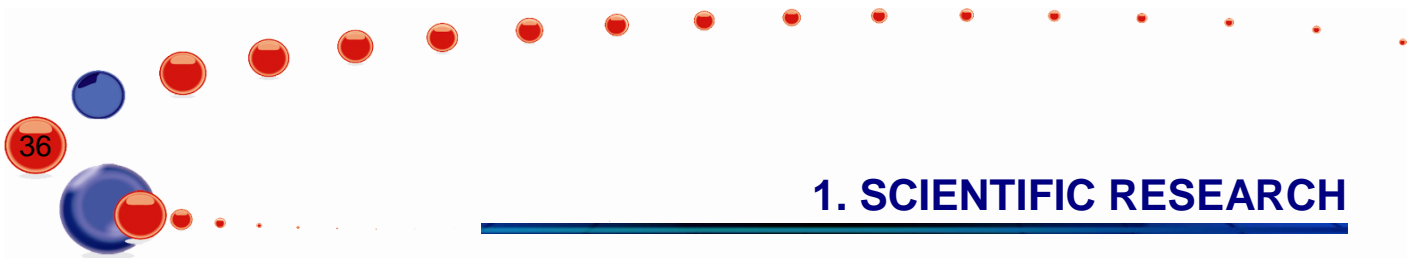


Fig. 1-II-8. Schematic energy level diagram of $\text{Eu}^{3+}/\text{Yb}^{3+}$ ions (a) and UCL spectrum of sample 1 recorded at room temperature under 976 nm laser excitation (b), CIE diagram of Eu^{3+} , Yb^{3+} co-doped initial glass (c).

Thus, in transparent glass-ceramics from the potassium-zinc-aluminum-silicate system co-doped with rare-earth ions (europium, ytterbium) and containing ZnO nanocrystals, strong red (~ 612 nm) luminescence in the visible region from intracenter transitions on Eu^{3+} ions and ultraviolet exciton luminescence (~ 380 nm) from ZnO crystals have been simultaneously observed



1. SCIENTIFIC RESEARCH

for the first time. Luminescence from triply charged europium ions has never been studied for this type of glass-ceramics.

3.0. Guest seminar

On October 16, 2016 a head of FLNP sector of Raman spectroscopy G.M.Arzumanyan gave a guest seminar at the A.M.Prokhorov General Physics Institute of the Russian Academy of Sciences (GPI RAS) in Moscow. The aim of his report was to familiarize the participants with a multimodal optical platform at JINR allowing one to conduct investigations in the field of spontaneous and stimulated Raman scattering, as well as with the first joint unique results on coherent surface-enhanced Raman scattering. A monolayer of molecules of 3,3'-dithiobis (6-nitrobenzoic acid, DTNB) adsorbed onto the surface of a dielectric metamaterial with gold nanoparticles immobilized on a nanostructured faceted surface of cerium dioxide film was used as a model sample. The Raman shift at 1344 cm^{-1} which is characteristic of the sample was used for surface-enhanced coherent mapping of the signal intensity with high contrast and high spatial resolution. The unique technique of registration of such signals has been developed at JINR (Dubna) in close cooperation with GPI RAS, ITAE RAS, MSU and IBCP RAS.

In the final discussion it was noted that the optical platform based on the "CARS" microscope at JINR can be considered as one of the best instruments in Russia for high-contrast and high-sensitive research in the field of Raman spectroscopy and microscopy.

1. SCIENTIFIC RESEARCH

III. NEUTRON NUCLEAR PHYSICS

In 2016, in FLNP the scientific activity in the field of neutron nuclear physics was carried out in the following traditional directions: investigations of time and space parity violation processes in neutron-nuclear interactions; studies of the fission process; experimental and theoretical investigations of fundamental properties of the neutron; gamma-spectroscopy of neutron-nuclear interactions; atomic nuclear structure, obtaining of new data for reactor applications and nuclear astrophysics; experiments with ultracold neutrons, applied research using NAA. The scientific program to study the inelastic scattering of fast neutrons made into a separate project "TANGRA" was successfully implemented. A number of investigations in the field of fundamental physics and ultracold neutron physics were performed on the neutron beams of nuclear research centers in Germany, China, USA, France, Switzerland.

1. Experimental and methodological investigations

1.1. Investigation of the mechanism of fragment excitation and prompt neutron emission and gamma-ray cascades by simultaneous spectroscopy of fission fragments, neutrons and gamma-rays.

Spontaneous fission and fission induced by thermal and resonance neutrons are classical examples of low-energy fission, which occurs either at zero excitation energy of the fissioning nucleus or at excitation energies close to the fission barrier. Nuclear fission is a consequence of the collective motion of nucleons, which can be considered as a deformation of the surface of a nuclear liquid drop consisting of nucleons interacting via Coulomb and nuclear forces. The Strutinsky shell correction to the classical nuclear fission liquid-drop model has made it possible to create an effective calculation model of the multimodal (MM) fission. One of the most popular versions of these models parameterizes the changing (with increasing deformation) shape of a fissioning nucleus by quasi-spheroids connected by a rather thick neck at the prescission stage. The trajectories in the multidimensional deformation space are selected by minimizing the deformation energy of the fissioning system calculated by the specified method. Moreover, the shape symmetry of the fissioning system can change in the so-called trajectory bifurcation points. It should be noted that during the evolution, the fissioning nucleus overcomes the first barrier having a shape of a symmetrical "dumbbell", but to overcome the second barrier the configuration can be both symmetrical and asymmetrical. Along with it, energetically favorable configurations are those from a particular set of prescission shapes that determine the properties of fission modes (FM). A random neck rupture (RNR) leads to the separation of fission fragments because of the Coulomb repulsion. The primary fission fragments formed after the neck rupture are relatively "cold" and highly deformed. After the deformation energy is transformed to the core heating, prompt fission neutrons (PFN) are emitted.

The number of PFN, $\bar{\nu}(A, TKE)$, emitted by FF with the mass number A and the total kinetic energy TKE is directly related to the FF excitation spectrum. The measurement of the function $\bar{\nu}(A, TKE)$ allows one to obtain the characteristics of PFN averaged over A or TKE by integrating over the corresponding variable if the mass-energy distribution (MED) of FF – $Y(A, TKE)$ is known. The examples of these averages together with the MED calibration are given below:

$$\bar{\nu}(A) = \frac{\int_0^{\infty} \bar{\nu}(A, TKE) Y(A, TKE) dTKE}{\int_0^{\infty} Y(A, TKE) dTKE}, \quad \bar{\nu} = \frac{\int_0^{\infty} \bar{\nu}(A, TKE) Y(A, TKE) dTKE dA}{\int_0^{\infty} Y(A, TKE) dTKE dA}, \quad 200 = \int_0^{\infty} Y(A, TKE) dTKE dA \quad (1).$$

1. SCIENTIFIC RESEARCH

Thus, the experimentally measured multiplicity of PFN is a superposition of distributions $\bar{\nu}_i(A)$ of various FM with a realization probability p_i :

$$\bar{\nu}(A) = \frac{\sum_{i=1}^N p_i Y_i(A) \bar{\nu}_i(A)}{\sum_{A=0}^{A_{\text{CN}}} p_i Y_i(A)} \quad (2).$$

The experimental data analysis on the measurement of PFN allows one to obtain the following formula:

$$\bar{\nu}(A, TKE) = \left\{ \frac{\partial \bar{\nu}}{\partial TKE}(A) [TKE_{\text{max}} - TKE(A)], \text{ if } TKE < TKE_{\text{max}} \right\} \quad (3).$$

During 2013-2016 the data obtained in the experiments at the EC-JRC-IRMM Institute (Belgium) on the PNF emission in spontaneous fissions of ^{252}Cf were analyzed. As a result, the errors in the data analysis were identified and eliminated, which made it possible to explain the discrepancies in the results of the experiments with high and low neutron detection efficiency. In addition, a setup has been designed to study the prompt neutron emission and gamma-ray cascades for the fragments with defined masses in coincidence with PFN in the resonance neutron induced fission of ^{235}U . It consists of a double ionization chamber with Frisch grids, an NE-213-scintillator-based fast neutron detector, a pair of gamma-ray NaI-based scintillation detectors (**Fig. 1-III-1**).

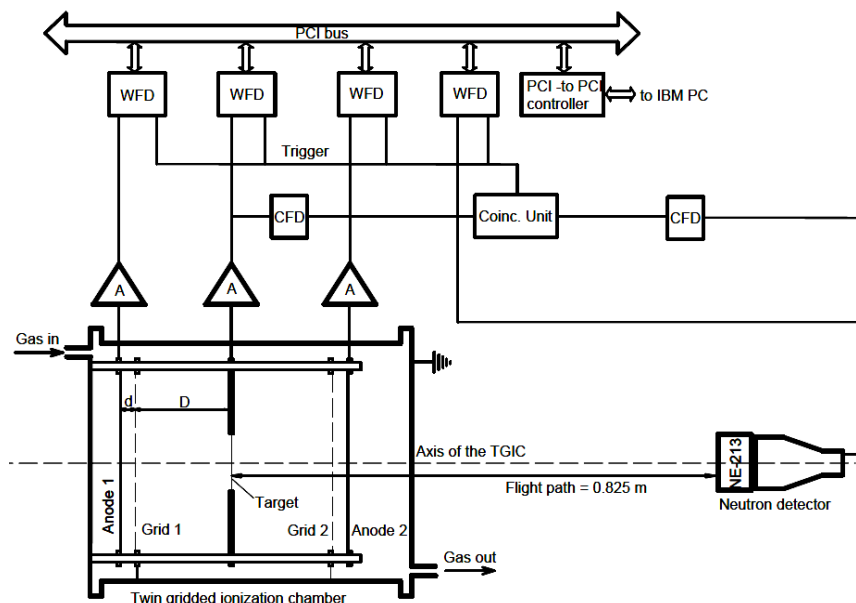


Fig. 1-III-1. Schematic of the experimental setup. Gamma-detectors are not shown.

The data acquisition system was implemented on the basis of an eight-channel system of synchronized pulse digitizers with a sampling rate of 250 MHz and amplitude resolution of 12 bits. The calibration experiments were carried out in the period from December 2015 to March 2016 on the IBR-2 thermal neutron beamline. At present, the data analysis and the setup upgrade involving the replacement of two NaI detectors with high-purity germanium detectors are in progress. Some results are presented in **Fig. 1-III-2, 1-III-3, 1-III-4**.

1. SCIENTIFIC RESEARCH

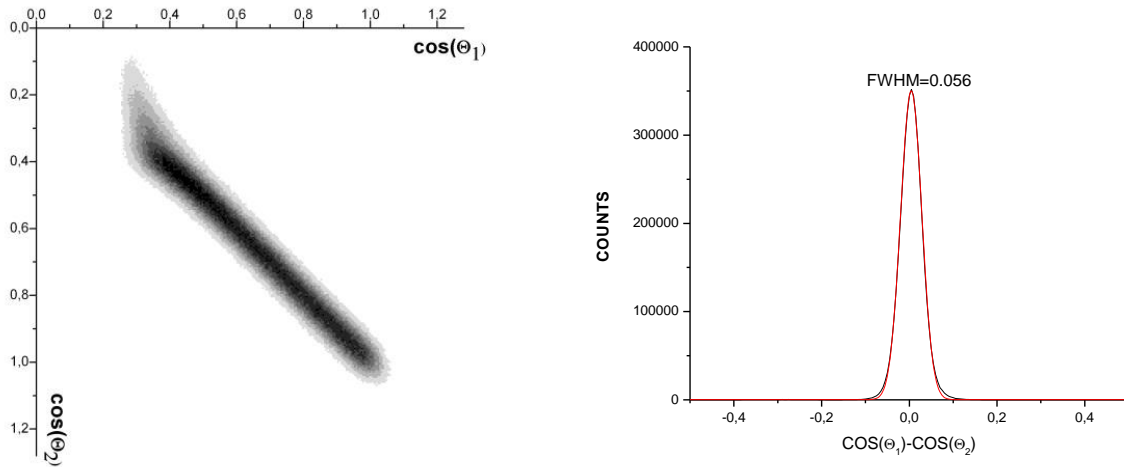


Fig. 1-III-2. Demonstration of the measuring accuracy for FF angular distributions.

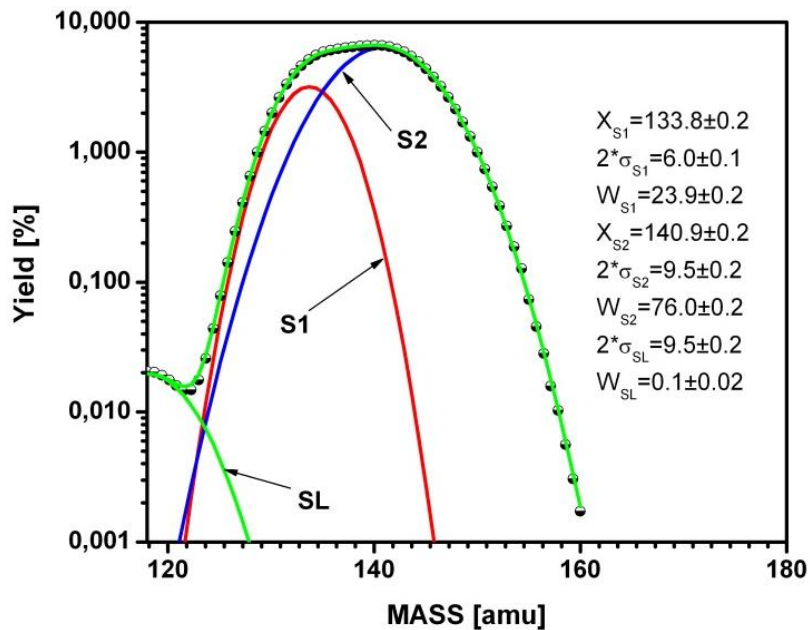


Fig. 1-III-3. Fission modes for the mass distribution of thermal neutron-induced fission fragments of ^{235}U according to the calculations within the MM-RNR model.

It also follows from the analysis of the experiment that for a fixed mass number A , $\bar{\nu}(A, TKE)$ becomes a linear function of TKE, so in practice it is sufficient to measure two functions $\bar{\nu}(A)$ and $TKE(A)$ to obtain $\bar{\nu}(A, TKE)$.

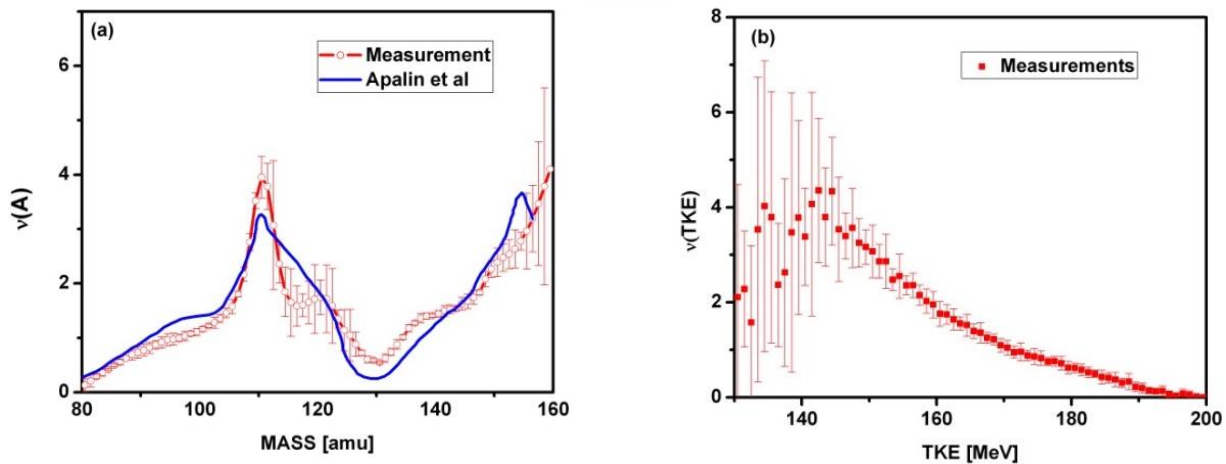


Fig. 1-III-4. The average number of PFN as a function of mass (left) and TKE FF (right) measured in the experiment $^{235}\text{U}(n,f)$.

The interest to the measurements of PFN multiplicity is primarily due to the fact that PFN carry information about the excitation energy of FF. In this regard, the information about the variations in the excitation energy depending on the FF mass is fundamental from the viewpoint of the fission process in the last stage of the evolution for the fissioning system from the saddle point on the potential energy surface to the point of rupture. In theoretical calculations of the fissioning nucleus excitation energy and its distribution between FF it is necessary to take account of a change in their excitation energy during the formation process. Recent experimental studies of the $^{237}\text{Np}(n,f)$ reaction in the range of incident neutron energy of 0.5 - 6.0 MeV have revealed that a growth of the incident neutron energy results in an increase in PFN emission mainly from a heavier fragment. This observation suggests that in the prescission configuration the excitation energy can be pumped from one forming FF to another through the neck. This process should have a strong impact on the PFN yield depending on the mass distribution between FF. The complete study of this effect requires more precise information about the level density in the forming FF, which for many years was calculated assuming that nucleons in the nucleus form a Fermi gas. This assumption, however, is not confirmed experimentally for the systems with low excitation energy. In this regard, it is necessary to conduct new experimental studies of the deexcitation process in FF by means of simultaneous measurements of PFN and prompt gamma-rays. For this purpose, a modern setup has been constructed, which provides simultaneous spectrometric measurements of FF masses, PFN and cascades of prompt gamma-rays. First experiments were carried out on the beam of thermal neutrons at IBR-2 at the end of 2015. At present, data processing and planning of new experiments at IREN are in progress.

1.2. Research of the dynamics of interaction between superfluid and normal phases of nuclear matter

The process of the phase transition of any nucleus under a change in its excitation energy can be theoretically studied in detail by analyzing the density of excited levels and partial widths of the nucleus transition between them. To obtain the reliable information, the accuracy in the determination of these functions at the level of no worse than a few tens of percent is required. Such an experimental level considering the possible existence of hidden (or undetermined so far) parameters of the process of the cascade gamma-decay of any compound state can only be achieved by using a modern mathematical model of the cascade decay of an arbitrary compound state.

1. SCIENTIFIC RESEARCH

The acquisition of coincidence statistics for the study of the process of cascade gamma-decay of the ^{172}Yb compound state at the DDR reactor in Dalat, Vietnam, has been completed. The accumulated gamma-gamma coincidences were processed in Dubna, FLNP JINR. The Cooper pair-breaking thresholds were determined up to the neutron binding energy. In **Fig. 1-III-5** the experimental intensity of the two-quantum cascades is compared with the results of the calculations in the framework of the existing representations of the nucleus as a statistical system of a Fermi gas and the Dubna model, which takes account of the interaction of the normal and superfluid phases of nuclear matter.

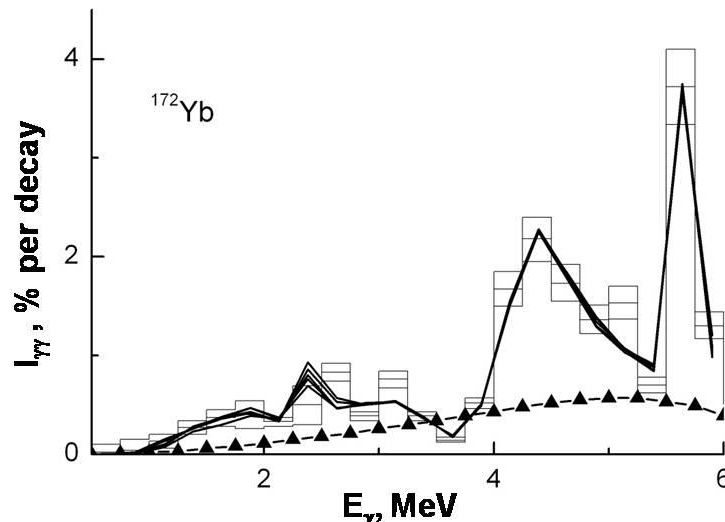


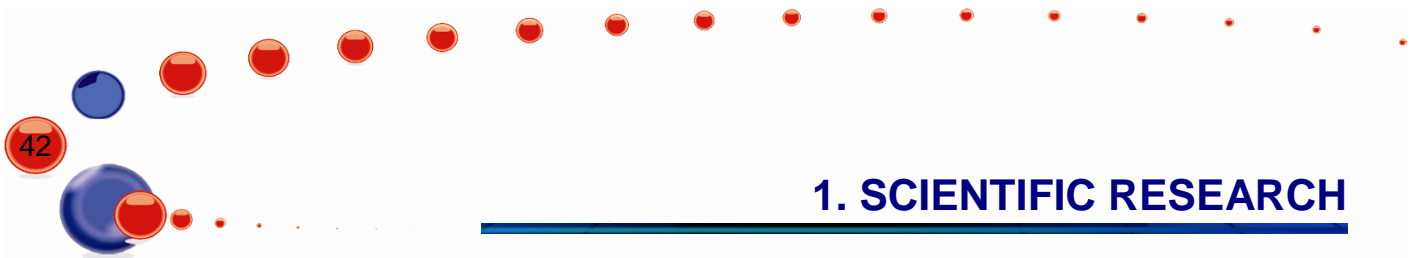
Fig. 1-III-5. Dependence of the cascade intensity on the energy of primary transition. Histogram – experiment with its errors. Broken lines – results of the best fits for 5 options for the variable ratio of the capture cross-section in the resonances with spins $J = 0$ and $J = 1$. Triangles – cascade intensity calculated according to the conventional models of the level density and radiation strength functions of the statistical nucleus model.

1.3. Investigations of (n,p), (n, α) reactions

On beamline №5 of EG-5, neutron-producing targets based on $\text{D}(d,n)^3\text{He}$ (solid and gas targets) and $^7\text{Li}(p,n)^7\text{Be}$ reactions have been designed and tested during measurements. The development of a PIXIE-4 based electronic system for acquisition and storage of multidimensional data from an alpha-spectrometer at EG-5 has been completed and followed up by tests on a fast neutron beam.

The experimental and theoretical investigations of the (neutron, charged particle) reactions induced by fast neutrons have been conducted. The experiments were carried out at the Van de Graaf accelerators EG-5 in FLNP JINR and EG-4.5 of the Institute of Heavy Ion Physics of Peking University. Data on the reactions with the emission of charged particles induced by fast neutrons are of much interest for studying the mechanisms of nuclear reactions and atomic nuclear structure as well as in choosing engineering materials and in performing calculations in the development of new facilities for nuclear power engineering.

The analysis of the data from the measurements of the $^{144}\text{Sm}(n,\alpha)^{141}\text{Nd}$ and $^{66}\text{Zn}(n,\alpha)^{63}\text{Ni}$ reactions at $E_n = 4.0, 5.0$ and 6.0 MeV has been completed. The data have been obtained for the first time. For ^{66}Zn there have been no measurements in the neutron energy range of 0-20 MeV, for ^{144}Sm there have been only two measurements at around 14 MeV. The experimental cross-sections have been compared with the available libraries and calculations using the TALYS-1.6 code (**Figs. 1-III-6**).



1. SCIENTIFIC RESEARCH

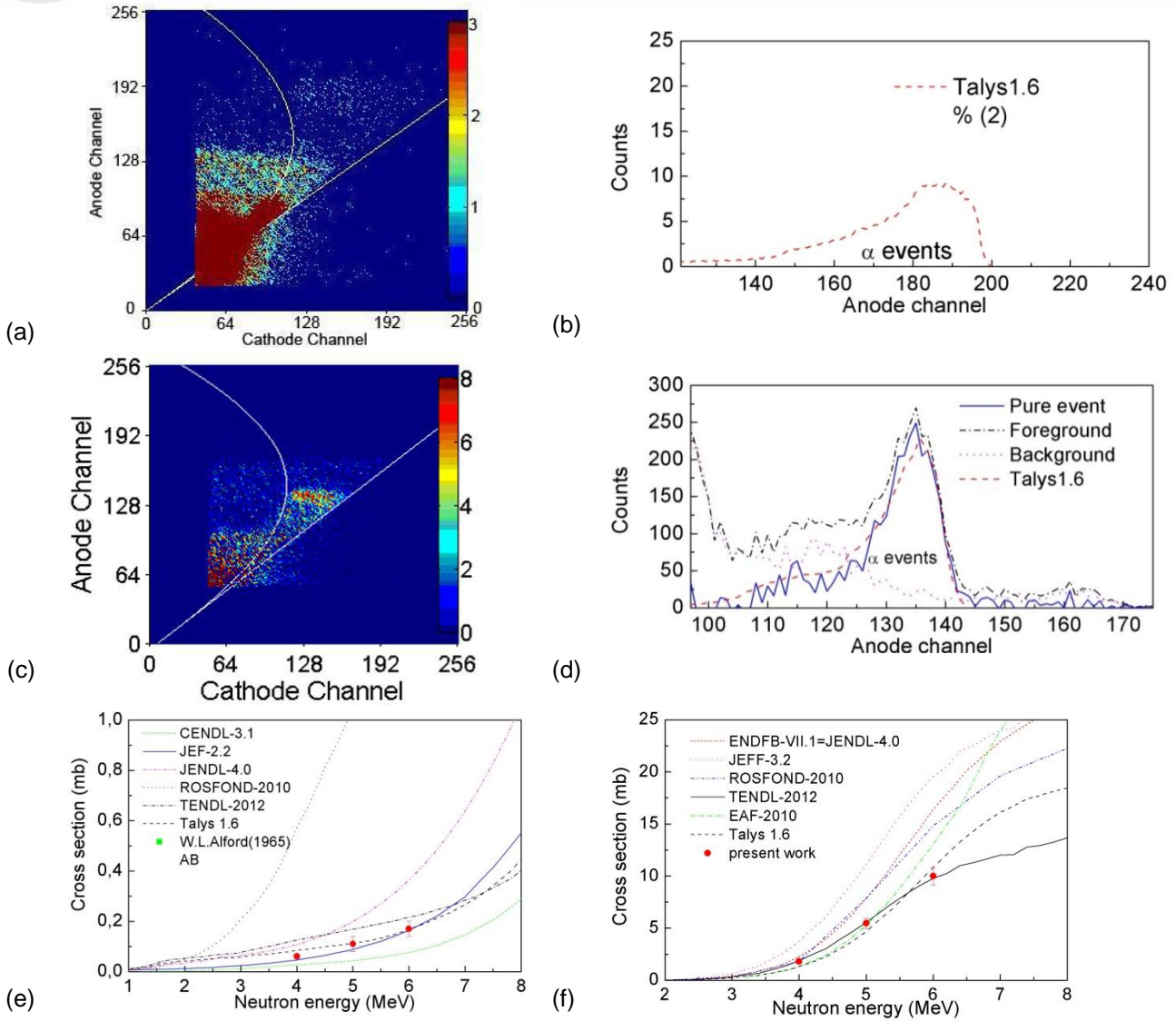


Fig. 1-III-6 (a) 2D spectrum of the $^{144}\text{Sm}(n,\alpha)^{141}\text{Nd}$ reaction at $E_n = 4.0$ MeV in the "forward" direction; (b) Spectrum from anode of the $^{144}\text{Sm}(n,\alpha)^{141}\text{Nd}$ reaction at $E_n = 4.0$ MeV in the "forward" direction; (c) 2D spectrum of the $^{66}\text{Zn}(n,\alpha)^{63}\text{Ni}$ reaction at $E_n = 5.0$ MeV in the "forward" direction (with the background subtracted); (d) Spectrum from anode of the $^{66}\text{Zn}(n,\alpha)^{63}\text{Ni}$ reaction at $E_n = 5.0$ MeV in the "forward" direction; (e) Cross-section of the $^{144}\text{Sm}(n,\alpha)^{141}\text{Nd}$ reaction in comparison with the existing measurements and estimates for the neutron energy range from 1.0 to 8.0 MeV; (f) Cross-section of the $^{66}\text{Zn}(n,\alpha)^{63}\text{Ni}$ reaction in comparison with the existing measurements and estimates for the neutron energy range from 2.0 to 8.0 MeV.

A systematic analysis of our experimental cross-sections of the (n,α) reaction in the energy range from 4 to 6.5 MeV has been performed. The dependence of the cross-sections on the parameter $(N-Z+0.5)/A$ in this energy range has been observed and explained in the framework of the statistical model. At the same time, formulas of the statistical model give overestimated values for the absolute cross-sections of the (n,α) reaction. This difference between the theoretical calculations and experiment can be eliminated by introducing a clustering factor for alpha particles in the nucleus, $Wp/\alpha = 4.5$. The results of the analysis can be used in astrophysical calculations, e.g. for the s-process, helium burning, and also allow one to estimate the cross-sections of unstable isotopes for which the measurements are difficult or impossible.

1. SCIENTIFIC RESEARCH

1.4. Measurements of gamma-spectra and angular distributions of gamma-rays for various nuclei using the tagged neutron method

In the framework of the "TANGRA" project, the angular correlations of γ -rays and neutrons, as well as gamma-spectra produced in the inelastic scattering of 14.1 MeV neutrons by various nuclei have been measured. These measurements are aimed at determining the partial cross-sections of the formation of nucleus excitation levels with the corresponding gamma-lines in inelastic neutron scattering reactions, as well as spin characteristics of these levels in the given reaction. This information is important for further development of the method of elemental analysis using tagged neutrons, in particular, to create a local database of characteristic gamma-rays for a broad set of elements, and for a detailed study of inelastic scattering reactions of fast neutrons by these nuclei. **Figure 1-III-7** shows samples for measuring gamma-spectra at the TANGRA facility.

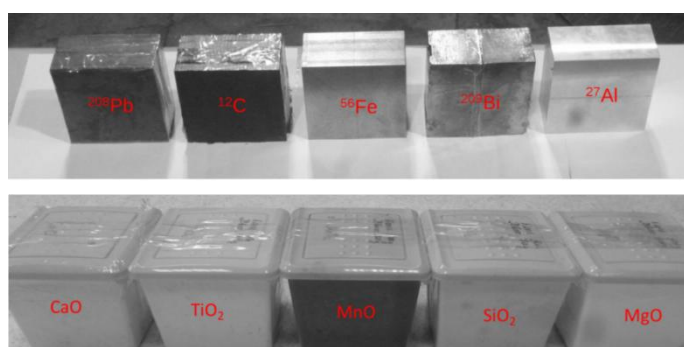


Fig.1-III-7. Samples for measuring gamma-spectra at the TANGRA facility.

A scheme of the experiment is presented in **Fig. 1-III-8**. As a source of 14.1-MeV neutrons we used a portable neutron generator ING-27 developed and manufactured at the N.L.Dukhov Russian Institute of Automatics (VNIIA). To form a flux of tagged neutrons, the generator comprises a built-in double-sided silicon strip detector with eight mutually perpendicular strips on each side, which form an 8x8 matrix of $6 \times 6 \text{ mm}^2$ pixels. The alpha-detector is located at a distance of 100 mm from the tritium target of the neutron generator (NG) and intended to detect 3.5-MeV alpha-particles produced in the reaction $(d + t \rightarrow \alpha(3,5 \text{ MeV}) + n(14,1 \text{ MeV}))$. Characteristic gamma-rays from the irradiated targets were detected by 22 detectors on NaI(Tl) crystals shaped as hexagons (distance between crystal faces – 85 mm, crystal height – 200 mm). The γ -ray detectors were arranged perpendicularly to the horizontal plane in a circle of radius of 370 mm with a target under study placed in its center. The angle between the axes of two adjacent NaI(Tl) crystals in the horizontal plane was 15° .

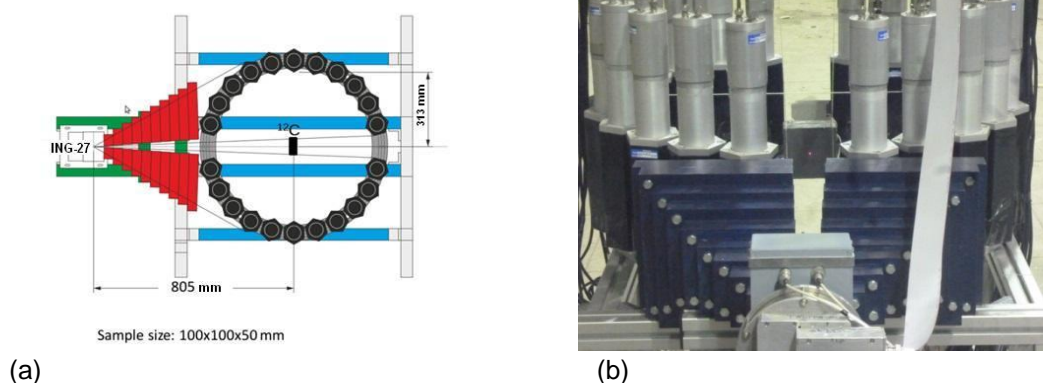


Fig. 1-III-8. A general view of the experiment (a) and the setup (b)

1. SCIENTIFIC RESEARCH

As an example, **Figure 1-III-9** shows spectra of gamma-rays measured by the detector positioned at an angle of 30° for different samples. A detailed analysis of the obtained experimental data is scheduled for 2017.

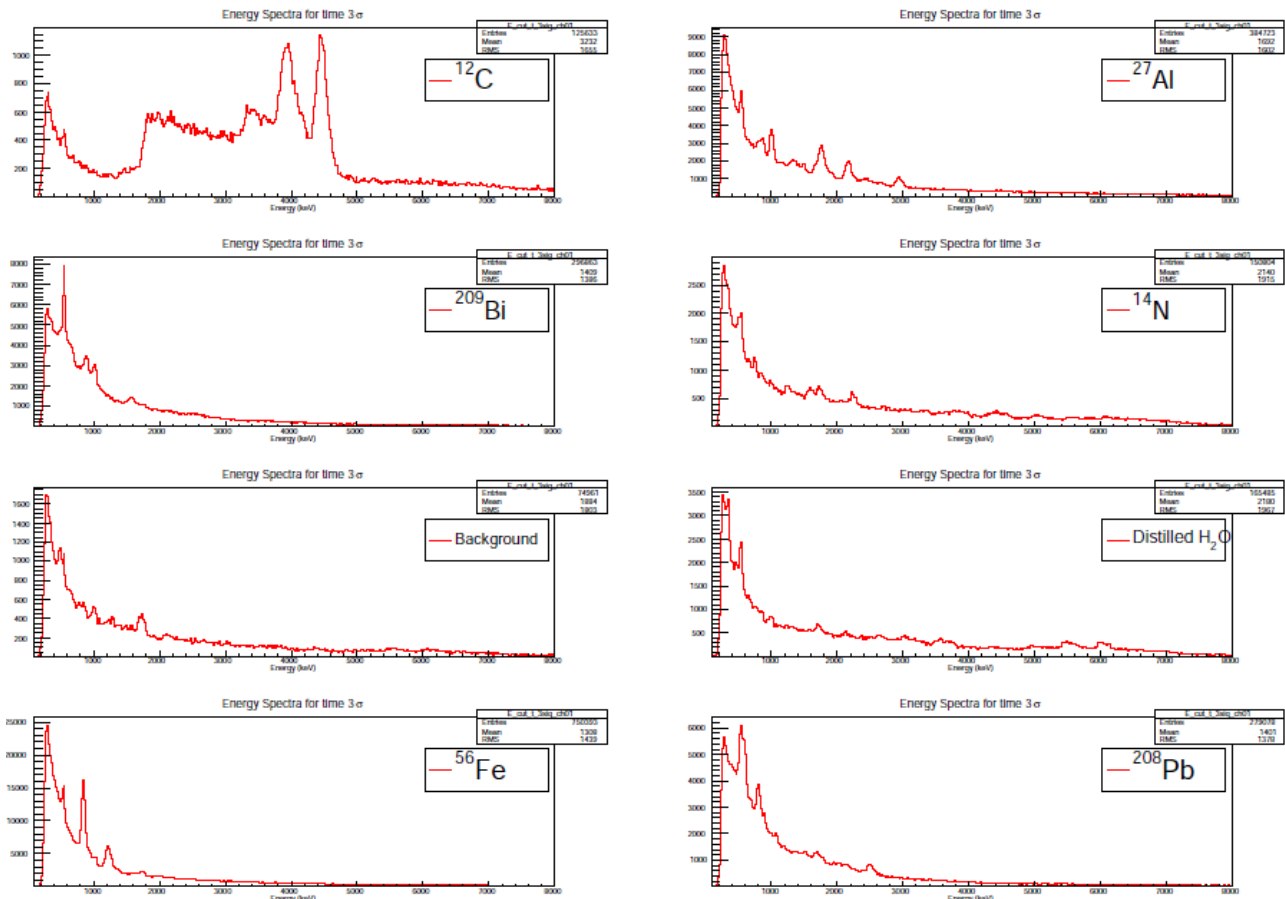


Fig. 1-III-9. Energy distribution of the events detected by the γ -detector positioned at an angle of 30° .

1.5. Measurement of T-odd effects in ^{235}U fission on a hot source of polarized neutrons

In the framework of the FLNP-ITEP-FRM2 collaboration a series of experiments have been continued to measure the ROT-effect in the emission of prompt γ -rays and neutrons in the binary fission of ^{235}U and ^{233}U induced by polarized cold neutrons. The experiments were carried out on the POLI instrument at the FRM-2 reactor (Garching, Germany).

For these experiments a neutron spin control system based on rectangular coils in magnetic screens was developed. The system to control the polarization vector of the neutron beam with a high accuracy (10^{-4}) was developed among other methods in Dubna in 1997-1999. This method uses the neutron spin precession in a magnetic field. The developers of the method had positive experience in using such systems (coils) to control the direction of neutron polarization. In the early eighties, they used the coils in magnetic screens for epithermal and resonance neutrons.

The main advantage of such coils is high magnetic field homogeneity in combination with small dimensions. Soft magnetic screens of the coils made of an alloy with high permeability allow one to use these devices as portable boxes with homogeneous magnetic fields (BHF). A simple

1. SCIENTIFIC RESEARCH

construction of the coil is shown in **Fig. 1-III-10** it consists of a rectangular coil frame with grooves to ensure high precision in winding aluminum wires.

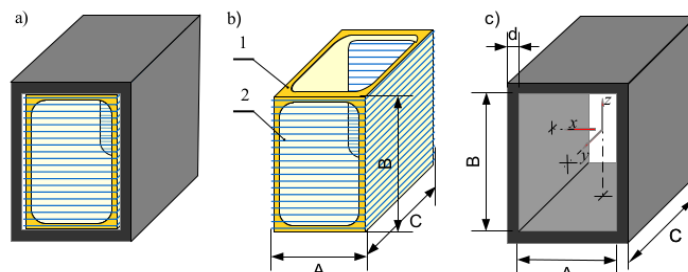


Fig. 1-III-10. Box with homogeneous magnetic field: a) box (BHF); b) rectangular coil frame (1) aluminum coils (2), and c) external magnetic screen. A, B, C – coil dimensions. D – yoke thickness.

When a neutron enters the coil with a homogeneous magnetic field B , it starts to precess around the direction of the field with a frequency f proportional to the external field. In particular, for a neutron with energy $E = 0.3$ eV the spin rotates by 90° at $l = 52$ mm, $B = 4\pi$ G and $I = 0.5$ A.

The schematic of the experiment with the location of all coils to control polarization is presented in **Fig. 1-III-11**.

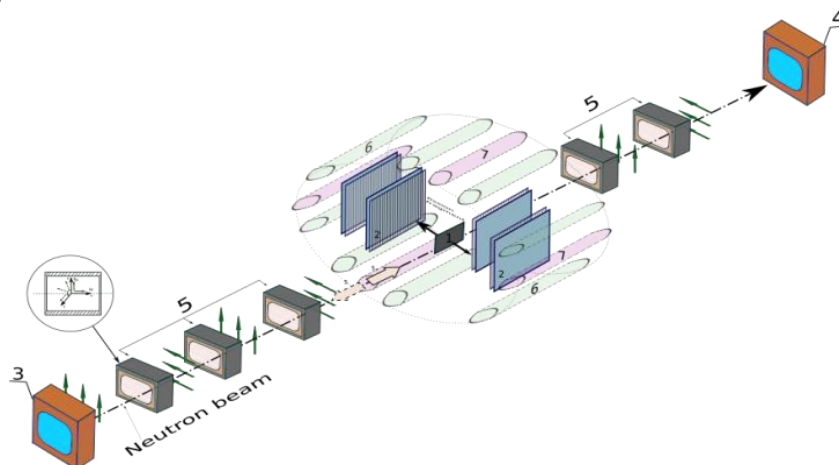


Fig. 1-III-11. Schematic of the experiment. 1) target; 2) multi-wire proportional chamber for the detection of fission fragments; 3) polarizer; 4) analyzer; 5) rectangular coils in magnetic screens (arrows show the magnetic field direction); 6) plastic scintillation detectors; 7) scintillation detectors of gamma-rays and neutrons.

Cells with polarized ^3He (length of approximately 13 cm and pressure of about 2.5 atm) were used as a polarizer and analyzer. The cells were placed in rectangular coils with a magnetic screen and homogeneous magnetic field providing ^3He relaxation time in the cells of about 40 hours. To control polarization, five similar coils of smaller dimensions allowing one to vary the current magnitude and direction in each of them were used, which made it possible to provide any neutron polarization direction in a given point along the neutron beam. One of the coils was used as a spin-flipper with a spin-flip frequency of the order of 1.3 s.

The experimental setup at the POLI instrument of the FRM2 reactor is shown in **Fig. 1-III-12**.

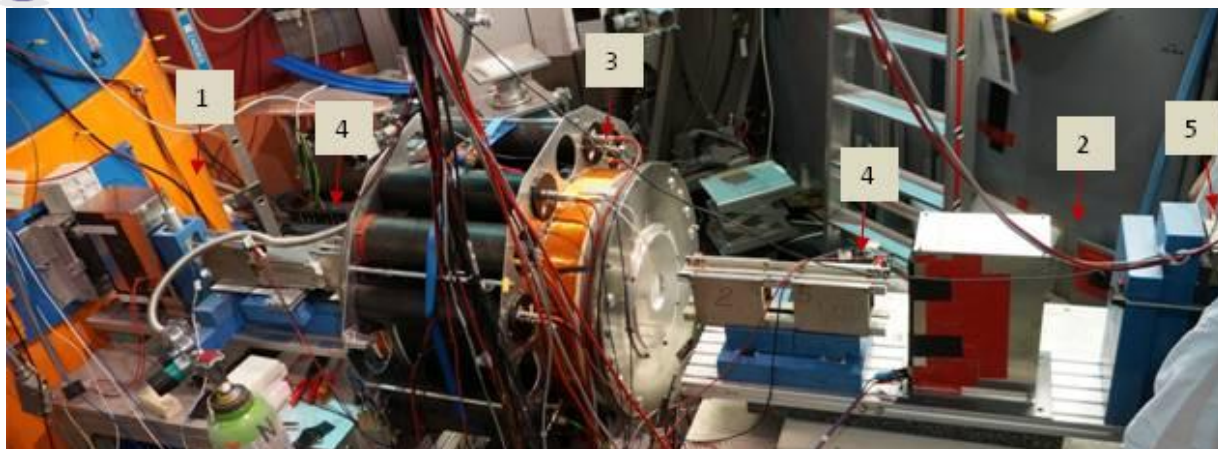


Fig. 1-III-12. Setup for measuring the ROT-effect at the POLI instrument (FRM2, Garching). 1 – neutron polarizer, 2 – analyzer, 3 – fission chamber surrounded by gamma-ray and neutron detectors, 4 – polarization control coils, 5 – neutron counter for measuring polarization

A beam of 0.3-eV neutrons was monochromatized by a mosaic single crystal diffractometer and focused on the target. A neutron polarizer on the basis of a polarized ^3He cell with an average polarization of $\sim 70\%$ was placed between the diffractometer and the target. The polarized neutron flux density at the target was $\sim 5 \times 10^6 \text{ n cm}^{-2}\text{s}^{-1}$. The polarization was controlled by a similar analyzer and measured by a neutron counter. Since the neutron beam should be horizontally polarized at the target and the polarization of neutrons after ^3He cells was vertical, rectangular coils in magnetic screens providing polarization control were installed on both sides of the chamber. The direction of the magnetic field in the first coil changed every 1.3 s, which created an analogue of a spin-flip and allowed us to measure the difference effect.

Fragments were detected by fast multi-wire detectors and could be separated into light and heavy ones by the time of flight. Gamma-rays and neutrons were detected by scintillation counters (plastic, NaI(Tl)) placed at specific angles to the direction of emission of the fragments. The so-called ROT-effect (effect of rotation of the fissioning system in or against the direction of the angular momentum transferred by a polarized neutron) for gamma-rays and neutrons was measured. Neutrons were separated from gamma-rays by the time-of-flight method.

The effect was measured for 9 days. As a result, the effect values (averaged over all detector position angles) were obtained:

- for gamma-rays: $(-4.6 \pm 2.7) \times 10^{-5}$;
- for neutrons: $(2.7 \pm 2.9) \times 10^{-5}$.

For gamma-rays, the value of the ROT effect differs from zero at the level of 2σ , for neutrons no statistically significant effect in the limits of errors was observed.

In 2017, a new experiment is planned, in which we expect to observe the effect or determine its upper limit with the accuracy comparable to that obtained on the cold neutron beam.

1.6. Measurement of the coefficients of P-odd angular correlations in the reactions of cold polarized neutrons with light nuclei.

The measurement of P-odd asymmetry in the emission of α -particles in the $^{10}\text{B}(n,\alpha)^7\text{Li}$ reaction was carried out on the cold polarized neutron beam of the PF1B instrument at the ILL reactor (Grenoble, France). A 24-section ionization chamber with insensitive gas gaps was used as a detector of α -particles. The P-odd asymmetry value was found to be $\alpha_{P\text{-odd}}^{^{10}\text{B},\alpha} = -(11.2 \pm 3.4) \cdot 10^{-8}$.

1. SCIENTIFIC RESEARCH

The result has been obtained for the first time in the world. This is only the second nucleus after ${}^6\text{Li}$ for which the P-odd effect was discovered.

1.7. Experiment to obtain a focused beam of very cold neutrons using a reflector of diamond nanoparticles

Ultracold neutrons (UCN) and very cold neutrons (VCN) intensively interact with nanoparticles due to the fact that the neutron wavelength and the particle size are of the same order of magnitude – a few nanometers, therefore, the cross-section of elastic coherent neutron scattering by particles is high. In [1] for the first time VCN with velocities of 40-160 m/s were reported to be stored in a trap with walls composed of diamond nanoparticles and effectively reflecting such neutrons.

One of the practical applications of nanoparticle reflectors can be a sharp increase in the VCN yield from the source, if we manage to form a narrow beam from the isotropic distribution and direct it to a neutron guide. In order to determine the possibility of the formation of such beams, a specialized experiment (scheme is shown in **Fig. 1-III-13**) was carried out.

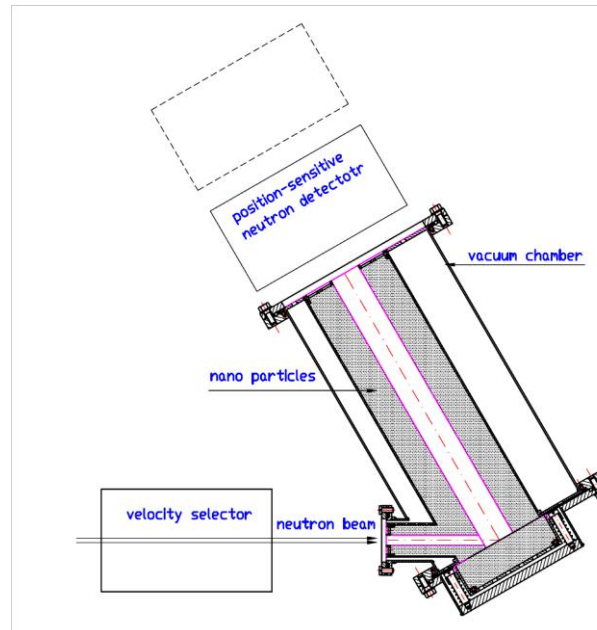


Fig. 1-III-13. Scheme of the experiment.

A beam of very cold neutrons (velocities 40-90 m/s) with a diameter of 8 mm passes through a velocity selector (with a resolution from 5% to 20%) and comes to the bottom of the trap through the inlet opening (\varnothing 10 mm). The trap is a thick-walled tube with an inner diameter of 30 mm and length of 30 cm. The walls of the tube consist of nanodiamond powder. Neutrons confined in a trap can be detected by a position-sensitive detector mounted on its exit end. By changing the distance from the trap exit to the detector, it is possible to measure the number of emitted neutrons and their angular distribution.

The preliminary results have shown that the number of escaping neutrons is ~ 1 -2% of the number of neutrons entering the trap, with the yield increasing as the neutron energy decreases. The beam formed has an angular divergence of 10^{-2} - 10^{-3} rad. These results indicate that the

covering of a VCN source with a nanoparticle reflector can result in a tenfold increase in the number of VCN in the neutron guide.

1.8. Experiment to study quasi-specular reflection of cold neutrons from the surface of nanopowder

The scattering of particles/rays at small angles in a medium (small-angle scattering) leads to the fact that for a beam of particles/rays falling on the medium at a glancing angle the angular distribution of reflected particles/rays has a pronounced maximum at an angle close to the angle of incidence, i.e. the so-called quasi-specular reflection is observed. A similar situation exists for neutrons when falling at a small angle on a medium with the effective small-angle scattering. Nanoparticles with a size of a few nanometers can effectively scatter cold neutrons at small angles. Therefore, for cold neutrons falling on the surface of a nanopowder a quasi-specular reflection (first described in [2]) can also be observed.

We experimentally measured the parameters of this phenomenon using the reflection of neutrons from a nanodiamond powder. For this purpose, we measured the dependence of the angular distribution of reflected neutrons for different wavelengths of incident neutrons and different angles of incidence (1° , 2° , 3° and 4°) of the neutron beam on the surface. The measurements were performed for a powder of nanoparticles of different sizes. The preliminary results of the measurements are presented in **Figs. 1-III-14 (a) and (b)**.

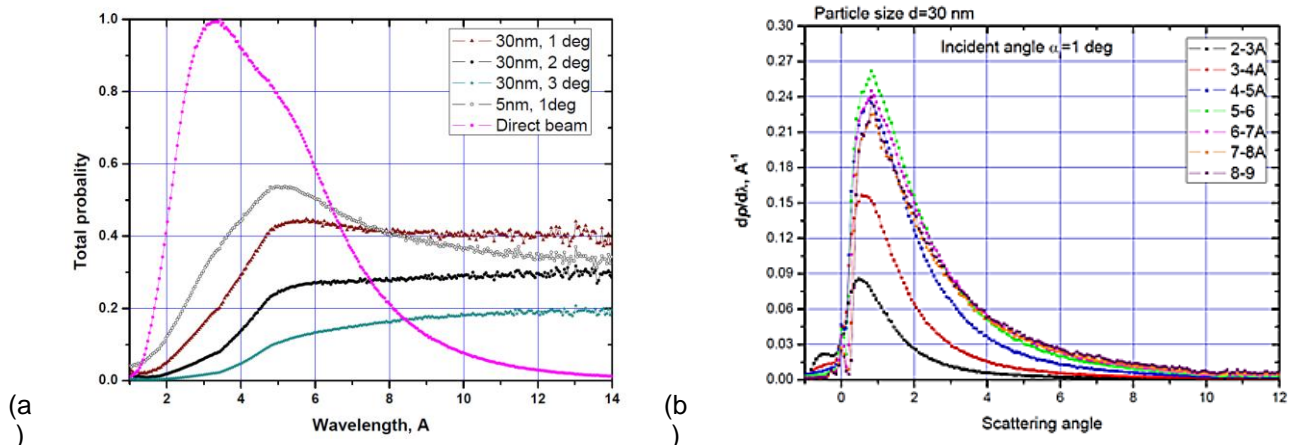


Fig. 1-III-14. (a) Total probability of reflection from the surface of nanopowders as a function of neutron wavelength for angles of incidence of 1° , 2° and 3° . The data for powders of two kinds of nanoparticles with an average size of 30 nm and 5 nm are presented. **(b)** Angular distribution of neutrons reflected from the surface of a powder of nanoparticles with an average size of 30 nm for different neutron wavelengths.

From the data presented in **Fig. 1-III-14** it can be clearly seen that for neutrons with longer wavelengths a more efficient reflector is that with large nanoparticles, for neutrons with shorter wavelengths – with small nanoparticles.

The findings can help in the construction of primary sections of mirror neutron guides for VCN and CN placed near a reactor core, which can significantly increase the neutron emission of the sources into the neutron guides.

1.9. Neutron diffraction by a moving grating

In the Institute of Laue-Langevin a new experiment to obtain UCN spectra for the diffraction by a moving grating (DMG) was performed. Its main purpose was to verify a theoretical prediction that at a certain height of the grating profile a significant suppression of the zero-order diffraction

1. SCIENTIFIC RESEARCH

may occur with a corresponding increase in the intensity of the lines of other orders. If this prediction is true, then by choosing a proper grating profile one can enhance the efficiency of the neutron energy transfer during DMG. The measurements of the spectra were carried out using the previously designed time-of-flight Fourier diffractometer of UCN (Fig. 1-III-15).

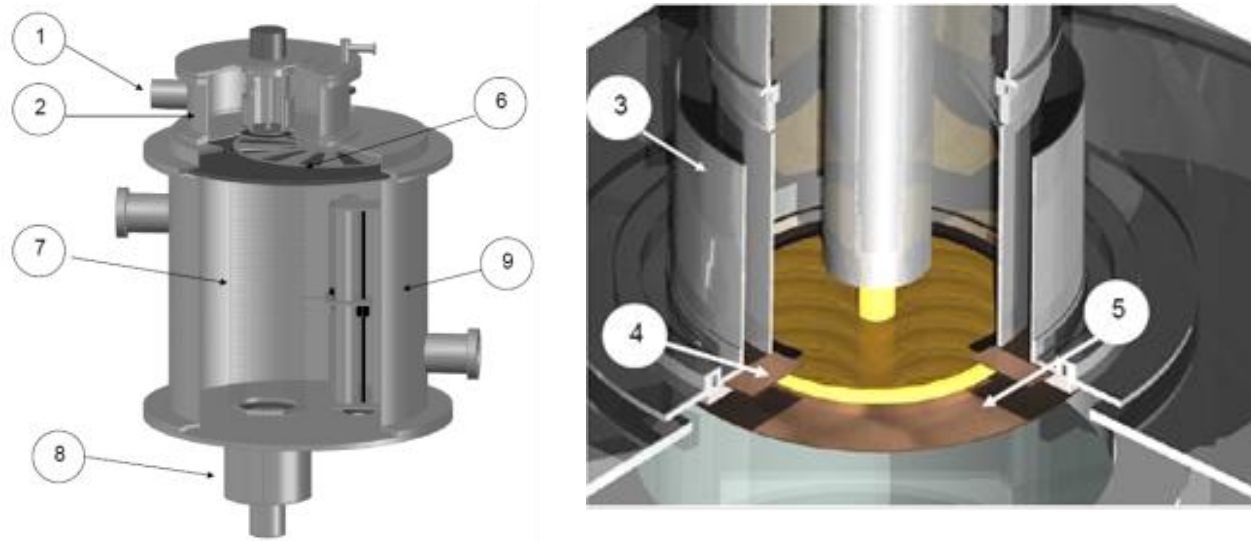


Fig. 1-III-15. Time-of-flight Fourier spectrometer: general view (left) and its upper part (right): 1 – leading neutron guide, 2 - inlet chamber, 3 - circular hall, 4 - filter-monochromator, 5 - grating 6 - rotor of Fourier chopper, 7 - vertical glass neutron guide, 8 - detector, 9 - vacuum chamber.

A new grating prepared as previously on the periphery of a silicon disc had 84000 radial grooves with a profile depth of $0.22\ \mu\text{m}$. The grating profile was analyzed using atomic force microscopy (Fig. 1-III-16). The spectra were obtained for four rotational speeds of the grating. It was found that the teeth and grooves of the grating follow rather a trapezoidal profile than a rectangular one.

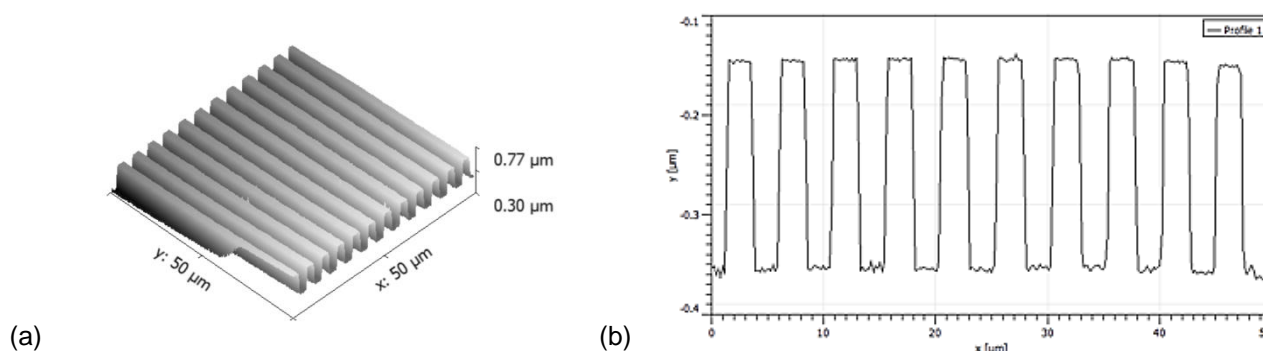


Fig.1-III-16. 3D image of a grating fragment obtained by atomic force microscopy (left) and its profile (right). The scales on the two axes are substantially different.

The comparison with the spectrum obtained for the grating with a less deep profile (Fig. 1-III-17, two bottom graphs) demonstrates the validity of the prediction about the possibility of a significant suppression of zero-order intensities. This is the main result of this experiment.

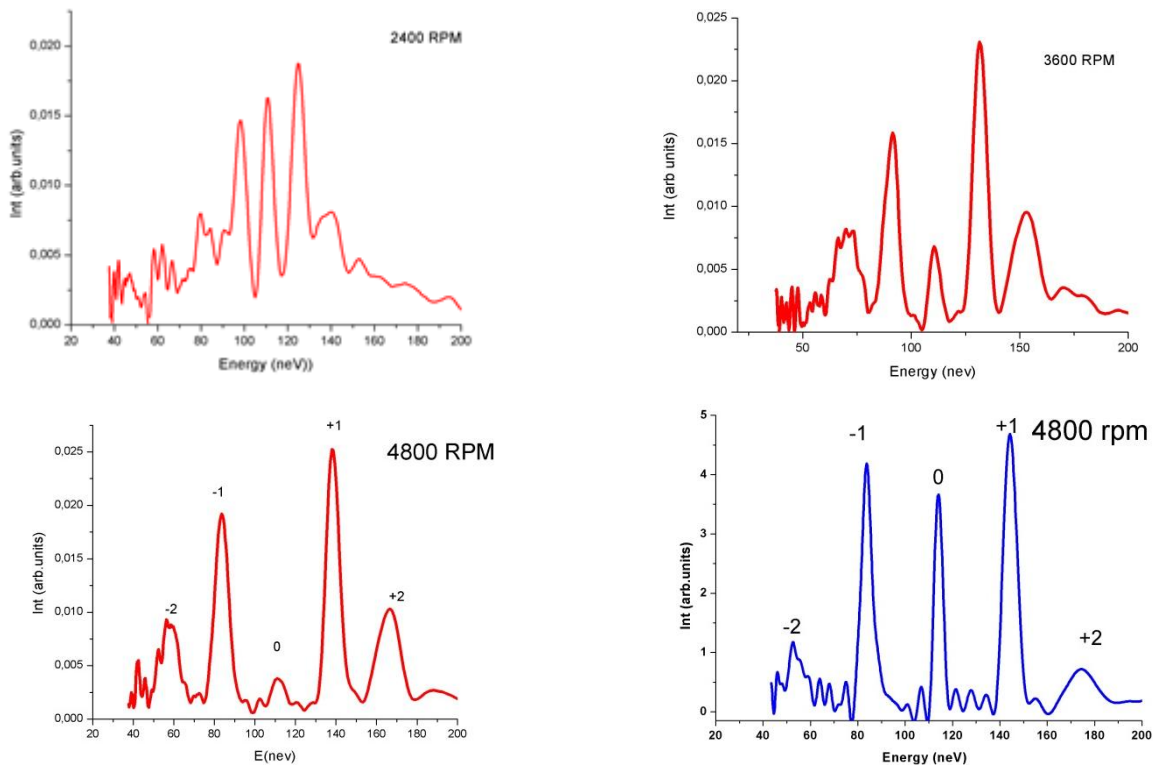


Fig. 1-III-17. Neutron spectra of diffraction by a moving grating with deep profile for three rotational speeds of the grating (2016). The bottom right figure shows the spectrum obtained in 2014 for the grating with a smaller profile depth. It can be seen that zero-order intensities are significantly different.

At the same time, the experimental spectra are not in full agreement with the results of the calculations. A reason for this discrepancy is not well understood for the moment, and its clarification requires a more thorough theoretical analysis of the DMG phenomenon together with the search for possible systematic effects inherent in the time-of-flight Fourier diffractometer of UCN.

1.10. Analysis of the accuracy of UCN time-of-flight measurement by Fourier spectroscopy

We are currently considering the possibility of a new experiment to test the weak equivalence principle. The experiment is based on the measurement of the time of flight of neutrons belonging to several diffraction orders in DMG. In this experiment, it will be necessary to ensure the accuracy of the time measurement at the level of $10 \mu\text{s}$. A test experiment was carried out to determine the possibility of using for this purpose a Fourier-diffractometer of UCN. The analysis showed that in the existing diffractometer presented above in **Fig. 1-III-15** there are sources of systematic effects leading to an absolute error in the measurement of time of flight, which reaches in some cases several hundred microseconds. Along with it, when measuring the time-of-flight difference there were no such problems.

In the considered experiment, the energy spectrum of UCN was formed by a five-layer planar nanostructure — neutron Fabry-Perot interferometer — placed in a vertical neutron guide. The interferometer transmitted UCN with a narrow energy spectrum with an average energy of about 114 neV. The time of flight of neutrons when falling down was 114 ms. It was measured for two positions of the interferometer differing in height by 5 mm. At the same time the neutron energy

1. SCIENTIFIC RESEARCH

changed by about 5 neV due to the Earth's gravity and the change in the time of flight was about 280 μs . The aim of the experiment was to measure the difference in the time of flight at two positions of the interferometer.

The procedure of accuracy evaluation was as follows. Two time-of-flight spectra were obtained for two positions of the monochromator. By fitting single peaks in each of the two spectra after the Fourier synthesis, a value of 290 μs was found for the difference in the time-of-flight values with uncertain accuracy at this step. Then, each of the raw data sets was divided into 30 groups and each group of data was considered as a result of an independent measurement. For each group its own spectrum with a single line was built using the Fourier synthesis and the line positions on the time scale were determined. The difference between the two averaged time-of-flight values was 300 μs . The experimental variances of these results were 80 and 90 μs . The fact that the distribution of the resulting values was close to the normal one made it possible to conclude about a purely statistical nature of the variance. This assumption leads to the total

accuracy estimation as $\delta t = \frac{\Delta t}{\sqrt{N}}$, where $\Delta t = 85 \mu\text{s}$ is the accuracy of one measurement and $N = 60$, which gives the estimate of $\Delta t \approx 11 \mu\text{s}$.

1.11. Experiment on the observation of neutron diffraction by surface ultrasonic waves

In collaboration with IPMT RAS (Chernogolovka) and Max Planck Institute (Munich, Germany) an experiment to observe neutron diffraction by surface ultrasonic waves was performed. The measurements were made on the N-REX reflectometer at the FRM II reactor, neutron wavelength of 4.3 \AA .

A single crystal of lithium niobate (LiNiO_3) was used as a sample. On its surface two interdigital transducers with a base frequency $f = 69 \text{ MHz}$ were designed using photolithography. They generated surface acoustic waves (SAW) in each of two directions. Under the application of voltage to the two transducers, a standing ultrasonic wave was produced on the surface.

The area of wave propagation was a stripe with a width of 6 mm and length of 60 mm. The SAW speed was 3590 m/s, about four times higher than the neutron velocity along the sample surface. The experiment was performed with SAW travelling in and against the direction of neutron wave propagation, as well as for the scattering by a standing ultrasonic wave. In all cases, an energy transfer to the neutron took place. If in the case of a travelling wave the phenomenon can be interpreted in terms of a quasi-classical Doppler frequency shift, then in the case of standing waves one deals with a non-stationary quantum effect. Thus, the given study expands a relatively short list of non-stationary quantum experiments with neutrons.

Figures 1-III-18 (a) and (b) shows a result of the measurement in the case of the opposite propagation direction for SAW and neutrons. In the right figure, the stripes of the diffraction scattering from SAW are clearly visible. **Figure 1-III-18 (c)** presents a similar picture for the case of neutron scattering by a standing wave. The stripes of the first order corresponding to the energy transfer $\Delta E = \pm \hbar \Omega$ are seen together with a stripe of the second order with the change in the neutron energy $\Delta E = -2\hbar \Omega$, where $\Omega = 2\pi f$. The value of the quantum of energy in the conditions of this experiment was $\Delta E_0 = \hbar \Omega = 3.276 \times 10^{-7} \text{ eV}$. We emphasize that here one deals with a non-stationary energy transfer, and purely diffraction beam splitting on a surface structure periodic in space is much smaller than the observed effect.

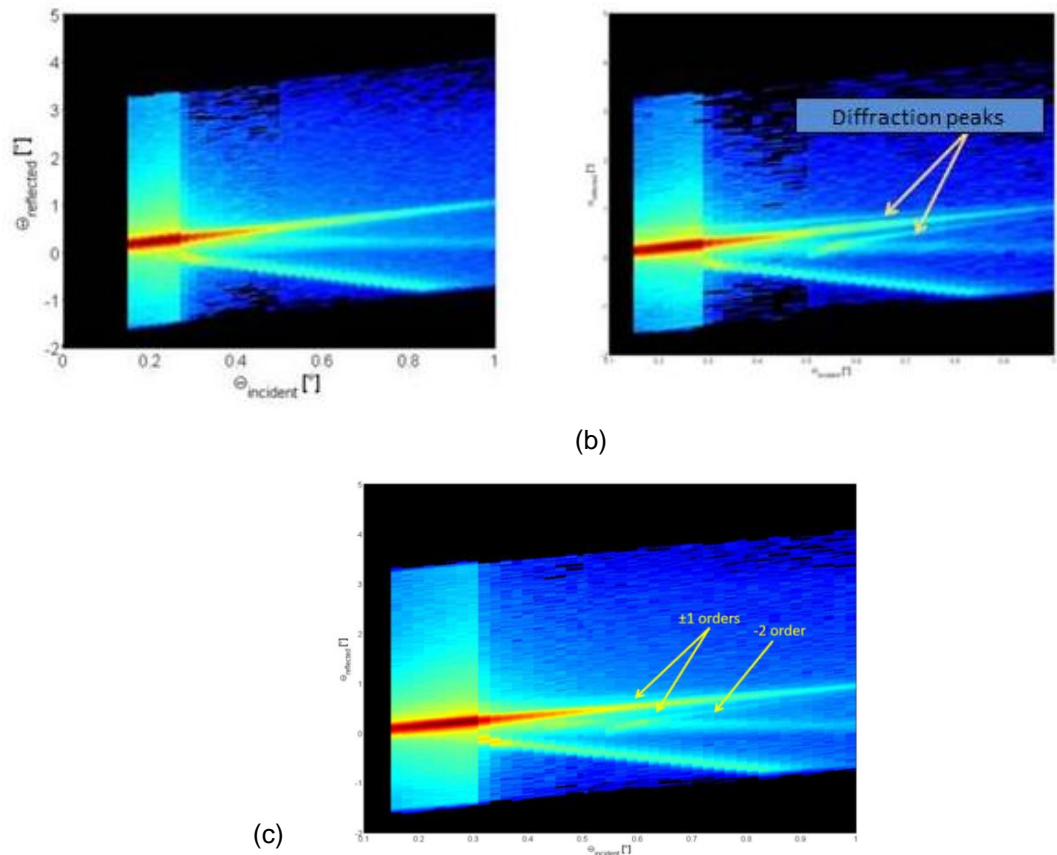


Fig. 1-III-18. 2D map of neutron scattering from the surface of lithium niobate in the absence (a) and after generator (b) of surface ultrasonic waves. (c) 2D map of neutron scattering from the surface of lithium niobate in the case of standing SAW.

1.12. Preparation of the experiment to observe the interaction of UCN with an oscillating barrier at giant accelerations

The purpose of the upcoming experiment is to verify the validity of the model of the effective potential at giant accelerations of the sample. An important step in the preparation of the experiment is quantum calculations of the interaction of the neutron wave packet with a potential structure oscillating in space at different magnitudes of the maximum acceleration of the object $w_{max} = A(2\pi f)^2$, where A and f are the oscillation amplitude and frequency, respectively. The calculations for the case of an oscillating potential barrier have shown that for the case of interest $w_{max} \approx 10^8 cm/s^2$ the observed non-stationary effects for the past state are very small. The calculations for the case of an oscillating resonant structure representing two barriers and a hole between them have revealed that in a wide range of amplitudes and frequencies in the past state, there are visible oscillations in the count rate. As a result, this geometry is selected as a priority geometry for further research. Possible approaches to the designing of the experiment to test the validity of the model of the effective potential at giant accelerations of the sample, have been considered.

The realization of the experiment requires samples whose surface can oscillate without significant deformations in a frequency range from 100 kHz to several MHz. We solve this problem in two ways. First, in collaboration with the Institute of Laue-Langevin the study of the topography

1. SCIENTIFIC RESEARCH

of the sample surface oscillating in space is in progress. Second, the experimental study of oscillating samples is under preparation. For this purpose, a special stand (vibrometer) for mapping the surface of oscillating samples (**Fig. 1-III-19**) has been designed. It consists of a laser interferometer and a two-coordinate table.



Fig. 1-III-19. Two-coordinate laser vibrometer.

The setup will make it possible to measure the surface shape synchronously with the phase of the sample movement. At present, the work to create and debug the mathematical software of the stand is underway.

2. Theoretical investigations

The characteristics of a spin-wave neutron interferometer (which consists of a pair of magnetic mirrors placed in a magnetic field non-collinear to the magnetization of the mirrors) in a magnetic field, have been investigated. The setup can be used for studying the properties of the neutron wave packet, as well as for measuring the scattering density correlations in thin films. On the basis of experimental data, the spectrometer sensitivity and the coherent neutron length have been estimated. The possibilities of using spin-echo spectroscopy to determine the coherent neutron length have been considered.

Contrary to the common opinion that the bound states always have discrete spectra, it has been shown that in the hydrogen atom there may be bound singular states with a continuous spectrum. The role of these states in the possible nuclear reactions of cold fusion and processes of star ignition has been discussed.

In the EPR paradox, a question on particle polarizations is under discussion: whether the source emits pairs of flying particles in an entangled state or in the form of individual particles with their own polarizations. To answer this question, a simple Bell's inequality for photons has been proposed. It can be tested in one measurement. A result of the possible measurement is being calculated taking into account the experimental constraints.

The concept of the coherence length of the neutron has been under consideration including the generally accepted definition of a Gaussian wave packet based on the beam formation method and a singular de Broglie wave packet of an individual neutron. Experiments to measure the coherence length have been proposed.

An explanation of the experimentally found small heating of UCN during the storage in traps has been proposed on the basis of the neutron wave packet properties. Due to the finite width of the packet, the transmission and reflection probabilities are accompanied by an increase and

1. SCIENTIFIC RESEARCH

decrease in the energy, respectively. The energy changes at the subcritical incidence of the de Broglie wave packet has been analytically calculated.

3. Methodological and applied research

3.1. Determination of the elemental composition of friable ores

The aim of the work is to study the technical possibilities of measuring the composition of friable ores using in real-time the technology of neutron activation analysis (NAA). In the framework of this study, the following tasks have been formulated: investigation of the influence of the type of gamma-ray detectors on the accuracy of the elemental composition determination for ore samples using Am-Be/Pu-Be sources; analysis of the impact of the position of neutron sources and detectors relative to the sample on the elemental composition determination accuracy; determination of optimal geometries for the equipment location relative to the sample; design of the logical circuit for processing signals from detectors; preparation of the primary design documentation.

In **Table 1-III-1** the rock composition determined by chemical analysis is given.

Table 1-III-1. Composition of the rock used in the study.

Results of analyses of ore elemental composition		
Controlled compound	Apatite concentrate, weight %	Tailings, weight %
P ₂ O ₅	38,98	0,9
Al ₂ O ₃	0,99	20,88
CaO	50,58	4,9
SiO ₂	2,38	42,16
Fe ₂ O ₃	0,68	8,02
K ₂ O	0,24	6,02
H ₂ O	0,06	0,15
TiO ₂	0,33	2,92
Na ₂ O	0,5	10,26

For the study, a PuBe neutron source with the intensity of $\sim 5 \cdot 10^6$ n/s was used. **Figures 1-III-20 (a) and (b)** shows a schematics of the experimental setup.

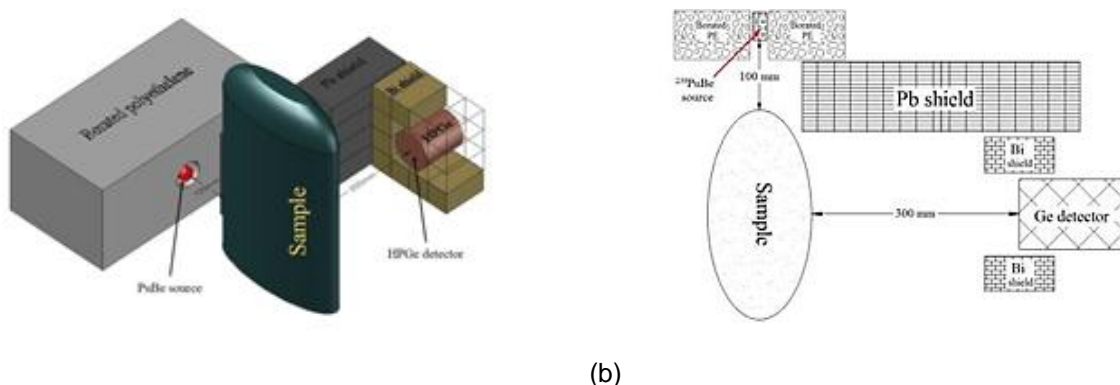


Fig. 1-III-20. (a) 3D representation of the experimental setup; **(b)** Experimental setup for determining the elemental composition of friable ores using an HPGe detector.

1. SCIENTIFIC RESEARCH

At the first stage, gamma-ray spectra of three irradiated ore samples with the content of P_2O_5 – 38, 98, 0,9% and their mixtures were measured using an HPGe detector. **Figure 1-III-21** shows the corresponding spectra for these samples.

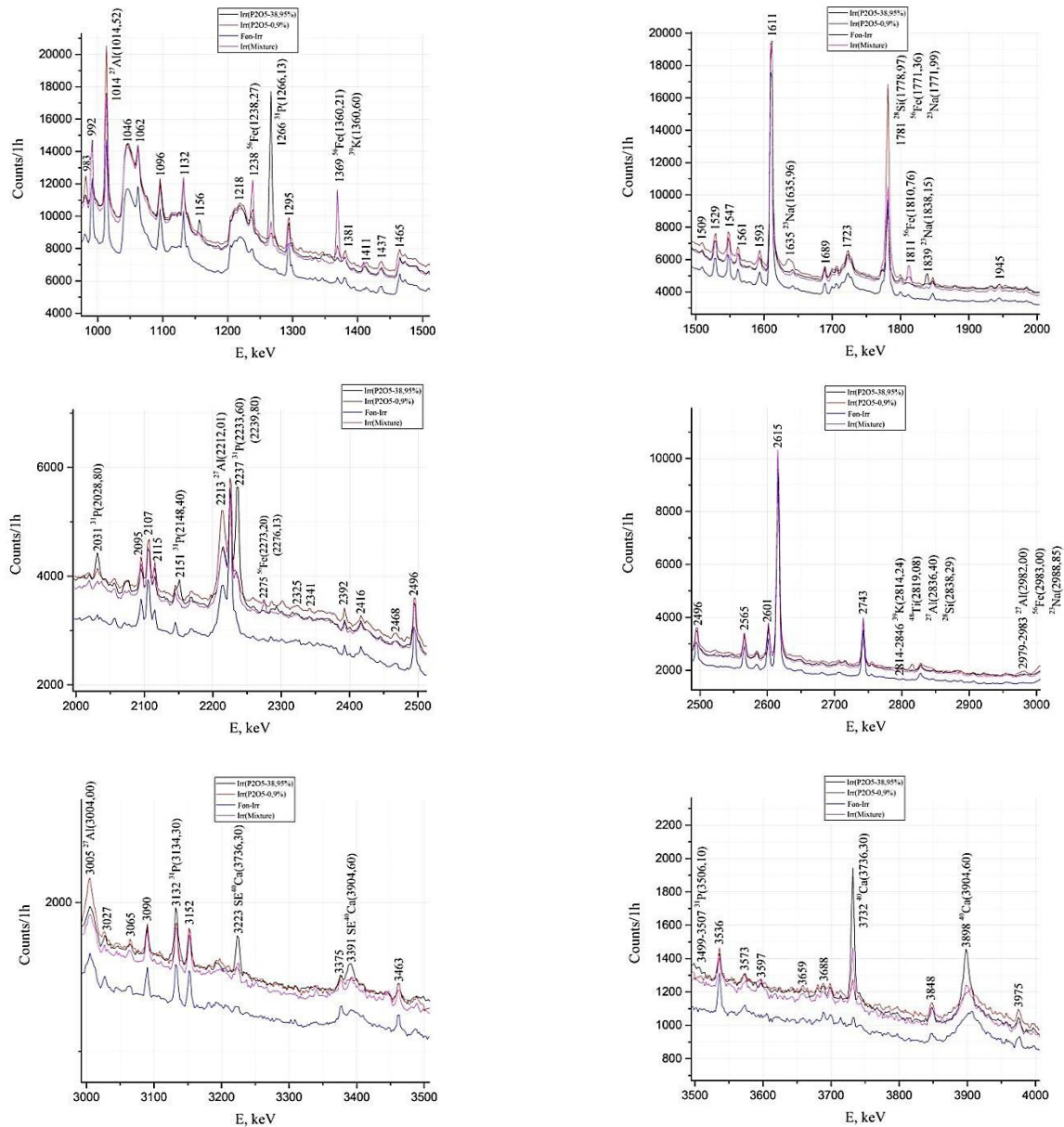


Fig. 1-III.21. Amplitude distributions of the events recorded by an HPGe-detector for ore samples (apatite concentrate, tailings and their mixtures) irradiated by neutrons from a PuBe-source. Background distributions of the recorded events obtained with the PuBe-source in the absence of the irradiated sample.

As one can see in the given spectra, there is a clearly observed difference in the results of the measurements of phosphorus (lines 1266 keV and 2237 keV) and calcium (lines 3732 keV and 3898 keV) contents, corresponding concentrations are at the levels of 38 and 0.9% (phosphorus) and 50 and 4.9% (calcium). This demonstrates the possibility of using the presented technique for

determining phosphorus and calcium concentrations with an accuracy that meets the requirements in the industrial extraction of ores of this class.

At the second stage, the measurements of gamma-spectra were made for the specified irradiated samples using a scintillation detector based on a BGO crystal.

A schematic of the experiments using a BGO-detector is given in **Fig. 1-III-22**.

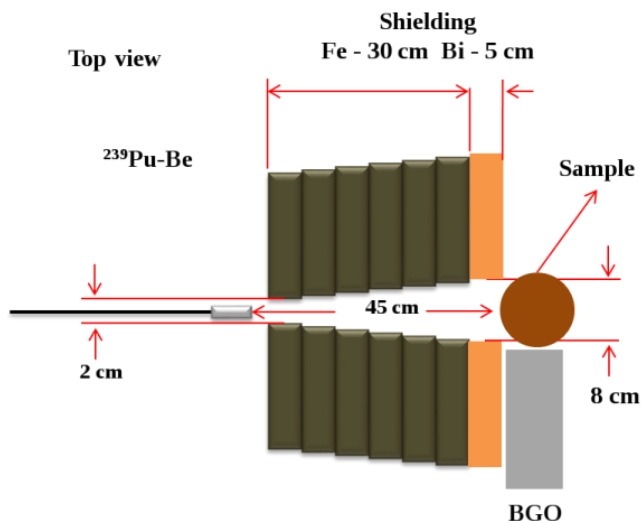


Fig. 1-III-22. Experimental setup for determining the elemental composition of friable ores using a BGO-detector.

In **Fig. 1-III-23**, the spectra of events recorded by HPGe and BGO detectors are given for comparison.

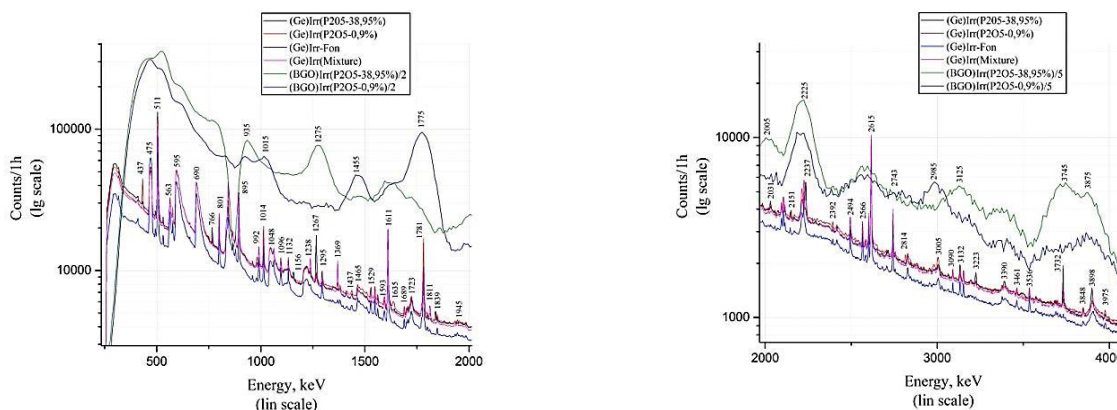


Fig. 1-III-23. Comparison of the amplitude distribution of events recorded by BGO- and HPGe-detectors.

As one can see in **Fig. 1-III-23**, there is no sufficiently clear difference in the results of the measurements of the content of phosphorus (lines 1266 keV and 2237 keV) and calcium (lines 3732 keV and 3898 keV) obtained using the BGO-detector as compared to the HPGe-detector. This is due to an essentially worse energy resolution and higher background for the BGO-detector in comparison with the HPGe-detector.

1. SCIENTIFIC RESEARCH

Nevertheless, BGO-detectors can still be used in measurements of the elemental content of friable ores. For this purpose, at this stage it is necessary to develop and create a highly efficient algorithm for the analysis of experimental data.

It is worth considering the question of using a gamma-ray detector based on $\text{LaBr}_3(\text{LaCr}_3)$ crystals.

3.2. Determination of the relative humidity of coke

The aim of this experiment is to verify the technical possibility of using detectors based on BGO and NaI (TI) crystals and standard neutron sources for real-time determination of the humidity of coke and other friable materials for industrial purposes. The method is based on the interaction of neutrons with hydrogen and oxygen nuclei constituting water molecules. Hydrogen effectively reacts with slow neutrons through the neutron capture, thereby forming deuterium, which emits 2223-keV gamma-rays. The main reaction for fast neutrons interacting with oxygen is inelastic scattering. In the process a cascade of characteristic gamma-rays is emitted with the most notable line at 6129 keV. These two lines were used for analysis of water content in the sample.

The studied sample is a closed volume of coke (coal). **Figure 1-III-24** shows a schematic of the experiment. A $^{239}\text{Pu-Be}$ neutron source with the intensity of $\sim 5 \cdot 10^6$ n/s is used for irradiating the sample. Gamma-rays from the sample were measured by the NaI or BGO detectors. A combined shield was installed between the detector and the neutron source to prevent the exposure of the detector to direct neutrons. To test the method, we used a sample weighing about 3 kg, to which water was added to the content from 2% to 80%.

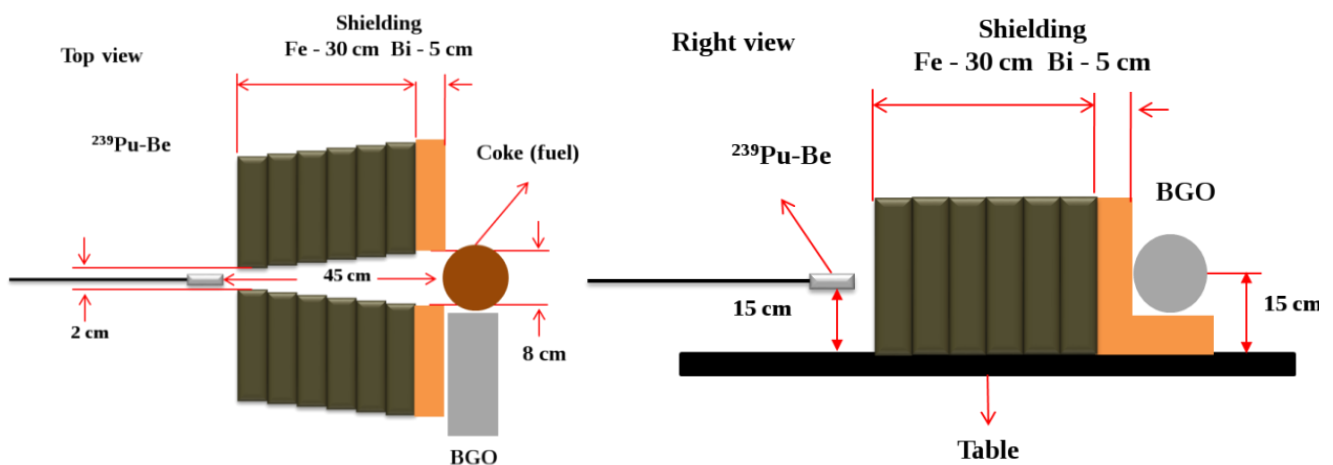


Fig. 1-III-24. The experimental setup for determining water content in samples (top view and right side view).

Figures 1-III-25 and **1-III-26** show the spectra of gamma-rays with the energies of 2223 keV and 6129 keV and their analysis for the water content of 6% and 42%, respectively.

1. SCIENTIFIC RESEARCH

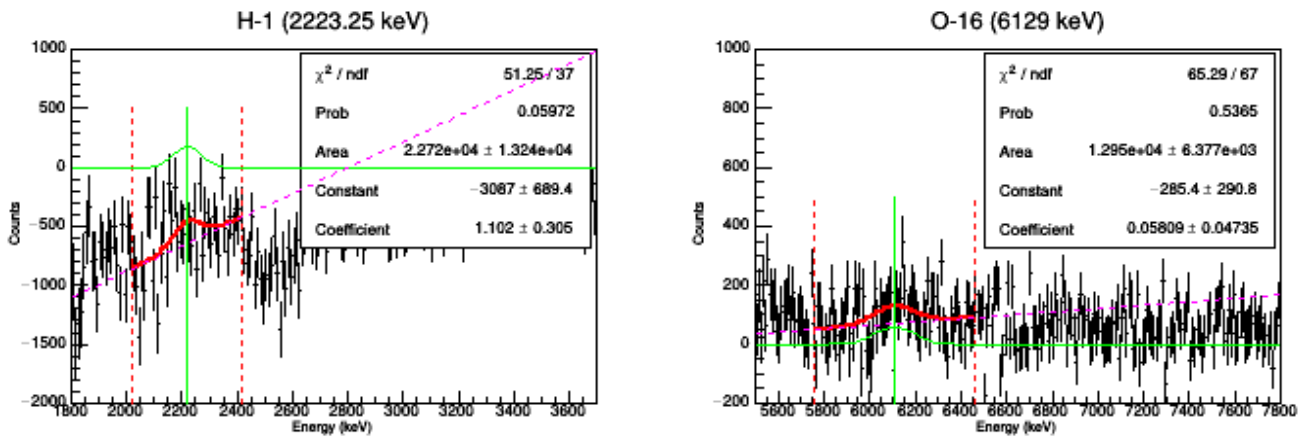


Fig. 1-III-25. Water content of 6%.

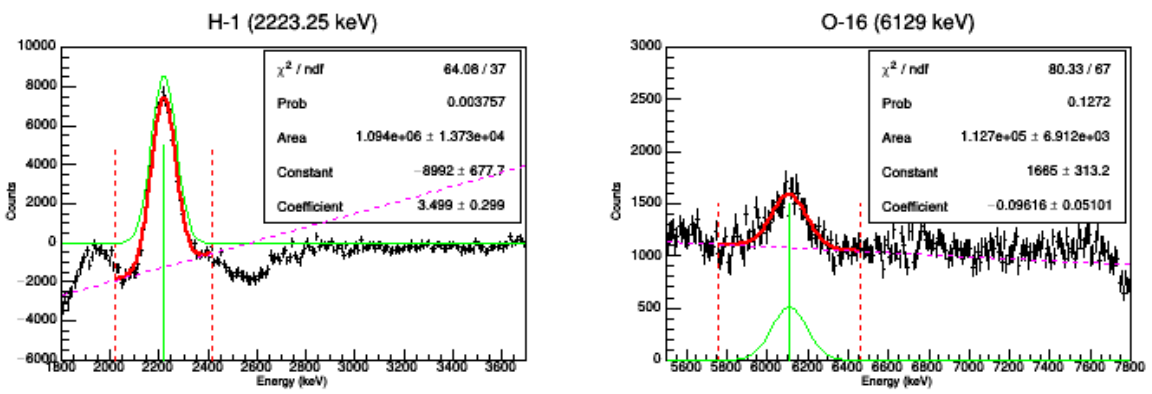


Fig. 1-III-26. Water content of 42%.

Figure 1-III-26 illustrates the dependence of the intensity of gamma-lines on the water content in the sample.

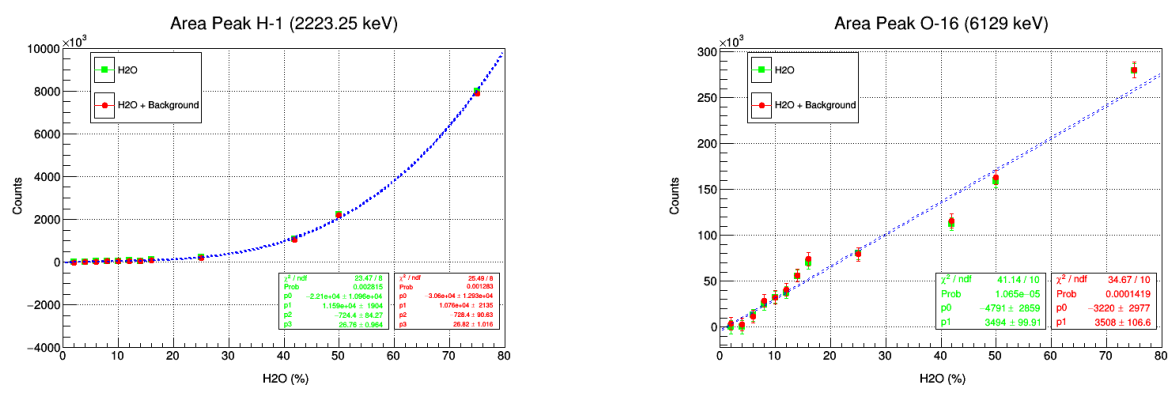


Fig. 1-III-26. Intensity of gamma-lines of 2223 keV and 6129 keV as a function of water content in the sample.

Thus, it has been demonstrated that the water content in coke can be determined by this method starting from the humidity of 5%. For industrial purposes, a higher accuracy is required. Therefore, these studies are planned to be continued to achieve the accuracy within 0-5%.

1. SCIENTIFIC RESEARCH

3.3. Analytical investigations on charged particle beams of the EG-5 accelerator

The research of elemental depth profiles of near-surface layers in various samples was the main direction of activity in 2016. The analytical studies were performed on the beams of charged particles with the energy from 1.0 MeV to 3.1 MeV using a variety of nuclear-physical analytical techniques including Rutherford backscattering (RBS), elastic recoil detection (ERD) and particle induced X-ray emission (PIXE). The investigations were carried out in collaboration with Moscow State University (Moscow), LETI (Saint-Petersburg), VSU (Voronezh), UMCS (Lublin, Poland), Institute of Electrical Engineering, Slovak Academy of Sciences (Bratislava), Institute of Physics, Vietnam Academy of Science and Technology (Hanoi, Vietnam). The changes in the elemental composition of the near-surface layers of GaAs crystal samples doped with different doses of heavy Ar^+ and Xe^+ ions were studied. In addition, the composition, structure and morphology of the surface of nanosized platinum-containing silicon films synthesized by the sol-gel technology were investigated. The influence of the irradiation by Xe^+ ions and neutrons on the structural characteristics of SiC and SiC(N) films prepared by the PECVD (Plasma Enhanced Chemical Vapour Deposition) technique was studied.

3.4. Analytical investigations at the IBR-2 reactor

In 2016, the REGATA facility was used for multi-element instrumental neutron activation analysis of about 3,000 environmental samples (vegetation, soil, air filters), a number of technological, biological and archaeological samples, as well as of samples of extraterrestrial origin in the framework of programs and grants of the JINR Member States and Protocols on scientific and technical cooperation with the JINR Non-Member States. Investigations of test samples were conducted for an interlaboratory comparison of the results under the IAEA program.

3.4.1. Development of the NAA&AR experimental base

Development of the software package for complex automation of multi-element neutron activation analysis (NAA) at the IBR-2 reactor was continued in 2016 (Pavlov et al., 2016). Work on the automation of NAA was carried out in the framework of the IAEA Coordinated Research Project «Development of an Integrated Approach to Routine Automation of Neutron Activation Analysis» (F1.20.25/CRP1888, Contract No. 17363).

3.4.2. Biomonitoring of air pollution

In 2016, the summing-up of the activities conducted in 2010-2015 in the framework of the international program "Heavy metal atmospheric deposition in Europe – estimations based on moss analysis" was done (Schroeder et al., 2016). In cooperation with the Laboratory of Information Technologies of JINR a cloud system has been developed to collect, store and process information on biomonitoring of atmospheric deposition of heavy metals and other toxic elements in the framework of the UN Programme on air of Europe (Ososkov, Frontasyeva et al., 2016). The comparison of moss species that grow in arid regions has become an important stage in this research. We have determined the species that have the same accumulating capacity as the three species used in the ICP Vegetation program (Gorelova, Frontasyeva et al., 2016). In the framework of the Serbia-JINR Cooperation Program a comparative analysis of air pollution in the so-called "street canyons" in Moscow and Belgrade has been performed (Goryainova et al., 2016). In cooperation with the Polish and French institutions a study of peat columns from Siberia was published in NATURE (Scientific Reports) (Fiałkiewicz-Kozieł et al., 2016).

3.4.3. Biotechnologies

In 2016, in collaboration with the Institute of Microbiology and Biotechnology of the Academy of Sciences of Moldova a new method of synthesis of selenium nanoparticles by cyanobacteria *Spirulina platensis* and *Nostoc linckia* was developed. Along with a number of optical and analytical methods, we used the neutron activation analysis at the IBR-2 reactor to characterize the selenium accumulation process by these cyanobacteria. The assessment of changes in the biochemical composition of cyanobacterium biomass (proteins, carbohydrates and others) in the process of selenium nanoparticles formation has been performed as well (Zinicovscaia, Chiriac et al. 2016, Zinicovscaia, Rudi et al. 2016). In 2016, work continued on the study of processes of extraction of toxic metals from wastewater using microalgae *Spirulina platensis* (Zinicovscaia, Cepoi et al. 2016). In collaboration with Institute of Experimental Physics, SAS in Košice a study on the extraction of heavy metals from model solutions using poplar sawdust was performed (Demcak et al., 2016). In cooperation with the University of Oulu, Finland, the application of NAA for analysis of pine sawdust used in wastewater treatment as a sorbent of metals has been studied (Keränen et al., 2016). In collaboration with the A.N. Frumkin Institute of Physical Chemistry and Electrochemistry of RAS in the framework of the projects supported by RFBR (15-05-08919 and 15-33-20069) work has been performed to study the processes of accumulation and biosorption of metals (vanadium, chromium, uranium, lanthanum) from mono- and multicomponent systems by microalgae *Spirulina platensis* and bacteria *Pseudomonas putida*. The results obtained showed that the concentrations of metals accumulated by the microbial biomass in the process of bioaccumulation were 15-40 times higher than in the biosorption process (Zinicovscaia, Safoniov et al. 2016). Studies have been conducted for biosorption of 13 metals by three types of organisms: bacteria, microalgae and yeast aimed at determination of the most effective sorbent for each metal. In cooperation with the Scientific-Production Association "Biosolar MSU", work has begun on the application of NAA to assess the efficiency of iodine and zinc accumulation by microalgae *Spirulina platensis* for industrial production of iodine- and zinc-containing medicines.

3.4.4. Environmental assessment

In 2016, work on the evaluation of industrial pollution of agricultural soils in one of the satellite cities of Cairo (Sadat City) was completed (Badawy et al., 2016). To continue the work on the assessment of the environmental situation in the basin of the Nile River and its delta, an additional neutron activation analysis of soil and sediment samples from the area of the Central Nile has been performed, and a statistical analysis of the whole amount of the results obtained earlier and in 2016 has been carried out. In collaboration with the National Research Center in Dokki, Cairo, work on modeling the coordinate bonds of several elements (Na, Mg, Ca, Fe, Ni, and Zn) with organic acids has been completed (Okahsa et al., in press). In 2016, the NAA of coral samples from the Red Sea as well as of brown and red algae from the Egyptian coastal aquatic areas of the Mediterranean sea was carried out in the framework of the Protocol on Cooperation with Cairo University. In collaboration with the A.O. Kovalevsky Institute of Marine Biological Research (Sevastopol) the analysis of the samples of macroalgae-biomonitor (red, green and brown) collected in the coastal zone of the Black Sea for the assessment of the state of the Crimea coastal ecosystem has been completed. The study of the seasonal variation of concentrations of 46 elements in the phytoplankton of coastal areas of the Black Sea has been completed. The obtained results have shown that phytoplankton can be successfully used as a biomonitor of aquatic ecosystems. In 2016, in cooperation with Moscow State University (Faculty of Biology) the investigation on the determination of the elemental composition of soil, bottom sediments, terrestrial and aquatic vegetation to assess the transport of pollutants in the strategically important areas of the Black Sea (coastal area of Anapa, Novorossiysk and Tuapse) was completed (P.Nekhoroshkov et al, 2016).

1. SCIENTIFIC RESEARCH

3.4.5. Material Sciences

In 2016, in the framework of the BRFBR-JINR joint grant and in cooperation with the Scientific and Practical Materials Research Center of the National Academy of Sciences of Belarus, the investigations of the crystallization processes and the characterization of artificial diamonds in the C-Mn-Ni-Fe system were conducted (Aleksiayenak et al., 2016). The NAA of 56 samples related to the topic "Studies on the phase formation and physical characteristics of the compounds in the Cu-Fe-S system at high pressures and temperatures" was carried out. Work has begun with the Institute of Nuclear Sciences "Vinca" in Belgrade (Serbia) to study the elemental composition of spider silk, which is of great interest both from the scientific and practical points of view.

3.4.6. Analysis of food products

The determination of mercury intake from the consumption of fish and seafood has been completed. This study carried out in collaboration with the specialists from the Analytical Center of the Geological Institute, Russian Academy of Sciences (Gorbunov et al., 2016).

3.4.7. Geology

In the framework of the joint JINR-Romania project, unconsolidated sediments of the western slope of the Romanian shore of the Black Sea have been studied in 2016 (Duliu, G.Oaie et al., 2016).

3.4.8. Archeology

Nine icons of the second half of the XVIII and XIX centuries, from different regions of Romania and Russia have been studied in detail using the epithermal neutron activation analysis (ENAA), X-ray fluorescence analysis (XRF), digital radiography (DR), Fourier transform infrared spectroscopy (FTIR) and IR-Raman spectroscopy. These methods were used to determine the chemical composition of pigments, as well as deeper layers of icons, while FTIR spectroscopy allowed us to identify the nature of binders. The results of this work have demonstrated the importance of the use of different methods for studying such complex objects as icons (Duliu, Sister Serafima (Dorina-Claudia Samoilescu) et al., 2016).

3.4.9. Analysis of materials of extraterrestrial origin

In 2016, a multi-element NAA of ferrous and carbonaceous meteorites received from the United States and Serbia was performed. For the first time, iridium content was determined in exotic clay samples from Serbia (originally from famous Fish Clay in the sea shore at Stevns Klint in Denmark). Most researchers believe that their Ir enrichments (on a ppb level) resulted from the impact of a chondritic asteroid striking the Earth at that time (about 65 millions years ago). Our results evidence for that hypothesis.

3.4.10. Medical plants

In 2016, we continued investigations in a new promising line of research – determination of the elemental composition of plants used in medicine. These studies are conducted in cooperation with the specialists from Mongolia, Bulgaria (Vasilev et al., 2016), Poland, China (Li Xuesong et al., 2016) and Portugal.

IV. NOVEL DEVELOPMENT AND CONSTRUCTION OF EQUIPMENT FOR THE SPECTROMETER COMPLEX OF THE IBR-2 FACILITY

1. Cryogenic neutron moderators

In 2016, a new device (diaphragm) was successfully tested on the laboratory test stand to measure the flow rate of gaseous helium in the pneumatic pipeline of the cold moderator.

A device for nitrogen-free charging of frozen pellets into the CM202 chamber has been developed and tested (**Fig. 1-IV-1**). The main advantage of this device is that in the process of loading of frozen pellets into the dosing machine, liquid nitrogen does not get into the pneumatic pipeline. This will make it possible to avoid problems related to the freezing of liquid nitrogen in the pipeline, namely, in the heat exchanger of the cold moderator.



Fig. 1-IV-1. A device for nitrogen-free charging of frozen pellets into the CM202 chamber.

An experimental comparison has been made of the cold neutron yield and radiation resistance of aromatic hydrocarbon triphenylmethane with those of mesitylene and m-xylene, already being used in the pelletized cold neutron moderator in the direction of IBR-2 beamlines № 7, 8, 10 and 11.

The comparison of the cold neutron yield from the surface of the materials under investigation has been carried out by experimentally studying the evolution of vibrational states as a function of temperature (**Fig. 1-IV-2**) on the DIN-2PI inelastic neutron scattering spectrometer. It can be seen from the figure that the intensity (yield) of scattered cold neutrons from the surface of the capsule with mesitylene and m-xylene is almost 2 times higher than the intensity of the triphenylmethane sample.

The comparison of radiation resistance has been done by comparing the yield of radiolytic hydrogen from the materials under irradiation on the radiation research facility (IBR-2 beamline 3) up to radiation doses corresponding to the real reactor experiment doses during the operation of the cold pelletized moderator at a reactor power of 2 MW.

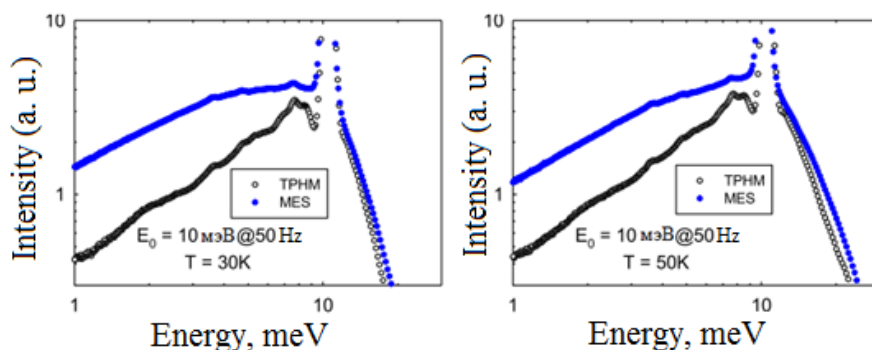


Fig. 1-IV-2. Evolution of vibrational states as a function of temperature (for 30 and 50 K) for an incident neutron energy of 10 meV (TPHM - powdered triphenylmethane, MES - solid frozen mesitylene mixed with m-xylene).

1. SCIENTIFIC RESEARCH

Figure 1-IV-3 presents a diagram of the yield of radiolytic gaseous hydrogen from aromatic hydrocarbons under irradiation to a fluence of $\sim 10^{18} \text{ n}\cdot\text{cm}^{-2}$ (dose $\sim 180 \text{ mGy}$). One can see that the hydrogen yield in the case of triphenylmethane, regardless of the form (whether it be powder or solid pellets) 9 times lower than the yield of hydrogen from a mixture of mesitylene and m-xylene, which points to a significantly higher radiation resistance of triphenylmethane as compared with the above-mentioned mixture.

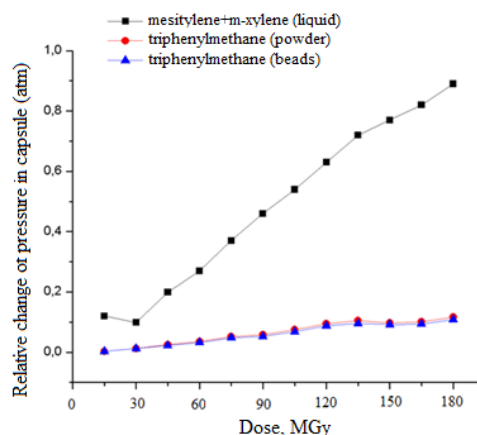


Fig.1- IV-3. Relative change of pressure in the capsule as a function of the absorbed dose for the mixture of mesitylene with m-xylene and triphenylmethane in the form of powder and solid pellets.

From these data we can make a preliminary conclusion that the neutron-physical properties of triphenylmethane make it possible to consider it as a material for a cold neutron pelletized moderator at IBR-2. To draw final conclusions, it is necessary to carry out a number of additional experiments on inelastic neutron scattering on the NERA spectrometer (IBR-2), neutron transmission on the IREN accelerator, pneumatic transport of triphenylmethane pellets, etc.

2. Radiation research facility

In 2016, the following activities were performed on the radiation research facility at IBR-2:

- in cooperation with FLNR a design specification was developed for a spectrometer of heavy nucleus fission products (VEGA – Velocity-Energy Guide-based Array) allowing the identification of primary (unmoderated) fission fragments by mass and energy in the experiments studying the rare modes of heavy nuclei fission;
- in collaboration with the Laboratory of Magnetic Sensors of the Lviv Polytechnic National University a study on the radiation resistance of magnetic sensors (3D Hall sensors) was carried out in the framework of the ITER international project (**Fig. 1-IV-4**);



Fig.1-IV-4. Samples of magnetic sensors under study.

- in collaboration with DLNP JINR the experiments on the irradiation of samples of silicon scintillators were conducted to study their electrical properties under irradiation;

1. SCIENTIFIC RESEARCH

- in collaboration with VBLHEP JINR we carried out preliminary studies on the nature of radiation defects in topaz samples after irradiation.

3. Calculations and simulation of spectrometers

During the period of 2016 the development of special mathematical models and related programs for simulating full reflectometric and GISANS experiments on samples, including multilayer rough samples and magnetic scattering has generally been completed. Various modifications of the kinematic approximation have been developed taking into account the penetration depth, refraction and renormalization of the collected data. The developed programs have the format of input and output data compatible with the known software package BornAgain that uses the Distorted Wave Born Approximation (DWBA) method.

Below are the results of the simulation of two virtual full reflectometric experiments (diffraction from gold columns on a silicon substrate (**Fig. 1-IV-5**)) in the modified kinematic approximation.

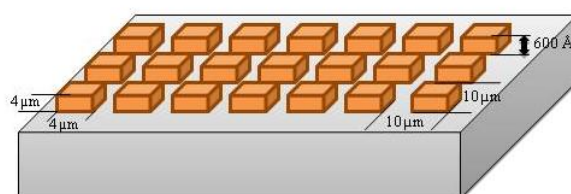


Fig. 1-IV-5. System of gold columns on a silicon substrate [1] (column height – 600 Å, column width – 4×4 μm, spacing in the horizontal plane – 10×10 μm).

The results of the simulation of the system presented in **Fig. 1-IV-5** for a full reflectometric experiment are shown in **Fig. 1-IV-6**.

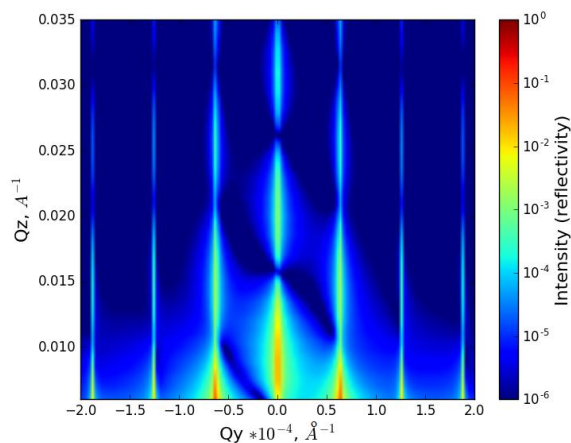


Fig. 1-IV-6. Simulation of a full reflectometric experiment in the modified kinematic approximation of the system of gold columns on a silicon substrate.

The results of the simulation of specular reflection of the system shown in **Fig. 1-IV-5** using four methods are presented in **Fig. 1-IV-7**:

- Parratt method, dynamic theory (the most accurate method);
- Born approximation;
- kinematic approximation with consideration of refraction from the columns;

1. SCIENTIFIC RESEARCH

- kinematic approximation with consideration of refraction from the columns and silicon substrate.

The modified kinematic approximation that takes into consideration the refraction from both the columns and substrate has demonstrated the best agreement with the Parratt method. Thus, taking account of refraction is crucial when using the kinematic approximation.

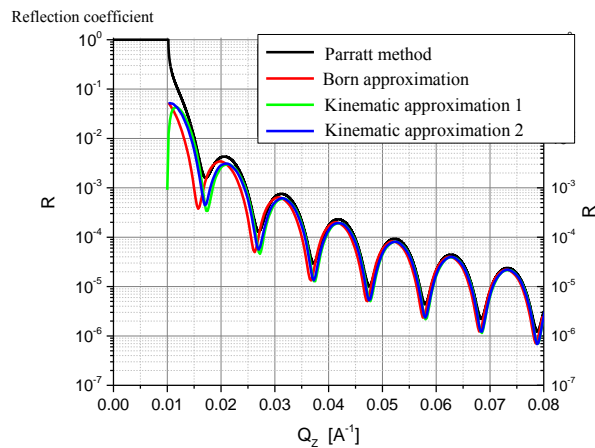


Fig. 1-IV-7. Simulation of specular reflection for the system presented in Fig. 1-IV-5 using various methods.

This is a very common situation when domains observed in multilayer magnetic structures are not ordered, but randomly oriented and randomly distributed in size. In [2], in particular, the analysis of the polarized neutron scattering from a multilayer lamellar iron-chromium system was performed. The magnetic iron layers were assumed to be divided into random domains, with the size distribution of the domains in the neighboring layers being identical, and the magnetization of the domains corresponding to the antiferromagnetic ordering in the adjacent layers. In the simulation, we chose the parameters of the structure similar to those used in [2]: the thickness of each iron layer was chosen to be 90 Å with a 10-Å thick chromium layer being between the iron layers, and the domain size distribution was described by an exponential function.

The result of simulation of the full experiment with magnetic roughness described by the exponential correlation function is shown in Fig. 1-IV-8.

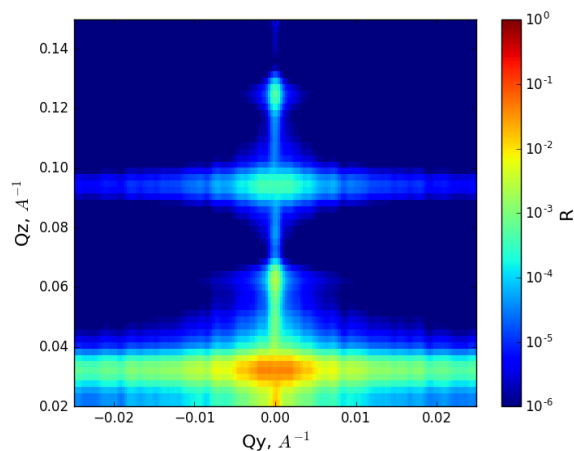


Fig. 1-IV-8. Simulation of iron-chromium multilayer magnetic structures in the modified kinematic approximation.

1. SCIENTIFIC RESEARCH

The simulation results in the modified kinematic approximation qualitatively are almost identical to the results published in [2] for such a system. What is more, this concerns both the measurements and the DWBA simulation.

4. Cryogenics

The following major activities were carried out in 2016 in the framework of the project “Development of PTH sample environment system for the DN-12 diffractometer at the IBR-2 facility”:

- a cryostat for a superconducting magnet with HTSC current leads and a cryostat for a high-pressure cell were manufactured (**Fig. 1-IV-9 (a)**);
- a machine for HTSC tape winding was manufactured (**Fig. 1-IV-9(b)**);
- magnet windings were produced;
- thermal measurements were carried out for both cryostats with a prototype of the magnet in a vertical position with a zero current (**Fig. 1-IV-(c)**);
- equipment and materials required for final assembling and commissioning of the PTH system were purchased.



(a)



(b)



(c)

Fig. 1-IV-9. (a) A cryostat for a superconducting magnet with HTSC current leads, with a cryostat for a high-pressure cell inserted into its shaft, in the mode of operating cryocoolers; (b) Manufacturing of magnet windings on a special machine; (c) Graphs of temperature in various parts of the cryostat versus time (temperature of magnet prototype – Input 6, 7; temperature of warm ends of HTSC current leads – Input 1, 3; sample temperature – Input 8).

1. SCIENTIFIC RESEARCH

The achieved terminal temperatures of the magnet prototype (13 K), warm ends of HTSC current leads (55-57 K), and sample (2.8 K) correspond to the design values.

5. Upgrade of control systems, actuators and sample temperature control systems on the IBR-2 spectrometers

During the reporting period a large amount of work has been carried out to upgrade the actuators of the IBR-2 spectrometers, neutron beam choppers, sample temperature control systems, as well as control systems of these devices. Below are a few examples of these devices.

On the YuMO spectrometer the position adjustment procedure for two detectors in the horizontal and vertical directions in the range of up to 100 mm has been automated, which allows one to accurately position the detectors relative to the beam along the whole path of their movement. A platform with a detector mounted on the position adjustment mechanism is shown in **Fig. 1-IV-10**.



Fig. 1-IV-10. A platform with a detector mounted on the position adjustment mechanism for moving in the horizontal and vertical directions.

The control systems of experimental setups have been upgraded on the HRFD and FSS spectrometers (**Fig. 1-IV-11**). They have become more technological, easy-to-operate and provide:

- connection of up to 5 devices via RS485 interface;
- control over 4 relay signals on the status of the setup;
- connection of additional 3 devices via a USB interface.

The interface converters have been replaced in the control systems as well.

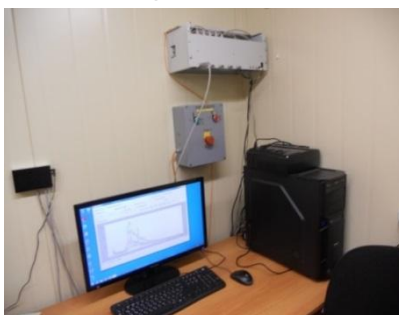


Fig. 1-IV-11. The control system of the setup status on the basis of AC4 (USB-RS485) and AC3-M (RS485-RS232) interface converters on the FSS diffractometer.

A control system of the Fourier-chopper on the FSS spectrometer has been put into operation. The chopper on beamline 9 of the IBR-2 reactor has been moved to the ring corridor. It has been tested with a standard control system and speed sensor on the basis of a reed switch

and magnet. It has been shown that the parameters of the sensor during the operation under high radiation conditions of the ring corridor do not worsen as compared to its operating characteristics in the restricted area.

6. Detectors and electronics

In 2016, the design of a new ring gas detector was developed for detecting small-angle scattering of thermal neutrons on the RTD diffractometer. Photos of the detector elements are presented in **Fig. 1-IV-12**.



Fig. 1-IV-12. Photos of the housing (left), internal part of the detector and 9 independent coaxial rings (right).

The detector is divided into 9 independent equidistant coaxial rings. The cathodes of each ring are divided into 16 independent sectors. The signal pickup is performed from anode wires (shared by all rings) and from each of the 16 cathodes. Thus, this detector system consists of 144 independent detectors. To eliminate the effect of impulse noise and reduce the electronic noise, the preamplifiers of detector elements are arranged inside the gas volume.

At present, the assembling of the detector mechanical units is underway. The digital data acquisition and accumulation electronics are based on the previously developed unified MPD modules.

In 2016, the spectrometer based on a recoil proton telescope, which had been developed in FLNP (see Annual Report 2015) was adjusted and put into trial operation in the National Fusion Research Institute (Daejeon, Republic of Korea) in accordance with Protocol №4519-4-15/17 of 15.06.2015 to study characteristics (in the first place, plasma temperature in the $D(d,n)^3He$ reaction) and perform diagnostics of the nuclear fusion reactor KSTAR (Korea Superconducting Tokamak Advanced Research fusion reactor). First physical data have been obtained and processed. The photo of the spectrometer is shown in **Fig. 1-IV-13**.

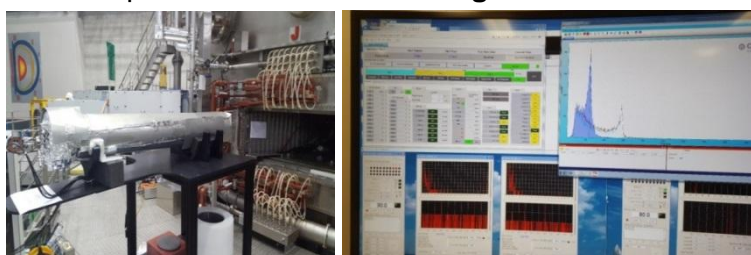


Fig. 1-IV-13. Spectrometer on the basis of a proton recoil telescope at the KSTAR nuclear fusion reactor.

Further development of these activities is proposed with the purpose of improving the energy resolution and enabling the operation in a wide range of neutron energies.

A new 2D position-sensitive detector (2D PSD) of thermal neutrons has been put into operation on the REMUR spectrometer. We have also conducted studies to determine the cause of high-frequency noise on this setup. Their source has been found to be a magnet of the spin-flipper.

1. SCIENTIFIC RESEARCH

Recommendations on the elimination of the problem have been made. The 2D PSD on the REMUR spectrometer and measurement results are shown in **Fig. 1-IV-14**. A similar detector has been put into service on the RTD diffractometer.

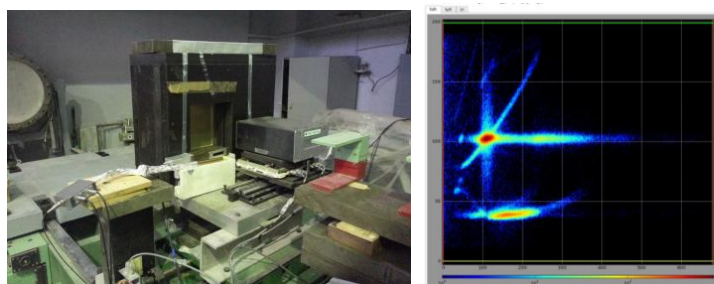


Fig. 1-IV-14. 2D PSD on the REMUR spectrometer (left) and measurement results (right).

We have carried out a series of methodological studies aimed at increasing the PSD service life and the optimization of its gas mixture for use in direct beams. A prototype of PSD on the basis of a multiwire proportional chamber with a ^{10}B converter has been developed and tested (**Fig. 1-IV-15**). These activities have been performed in the framework of the collaborative work on the ESS project (Lund, Sweden).

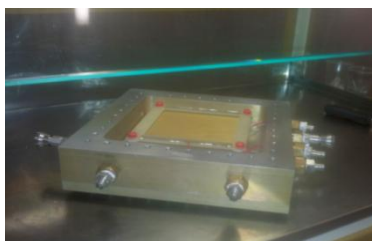


Fig. 1-IV-15. A prototype of PSD with a 10B converter.

In 2015, we completed the manufacturing and commissioning of scintillation counters of the fourth section of the ASTRA detector on the FSD diffractometer. In the process of this work a new design of the counters and a more convenient scheme of their arrangement in the ASTRA detector were proposed. The new design makes it possible to significantly reduce the material and human resources required for the manufacturing of the detector. In 2016, the necessary calculations of the geometry of the detector and its optimization were done for the maximum unification of elements. A 3D model of one of the planes of the new “Astra” detector is shown in **Fig. 1-IV-16**. A technical project for the detector system has been developed.

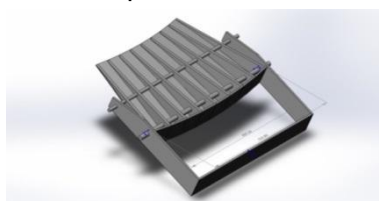


Fig. 1-IV-16. A 3D model of one of the planes of the new “Astra” detector.

The research and optimization of the scintillation detector on the FSD spectrometer have been carried out. High-voltage power sources have been replaced on FSD and HRFD. For acquisition and accumulation of data from two lithium-glass scintillation detectors of the FSS spectrometer the detector electronics modules received from GKSS (Germany) have been

1. SCIENTIFIC RESEARCH

adjusted. In addition, a 32-channel discriminator module and controller MPD-32 have been manufactured and adjusted (**Fig. 1-IV-17**).



Fig. 1-IV-17. Electronics of high-voltage power supply of detectors (top crate), modules of detector electronics and data acquisition electronics (bottom crate).

Methodological work has been carried out on the investigation of possibilities of using multichannel digitizers to acquire data from position-sensitive neutron detectors. At the requests of the researchers measurements of the neutron beam profiles on the 5, 9 and 13 beamlines of the IBR-2 reactor have been performed using a PSD.

7. Software and computer infrastructure

In 2016, in the framework of development of the software package Sonix+ the following activities were done:

- Modules to support new devices on the spectrometers were developed and put into service:
 - new Fourier chopper (HRFD);
 - new sample temperature control systems (HRFD, RTD, DN-6 and REMUR);
 - magnetometer and power sources (REMUR).
- The FSD spectrometer was put under control of OS Windows 7.
- A standard version of the user interface was installed on the DN-6 and DN-12 spectrometers.
- At the requests of the experimenters we carried out work on improving the user interface, position adjustment program and some process execution modules.
- Conversion of Python-based programs from Python 2.6 to Python 3 started.
- A new, more reliable and secure version of WebSonix was prepared.

The installation of an FLNP LAN standby server *nfserv-d* (CPU: E5-2650 V3 (2×10 cores); 64 GB RAM; 12 TB disk space) has been completed, on which the Linux operating system is installed. The server is put into trial operation and used for computational purposes, as well as for methodological studies to enhance the fault tolerance and operational efficiency of LAN servers.

References

[1] Metting Christopher Jason. (2011). Characterization and modeling of off-specular neutron scattering for analysis of two dimensionally ordered structures, Dissertation submitted to the Faculty of the Graduate School of the University of Maryland, College Park in partial fulfillment of the requirements for the degree of Doctor of Philosophy.

drum.lib.umd.edu/bitstream/1903/12439/1/Metting_umd_0117E_12778.pdf

[2] Lauter H., Lauter-Pasyuk V., Toperverg B. et al. // J. Magn. Magn. Mat. 2003. V. 258–259. p. 338.

2. NEUTRON SOURCES

I. THE IBR-2 PULSED REACTOR

In 2016, the activities on the research nuclear facility IBR-2 (RNF IBR-2) were carried out in accordance with the objectives of the theme "Development of the IBR-2 Facility with a Complex of Cryogenic Neutron Moderators"

At the RNF IBR-2 a cyclic mode of operation is adopted, in which the reactor is operated continuously at a power for 180÷400 hours in accordance with its schedule of operation for the current year.

In 2016, the IBR-2 research nuclear facility was operated in a nominal on-power mode under Rostekhnadzor license № valid until 30.09.2022.

Statistical data on the IBR-2 operation of IBR-2 for physics experiments are presented in **Table 2-I-1**.

Table 2-I-1. presents data on the IBR-2 operation for physics experiments.

No cycle	Period	Reactor operation for physics experiments, hr	Moderator type
1	18.01-29.01	262	water
2	08.02-19.02	262	water
3	14.03-28.03	328	water
4	04.04-18.04	328	water
5	16.05-27.05	120	water
6	26.09-07.10	canceled due to technical reasons	
7	17.10-03.11	408	water
8	15.11-25.11	237	cryogenic
9	05.12-26.12	502	water
TOTAL		2447	

The reasons for the IBR-2 shutdowns in 2016 were:

- The emergency shutdown on 06.04.2016 at 16:32 was caused by a voltage drop in the 10-kV bus section I of the main step-down substation GPP-2 as a result of an outage of the power transmission line PTL-110 kV "Tempy-Dubna-2" (outside the area of responsibility of JINR).
- The safety shutdown system was activated on 20.05.2016 at 04:40 because of a short-term power outage of the RNF IBR-2 caused by a voltage drop in the 10-kV bus section I of GPP-2 as a result of a failure of the bushing insulators of line 11 of the feeder of the central power distribution station CRP-1 of GPP-2 (in the area of responsibility of JINR).
- The emergency shutdown on 26.05.2016 at 16:06 was caused by a voltage drop in the 10-kV bus section I of GPP-2 as a result of short circuits in the municipal electric power supply system (outside the area of responsibility of JINR).
- The safety shutdown system was triggered on 27.05.2016 at 10:49 because of a voltage drop in the 10-kV bus section I of GPP-2 as a result of actuation of ground-fault protection in box №3 "Atoll" at CRP-8 (outside the area of responsibility of JINR).

Due to multiple power supply failures in May 2016 caused by voltage drops, cycle №5 of IBR-2 operation for physical experiments was terminated before the scheduled date with a loss of about 130 hours of experimental beam time.

II. IREN FACILITY

At the end of 2015 the second accelerating section was installed instead of the drift gap at the LUE-200 accelerator. In the early 2016 the connection of technical systems for the second accelerating section was made and a complex check of all systems of the accelerator was done. The existing accelerator configuration: the first section is powered by an E3730A Toshiba klystron, the second one – by a 2129 Thomson klystron. The power supply of klystrons is provided by Dawonsys modulators.

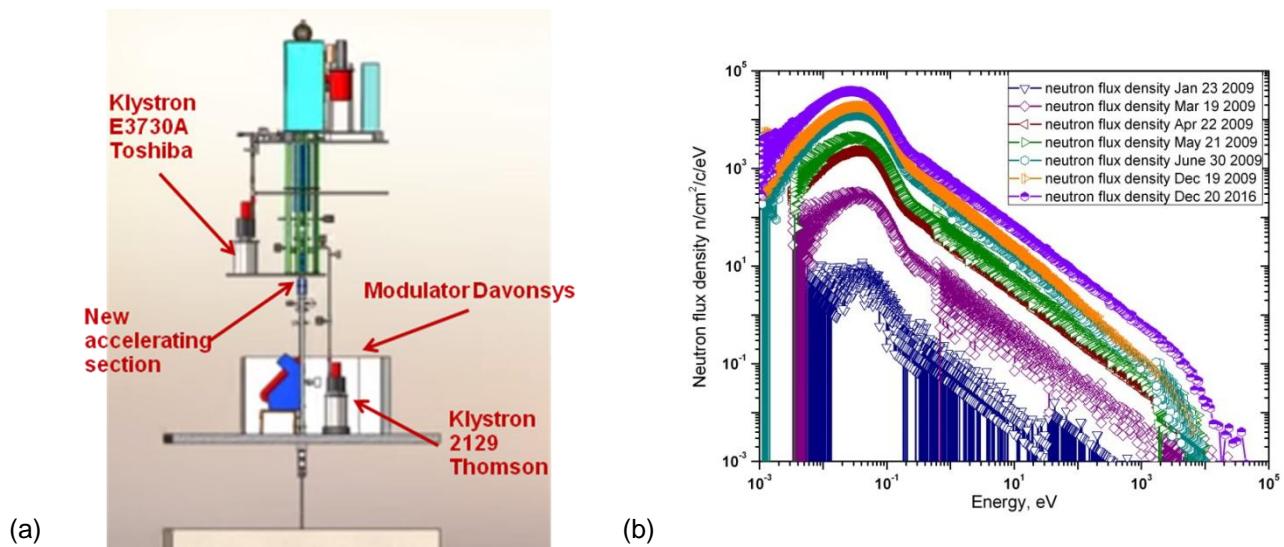


Fig. 2-II-1. (a) Scheme of a new configuration of the accelerator; (b) Spectra of neutron flux density from IREN obtained during the development of the facility.

During 2016 the training of the accelerating systems with the gradual achievement of nominal operating parameters was carried out. In December the facility operated within nominal parameters at a frequency of 50 Hz without any failures during one week. Preliminary measurements of the neutron flux were carried out. The estimation showed an increase of the neutron yield by at least 3 times in comparison with the operation with one section.

III. EG-5 ACCELERATOR

In 2016, the EG-5 accelerator operated for experiments for 620 hours. Experimental studies on charged particle beams using nuclear analytical methods of Rutherford backscattering (RBS) and elastic recoil detection (ERD) were conducted in cooperation with representatives of various institutes of the JINR Member States (Institute of Applied Physics of NAS, Sumy, Ukraine; Institute of Electrical Engineering of SAS, Bratislava, Slovakia; Maria Curie-Skłodowska-University, Lublin, Poland), Russian institutes (A.M.Prokhorov General Physics Institute of RAS, Moscow; B.P.Konstantinov Petersburg Nuclear Physics Institute, Gatchina; Voronezh State University), as well as of the JINR laboratories (DLNP, FLNR). Samples of different elemental composition and various preparation technologies were analyzed. The structure and properties of silicon and oxide films, the processes of accumulation and distribution of hydrogen and deuterium in the samples, the effect of proton irradiation on the characteristics of composite HTSC materials were investigated.

3. PUBLICATIONS

PUBLISHED PAPERS

DEPARTMENT OF NEUTRON INVESTIGATION OF CONDENSED MATTER

Atomic and magnetic structures (diffraction)

1. Аксенов В.Л., Балагуров А.М. "Дифракция нейтронов на импульсных источниках". **УФН**, 2016, т. 186 (3), с. 293-320.
2. Аксенов В.Л., Балагуров А.М., Козленко Д.П. "Исследования конденсированного состояния вещества на модернизированном реакторе ИБР-2: от функциональных материалов до нанобиотехнологий". **ЭЧАЯ**, 2016, т.47(4), с. 1154-1191. (Aksenov V.L., Balagurov A.M. and Kozlenko D.P. "Condensed Matter Research at the Modernized IBR-2 Reactor: from Functional Materials to Nanobiotechnologies". **Physics of Particles and Nuclei**, 2016, v. 47 (4), p. 627-646.)
3. Балагуров А.М., Бобриков И.А., Сумников С.В., Юшанхай В.Ю., Миронова-Улмане Н. "Магнитно-структурные фазовые переходы в NiO и MnO: нейтронные дифракционные данные". **Письма в ЖЭТФ**, 2016, т.104 (2), с.84-90.
4. Балагуров А.М., Бобриков И.А., Мухаметулы Б., Сумников С.В., Головин И.С. "Когерентное кластерное упорядочение атомов в интерметаллиде Fe-27Al". **Письма в ЖЭТФ**, 2016, т. 104(8), с. 560-567.
5. Бобриков И. А., Мухаметулы Б., Балагуров А. М. "Нейтроннографический анализ микроструктуры дисперсионно-твердеющих сталей". **ФММ**, 2016, т. 117 (10), с. 1082-1088. (Bobrikov I.A., Mukhametuly B., Balagurov A.M. "Neutron Diffraction Analysis of the Microstructure of Dispersion-Hardening Steels" **The Physics of Metals and Metallography**, 2016, Vol. 117, No. 10, p.1047-1053.)
6. Бобриков И.А., Самойлова Н.Ю., Балагуров Д.А., Иваньшина О.Ю., Дрожжин О.А., Балагуров А.М. "Анализ структурных трансформаций в литий-ионном аккумуляторе с помощью дифракции нейтронов". **Электрохимия**, 2017, том 53, № 2, с. 1-10.
7. Сиколенко В.В., Ефимов В.В., Ефимова Е.А., Тютюнников С.И., Карпинский Д.В., Троянчук И.О., Селютин А.Г., Keller L., Ritter C. "Нейтроннографические исследования перехода антиферромагнит-ферромагнит в кобальтах с дефицитом анионов". **Поверхность. Рентгеновские, синхротронные и нейтронные исследования**. 2016, № 11, с. 12-16.
8. Ata-Allah S.S., Balagurov A.M., Hashhash A., Bobrikov I.A., Hamdy Sh. "Refinement of atomic and magnetic structures using neutron diffraction for synthesized bulk and nano nickel zinc gallate ferrite". **Physica B**, 2016, v. 481, p. 118-123.
9. Balagurov A.M., Bobrikov I.A., Sumnikov S.V., Yushankhai V.Yu., Grabis J., Kuzmin A., Mironova-Ulmane N., Sildos I. "Neutron diffraction study of microstructural and magnetic effects in fine particle NiO powders". **Physica status solidi (B)**, 2016, vol. 253(8), p. 1529-1536.
10. Balagurov A.M., Bobrikov I.A., Golovin I.S., Cheverikin V.V., Golovin S.A. "Stabilization of bcc-born phases in Fe-27Ga by adding Tb: Comparative in situ neutron diffraction study". **Materials Letters**, 2016, vol.181, p. 67-70.
11. Burzo E., Kozlenko D.P., Dang N.T., Kichanov S.E., Golosova N.O. "Structural and magnetic properties of Ca_{1.5}La_{0.5}FeMoO₆ perovskite at high pressures". **Journal of Alloys and Compounds**, 2016, vol. 664, p. 363-368.
12. Dang N.T., Kozlenko D.P., Phan T.L., Kichanov S.E., Dang N.V., Thanh T.D., Khiem L.H., Jabarov S.H., Tran T.A., Vo D.B., Savenko B.N. "Structural Polymorphism of Mn-Doped BaTiO₃". **Journal of Electronic Materials**, 2016, vol. 45, p. 2477-2483.
13. Dang N.T., Zakhvalinskii V.S., Kozlenko D.P., Nekrasova Yu. S., The-Long Phan, Ta Thu Thang, Kichanov S.E., Thanh T.D., Savenko B.N., Khiem L.H., Taran S.V., Jabarov S.G. "Crystal structure, magnetic properties and conductivity mechanisms of La_{0.7}Ca_{0.3}Mn_{0.5}Fe_{0.5}O₃". **Ferroelectrics**, 2016, vol. 501, p. 129-144.
14. Efimov V.A., Ignatov A., Troyanchuk I.O., Sikolenko V.V., Rogalev A., Wilhelm F., Efimova E., Karpinsky D., Kriventsov V., Yakimchuk E., Molodtsov S., Sainctavit P., Prabhakaran D. "Co K-edge magnetic circular dichroism across the spin state transition in LaCoO₃ single crystal". **Journal of Physics: Conference Series**, 2016, vol. 712, p. 012111.
15. Golosova N.O., Kozlenko D.P., Kichanov S.E., Lukin E.V., Dubrovinsky L.S., Mammadov A.I., Mehdiyeva R.Z., Jabarov S.H., Liermann H-P, Glazyrin K.V., Dang T.N., Smotrakov V.G., Eremkin V.V, Savenko B.N. "Structural, magnetic and vibrational properties of multiferroic GaFeO₃ at high pressure". **Journal of Alloys and Compounds**, 2016, vol. 684, p. 352-358.
16. Golovin I.S., Balagurov A.M., Palacheva V.V., Bobrikov I.A., Zlokazov V.B. "In situ neutron diffraction study of bulk phase transitions in Fe-27Ga alloys". **Materials and Design**, 2016, vol. 98, p. 113-119.
17. Golovin I.S., Balagurov A.M., Bobrikov I.A., Cifre J. "Structure induced anelasticity in Fe₃Me (Me = Al, Ga, Ge) alloys". **Journal of Alloys and Compounds**, 2016, vol. 688, p. 310-319.
18. Golovin I.S., Balagurov A.M., Bobrikov I.A., Palacheva V.V., Cifre J. "Phase transition induced anelasticity in Fe-Ga alloys with 25 and 27%Ga". **Journal of Alloys and Compounds**, 2016, vol. 675, p.393-398.
19. Gridnev S.A., Kamynin A.A., Shportenko A.S., Kulakov P.V., Hahlenkov M.V., Kozlenko D.P., Savenko B.N., Kichanov S.E., Lukin E.V. "Dielectric relaxation in magnetoelectric composite 0.85 BiFeO₃-0.15 MgFe₂O₄". **Bulletin of the Russian Academy of Sciences: Physics**, 2016, vol.80, № 9, p.1092-1096.
20. Istomin S.Ya., Karakulina O.M., Rozova M.G., Kazakov S.M., Gippius A.A., Antipov E.V., Bobrikov I.A., Balagurov A.M., Tsirlin A.A., Micheau A., Biendicho J.J., Svensson G. "Tuning the high-temperature properties of Pr₂NiO_{4±δ} by simultaneous Pr- and Ni- cations replacement". **RSC Advances (Royal Society of Chemistry)**, 2016, vol. 6, p. 33951-33958.
21. Istomin S.Ya., Chernova V.V., Antipov E.V., Lobanov M.V., Bobrikov I.A., Yushankhai V.Yu., Balagurov A.M., Hsu K. Y., Lin J.-Y., Chen J. M., Lee J. F., Volkova O.S., Vasiliev A.N. "Wide range tuning of Mo oxidation state in La_{1-x}Sr_xFe_{2/3}Mo_{1/3}O₃ perovskites". **European Journal of Inorganic Chemistry**, 2016, vol. 2016 (18), p. 2942-2951.
22. Ivanshina O.Yu., Bobrikov I.A., Sumnikov S.V. and Balagurov A.M. "The methodology of electrode manufacturing for special designed lithium-ion cells". **Сборник трудов ОМУС-2016**, 2016, № 181, p. 37.
23. Kamynin A.A., Gridnev S.A., Kozlenko D.P., Kichanov S.E., Lukin E.V., Savenko B.N. "Features of the electrical

- resistance in magnetoelectric ceramics (1-x) BiFeO₃-x MgFe₂O₄". **Ferroelectrics**, 2016, vol. 501, p.114-121.
24. Karpinsky D.V., Troyanchuk I.O., Zheludkevich A.L., Ignatenko O.V., Silibin M.V. and Sikolenko V.V. "Crystal Structure and Piezoelectric and Magnetic Properties of Bi_{1-x}Sm_xFeO₃ Solid Solutions". **Physics of the Solid State**, 2016, vol. 58, p. 1590-1595.
 25. Karpinsky D.V., Troyanchuk I.O., Silibin M.V., Gavrilov S.A., Bushinsky M.V., Sikolenko V., Frontzek M. "Structure and magnetic interactions in (Sr,Sb)-doped lanthanum manganites". **Physica B**, 2016, vol. 489, p. 45-50.
 26. Kosova N.V., Bobrikov I.A., Podgornova O.A., Balagurov A.M., Gutakovskii A.K. "Peculiarities of structure, morphology, and electrochemistry of the doped 5-V spinel cathode materials LiNi_{0.5-x}Mn_{1.5-y}M_{x+y}O₄ (M = Co, Cr, Ti; x+y=0.05) prepared by mechanochemical way". **Journal of Solid State Electrochemistry**, 2016, vol. 20, p. 235-246.
 27. Kosova N.V., Podgornova O.A., Bobrikov I.A., Kaichev V.V., Bukhtiyarov A.V. "Approaching better cycleability of LiCoPO₄ by vanadium modification". **Materials Science and Engineering B**, 2016, vol. 213, p. 105–113.
 28. Kozlenko D.P., Dang N.T., Kichanov S.E., Dang N.V., Khiem L.H., Lukin E.V., Savenko B.N. "Neutron-diffraction study of the crystal structure of BaTiO₃ ferroelectric doped with iron". **Journal of Surface Investigation. X-ray, Synchrotron and Neutron Techniques**, 2016, vol. 10, № 2, p. 370-374.
 29. Kurlov A.S., Gusev A.I., Gerasimov E.Yu., Bobrikov I.A., Balagurov A.M., Rempel A.A. "Nanocrystalline ordered vanadium carbide: Superlattice and nanostructure". **Superlattices and Microstructures**, 2016, vol. 90, p. 148-164.
 30. Ovsyannikov S.V., Bykov M., Bykova E., Kozlenko D.P., Tsirlin A.A., Karkin A.E., Shchennikov V.V., Kichanov S.E., Gou H., Abakumov A.M., Egoavil R., Verbeeck J., McCammon C., Dyadkin V., Chernyshov D., S. van Smaalen, Dubrovinsky L.S. "Charge-ordering transition in iron oxide Fe₄O₅ involving competing dimer and trimer formation". **Nature Chemistry**, 2016, vol. 8, № 5, p. 501-508.
 31. Sherstobitova E.A., Gubkina A.F., Bobrikov I.A., Kalashnova A.V., Pantyukhin M.I. "Bottle-necked ionic transport in Li₂ZrO₃: high temperature neutron diffraction and impedance spectroscopy". **Electrochimica Acta**, 2016, vol. 209, p. 574–581.
 32. Sikolenko V., Troyanchuk I., Efimov V., Efimova E., Karpinsky D., Pascarelli S., Zakharko O., Ignatov A., Aquilanti D., Selutin A., Shmakov A., Prabhakaran D. "EXAFS and X-Ray diffraction study of LaCoO₃ across the spin-state transition". **Journal of Physics: Conference Series**, 2016, vol. 712, p. 012118.
 33. Sikolenko V., Troyanchuk I., Karpinsky D., Schorr S., Silibin M., Ritter C., Schilling F.R. "High pressure effects on the magnetic and crystal structure of La_{0.75}Ba_{0.25}CoO₃". **Material Chemistry and Physics**, 2016, vol. 181, p. 78-81.
 34. Troyanchuk I.O., Tereshko N.V., Silibin M.V., Gavrilov S.A., Nekludov K.N., Sikolenko V., Schorr S., Szymczak H. "Magnetic Ordering in Manganites Doped by Ti and Al". **Ceramics International**, 2016, online available DOI: 10.1016/j.ceramint.2016.09.132.
 35. Trukhanov S.V., Trukhanov A.V., Turchenko V.A., Kostishin V.G., Panina L.V., Kazakevich I.S., Balagurov A.M. "Crystal structure and magnetic properties of the BaFe_{12-x}In_xO₁₉ (x=0.1–1.2) solid solutions". **Journal of Magnetism and Magnetic Materials**, 2016, vol. 417, p. 130-136.
 36. Trukhanov S.V., Trukhanov A.V., Turchenko V.A., Kostishyn V.G., Panina L.V., Kazakevich I.S., Balagurov A.M. "Structure and magnetic properties of BaFe_{11.9}In_{0.1}O₁₉ hexaferrite in a wide temperature range". **Journal of Alloys and Compounds**, 2016, vol. 689, p. 383-393.
 37. Turchenko V., Trukhanov A., Trukhanov S., Bobrikov I., Balagurov A.M. "Features of crystal and magnetic structures of solid solutions BaFe_{12-x}D_xO₁₉ (D = Al³⁺, In³⁺; x = 0.1) in a wide temperature range". **The European Physical Journal plus**, 2016, vol. 131, p. 82.
 38. Valkov S., Neov D., Luytov D. and Petrov P. "Neutron Diffraction of Titanium Aluminides Formed by Continuous Electron-Beam Treatment". **19th International Summer School on Vacuum, Electron and Ion Technologies (VEIT2015)**, 21 – 25 September 2015, Sozopol, Bulgaria, **Journal of Physics: Conference Series**, 2016, vol. 700, p. 012034.
 39. Vu M.T., Kozlenko D.P., Kichanov S.E., Troyanchuk I.O., Lukin E.V., Khiem L.H., Savenko B.N. "Pressure induced antiferromagnetism in the manganite La_{0.7}Sr_{0.3}Mn_{0.83}Nb_{0.17}O₃". **Journal of Alloys and Compounds**, 2016, vol. 681, p. 527-531.

Nanostructured materials (small-angle scattering and diffraction)

40. Samoilenko S.O., Kichanov S.E., Kozlenko D.P., Ivankov O.I., Gurin V.S., Rachkovskaya G.E., Zakharevych G.B., Bulavin L.A., Islamov A. Kh., Savenko B.N. "Study of silicate glasses with PbS nanoparticles using small-angle neutron scattering". **Journal of Surface Investigation. X-ray, Synchrotron and Neutron Techniques**, 2016, vol. 10, № 1, p. 187-190.
41. Doroshkevich O., Shylo A., Lyubchik A., Kirilov A., Glazunova V., Zelenyak T., Burkhovetsky V., Troitskiy G., Vasilenko T., Bacherikov Yu., Sinyakina S., Akhkozov L., Turchenko V., Bodnarchuk V., Doroshkevich V., Kholmurodov Kh. Konstantinova T. "Investigation of nanopowder dispersed system based on zirconia by transmission electron microscopy, electrochemical impedance spectroscopy and spin-echo". **Material Science. Nonequilibrium phase transformations**, 2016, Issue 1, p. 22-25.
42. Doroshkevych A.S., Shilo A.V., Volkova G.K., Glazunova V.A., Perekrestova L.D., Lyubchik S.B., Konstantinova T.E. "Formation of nanostructured state in LaBGeO₅ monolithic glass using pulsed magnetic fields". **Semiconductor Physics, Quantum Electronics and Optoelectronics**, 2016, vol.19, № 3, p. 267-272.

Soft matter, liquids (small angle scattering and diffraction)

43. Кизима Е.А., Кузьменко М.О., Булавин Л.А., Петренко В.И., Михеев И.В., Заболотный М.А., Кубовскава М., Корсанский Р., Коробов М.В., Авдеев М.В., Аксенов В.Л. "Влияние физиологической среды на агрегационное состояние фуллеренов C₆₀ и C₇₀". **Поверхность. Рентгеновские, Синхротронные и Нейтронные Исследования**, 2016, № 11, стр. 3–6.
44. Петренко В.И., Авдеев М.В., Булавин Л.А., Алмаши Л., Григорьева Н.А., Аксенов В.Л. "Влияние избытка поверхностно-активных веществ на устойчивость магнитных жидкостей на основе слабополярного растворителя по данным малоуглового рассеяния нейтронов". **Кристаллография**, 2016, т. 61, № 1, стр. 132-137. (Petrenko V.I., Avdeev M.V., Bulavin L.A., Almasy L., Grigoryeva N.A., Aksenov V.L. "Effect of

3. PUBLICATIONS

- surfactants excess on the stability of low-polarity ferrofluids probed by small-angle neutron scattering". **Crystallography reports**, 2016, vol. 61, Issue 1, p. 121-125).
45. Tropin T.V., Schmelzer J.W.P., Aksenov V.L. "Modern aspects of the kinetic theory of glass transition". **Physics – Uspekhi**, 2016, vol. 59, Issue 1, p. 42-66 (Тропин Т.В., Шмельцер Ю.В.П., Аксенов В.Л. "Современные аспекты кинетической теории стеклования". **Успехи физических наук**, 2016, т. 186, №1, стр. 47-73).
 46. Хусенов М.А., Холмуродов Х.Т. "Молекулярно-динамическое моделирование ван-дер-ваальсовой системы из нуклеотидной цепочки с наночастицами золота в матрице углеродной нанотрубки". **Вестник Воронежского государственного технического университета**, 2016, том 12, Выпуск №1, стр. 81-87.
 47. Anitas E.M., Osipov V.A., Kuklin A.I., Cherny A.Yu. "Influence of randomness on small-angle scattering from deterministic mass fractal". **Romanian Journal of Physics**, 2016, vol.61, nos. 3-4, p. 457-463, Bucharest.
 48. Avdeev M.V., Tomchuk O.V., Ivankov O.I., Alexenskii A.E., Dideikin A.T., Vul' A.Ya. "On the structure of concentrated detonation nanodiamond hydrosols with a positive ζ potential: analysis of small-angle neutron scattering". **Chemical Physics Letters**, 2016, vol. 658, p. 58-62.
 49. Balasoiu M., Bica I., "Composite magnetorheological elastomers as dielectrics for plane capacitors: effects of magnetic field intensity". **Results in Physics**, 2016, vol. 6, p. 199-202.
 50. Bica I., Balasoiu M., Bunoiu M., Iordaconiu I., „Microparticles and electroconductive magnetorheological suspensions". **Romanian Journal of Physics**, 2016, vol. 61, № 5-6.
 51. Bodale I., Oprisan M., Stan C., Tufescu F., Racuciu M., Creanga D., Balasoiu M. "Nanotechnological Application Based on CoFe₂O₄ Nanoparticles and Electromagnetic Exposure on Agrotechnical Plant Growth", **Chapter 3rd International Conference on Nanotechnology and Biomedical Engineering**, 2016, Volume 55, Series IFMBE Proceedings, Springer Singapore, ISBN 978-981-287-735-2, p. 153-156.
 52. Bulavin L., Kutsevol N., Chumachenko V., Soloviov D., Kuklin A. & Marynin A. "SAXS Combined with UV-vis Spectroscopy and QELS: Accurate Characterization of Silver Sols Synthesized in Polymer Matrices". **Nanoscale research letters**, 2016, vol. 11(1), p. 1-8.
 53. Byvshhev I.M., Vangeli I.M., Murugova, T.N., Ivankov O.O., Kuklin A.I., Popov V.I. & Yaguzhinsky L.S. "On the existence of two states of OXPHOS system supercomplex in heart mitochondria". **Biochimica et Biophysica Acta (BBA)-Bioenergetics**, 2016, vol. 1857, e35-e36.
 54. Davide B., Lagana G., Toscano G., Calandra P., Kiselev M.A., Lombardo D., Bellocco E. "The interaction and binding of flavonoids to human serum albumin modify its conformation, stability and resistance against aggregation and oxidative injuries". **Biochimica et Biophysica Acta**, 2016. In press. BBAGEN-28417; No. of pages: 9.
 55. Dordovic V., et al., "Cation-sensitive compartmentalization in metallacarborane containing polymer nanoparticles". **RSC Advances**, 2016, vol. 6 (12), p. 9884-9892.
 56. Egorov V.V., Gorshkov A.N., Murugova T.N., Vasin A.V., Lebedev D.V., Isaev-Ivanov V.V. & Kiselev O.I. "Characterization of oligomerization of a peptide from the ebola virus glycoprotein by small-angle neutron scattering". **Crystallography Reports**, 2016, vol. 61(1), p. 94-97.
 57. Egorov V.V., Shaldzhyan A.A., Gorshkov A.N., Zabrodskaya Y.A., Lebedev D.V., Kuklin A.I. & Isaev-Ivanov V.V. "On the structural features of influenza A nucleoprotein particles from small-angle X-ray scattering data". **Journal of Surface Investigation. X-ray, Synchrotron and Neutron Techniques**, 2016, vol. 10(2), p. 322-325.
 58. Gorshkova Yu.E., Kuklin A.I. and Gordeliy V.I. "Structure and Phase Transitions of ДМФХ Multilamellar Vesicles in the Presence of Ca²⁺ Ions". **Journal of Surface Investigation: X-ray, Synchrotron and Neutron Techniques**, 2016, vol. 10, № 6, p. 1154–1164. DOI: 10.1134/S1027451016050499.
 59. Jargalan N., Tropin T.V., Avdeev M.V., Aksenov V.L. "Investigation and modeling of evolution of UV-Vis spectra of C60/NMP solution". **Nanosystems: physics, chemistry, mathematics**, 2016, vol. 7, Issue 1, p. 99-103.
 60. Kadochnikov V.V., Egorov V.V., Shvetsov A.V., Kuklin A.I., Isaev-Ivanov V.V. & Lebedev D.V. "Modeling of conformational transitions of fibrillogenic peptide, homologous to beta-domain of human alpha-lactalbumin". **Crystallography Reports**, 2016, vol. 61(1), p. 98-105.
 61. Khusenov M.A., Dushanov E.B., Kholmurodov Kh.T., Zaki M.M., Sweilam N.H. "On Correlation Effect of the Vander-Waals and Intramolecular Forces for the Nucleotide Chain - Metallic Nanoparticles - Carbon Nanotube Binding". **The Open Biochemistry Journal**, 2016, vol. 10, p.17-26. DOI: 10.2174/18744091X01610010017.
 62. Kulvelis Y.V., et al. "Structure and properties optimization of perfluorinated short side chain membranes for hydrogen fuel cells using orientation stretching". **RSC Advances**, 2016, vol. 6, p. 108864–108875.
 63. Lombardo D., Calandra P., Barreca D., Magazu S., Kiselev M.A. "Soft Interaction in Liposome Nanocarriers for Therapeutic Drug Delivery". **Nanomaterials**, 2016, vol. 6, № 125, p. 2-26; doi:10.3390/nano6070125, www.mdpi.com/journal/nanomaterials.
 64. Lombardo D., Calandra P., Bellocco E., Lagana G., Barreca D., Magazu S., Wanderlingh U., Kiselev M.A. "Effect of anionic and cationic polyamidoamine (PAMAM) dendrimers on a model lipid membrane". **Biochimica et Biophysica Acta**, 2016, vol. 1858, p. 2769–2777. <http://dx.doi.org/10.1016/j.bbamem.2016.08.001>. Elsevier B.V.
 65. Majorosova J., Petrenko V.I., Siposova K., Timko M., Tomasovicova N., Garamus V.M., Koralewski M., Avdeev M.V., Leszczynski B., Jurga S., Gazova Z., Hayryan Sh.,Hu Chin-Kun, Kopcansky P. "On the adsorption of magnetite nanoparticles on lysozyme amyloid fibrils". **Colloids and Surfaces B**, 2016, vol.146, p. 794–800.
 66. Nagornyi A.V., Petrenko V.I., Avdeev M.V., Solopan S.O., Yelenich O.V., Belous A.G., Veligzhanin A.A., Gruzinov A.Yu., Zubavichus Ya.V., Bulavin L.A. "Structure of water-based magnetic liquids by small-angle x-ray scattering". **Romanian Journal of Physics**, 2016, vol. 61, Issues 3-4, p. 483-490.
 67. Ordon M., Gorshkova Y. & Ossowska-Chruściel M.D. "Lithocholic acid derivative in the presence of dimethyl sulfoxide: Morphology and phase transitions". **Thermochemica Acta**, 2016, vol. 643, p. 1-12.
 68. Petrenko V.I., Ivankov O.I., Avdeev M.V., Nikolaienko T.Yu. "Spatial structure of liquid systems with organic-coated magnetite nanoparticles". **Bulletin of Taras Shevchenko National University of Kyiv Series Physics & Mathematics**, 2015, Issue 3, p. 203-206.

3. PUBLICATIONS

69. Prylutsky Y., Borowik A., Goluński G., Woziwodzka A., Piosik J., Kyzyma O., Pashkova I., Ritter U., Evstigneev M. "Biophysical characterization of the complexation of C60 fullerene with doxorubicin in a prokaryotic model". **Materialwissenschaft und Werkstofftechnik**, 2016, vol. 47, issue 2-3, p. 92–97, <http://onlinelibrary.wiley.com/doi/10.1002/mawe.201600463/full>.
70. Prylutsky Yu.I., Cherepanov V.V., Kostjukov V.V., Evstigneev M.P., Kyzyma O.A., Bulavin L.A., Ivankov O., Davidenko N.A. and Ritter U. "Study of the complexation between Landomycin A and C60 fullerene in aqueous solution". **RSC Advances**, 2016, vol. 6, p. 81231-81236.
71. Puscasu E, Sacarescu L., Lupu N., Grigoras M., Oanca G., Balasoiu M., Creanga D., "Iron oxide-silica nanocomposites yielded by chemical route and sol-gel method". **Journal of Sol-Gel Science and Technology**, 2016, vol. 79(3), p. 457–465, doi10.1007/s10971-016-3996-1.
72. Puscasu E., Sacarescu L., Domocos A., Leostean C., Turcu R., Creanga D., Balasoiu M., "Hydrophilic Versus Hydrophobic Oleate Coated Magnetic Particles". **Romanian Journal of Physics**, 2016, vol. 61, p. 5-6.
73. Rada M., N.Aldea, Z.H.Wu, Z.Jing, S.Rada, E.Culea, S.Macavei, R.Balan, R.C.Suciu, R.V.Erhan, V.Bodnarchuk. "Evolution of the germanium–oxygen coordination number in lithium–lead–germinate glasses". **Journal of Non-Crystalline Solids**, 2016, vol. 437, p. 10–16.
74. Rajewska A., Medrzycka K., Hallmann E. & Soloviov D.V. "Small-angle neutron scattering study of the structure of mixed micellar solutions based on heptaethylene glycol monotetradecyl ether and cesium dodecyl sulfate". **Crystallography Reports**, 2016, vol. 61(1), p. 126-128.
75. Ryzhkov A., Melenev P., Raikher Yu., Balasoiu M., "Structure organization and magnetic properties of microscale ferrogels: the effect of particle magnetic anisotropy". **Journal of Chemical Physics** 2016, vol. 145, p. 074905, <http://dx.doi.org/10.1063/1.4961299>.
76. Schmidt A.E., Shvetsov A.V., Kuklin A.I., Lebedev D.V., Surzhik M.A., Sergeev V.R. & Isaev-Ivanov V.V. "Small-angle scattering study of Aspergillus awamori glycoprotein glucoamylase". **Crystallography Reports**, 2016, vol. 61(1), p. 149-152.
77. Stan C., Balasoiu M., Ivankov A.I., Cristescu C.P., "Multifractal Analysis of CoFe₂O₄/2DBS/H₂O Ferrofluid from TEM and SANS Measurements". **Romanian Reports in Physics**, 2016, vol. 68 (1), p. 270–277.
78. Vlasov A., Kovalev Y., Ryzhykau Y., Frolov F., Zinovev E., Rogachev A., Kuklin A., Gordeliy V. "Light-induced electrical properties of bacteriorhodopsin in purple membranes". **FEBS Journal**, 2016, vol. 283, Issue Supplement S1, p.218.
79. Zelenyak T.Y., Kholmurodov K.T., Tameev A.R. et al. "Molecular dynamics study of perovskite structures with modified interatomic interaction potentials". **High Energy Chemistry**, 2016, vol. 50, p. 400-405, DOI:10.1134/S0018143916050209 <http://link.springer.com/journal/10733>.
80. Zemlyanaya E.V., Kiselev M.A., Zhabitskaya E.I., Gruzinov A.Yu., Aksenov V.L. "SFF analysis of the small angle scattering data for investigation of a vesicle systems structure". **Journal of Physics: Conference series**, 2016, vol. 724, 012056, p. 1-5; DOI: 10.1088/1742-6596/724/1/012056.
81. Zhabitskaya E., Zemlyanaya E., Kiselev M., and Gruzinov A. "The Parallel Asynchronous Differential Evolution Method as a Tool to Analyze Synchrotronous Scattering Experimental Data from Vesicular Solutions". **The European Physical Journal Web of Conferences**, 2016, vol. 108, p.02047, DOI: 10.1051/epjconf/201610802047. Article available at <http://www.epj-conferences.org> or <http://dx.doi.org/10.1051/epjconf/201610802047>.

Thin films (reflectometry, polarized neutrons)

82. Жакетов В.Д., Никитенко Ю.В., Раду Ф., Петренко А.В., Csik A., Борисов М.М., Мухамеджанов Э.Х., Аксёнов В.Л. "Магнетизм в структурах с ферромагнитными и сверхпроводящими слоями". **ЖЭТФ**, 2016, том. 150, Вып. 5(11)1-19.

Atomic and magnetic dynamics (inelastic neutron scattering)

83. Drużbicki K., Pajzderska A., Kiwiłsza A., Jencyk J., Chudoba D., Jarek M., Mielcarek J., Wąsicki J., "In search of the mutual relationship between the structure, solid-state spectroscopy and molecular Dynamics In selected calcium channel blockers". **European Journal of Pharmaceutical Sciences**, 2016, vol. 85, p. 68-83.
84. Drużbicki K., Pinna R.S., Rudić S., Jura M, Gorini G., Fernandez-Alonso F. "Unexpected Cation Dynamics in the Low-temperature Phase of Me-thylammonium Lead Iodide – The Need for Improved Models". **The Journal of Physical Chemistry Letters**, 2016, vol. 7 (22), p. 4701–4709. DOI: 10.1021/acs.jpcllett.6b01822.
85. Laine M., Barbosa N.A., Kochel A., Osiecka B., Szewczyk G., Sarna T., Ziółkowski P., Wieczorek R., Filarowski A. "Synthesis, structural, spectroscopic, computational and cytotoxic studies of BODIPY dyes." **Sensors and Actuators B: Chemical**, 2017, vol. 238, p. 548-555.
86. Laine M., Barbosa N.A., Wieczorek R., Melnikov M.Ya., Filarowski A., "Calculations of BODIPY dyes in the ground and excited states by M06-2X and PBE0 functionals". **Journal of Molecular Modeling**, 2016, vol. 22, p. 260. DOI: 10.1007/s00894-016-3108-8.
87. Łuczynska K., Drużbicki K., Lyczko K., Dobrowolski J.Cz. "Structure-Spectra Correlations in Anilate Complexes with Picolines". **Crystal Growth & Design**, 2016, p. 6069–6083.
88. Łuczynska K., Drużbicki K., Lyczko K., Dobrowolski J. Cz. "Computationally assisted low-wavenumber spectroscopy of hydrogen-bonded supramolecular synthons". **Annual Report Institute of Nuclear Chemistry and Technology**, 2015, 2016, p. 46-50.
89. Pajzderska A., Drużbicki K., Kiwiłsza A., Gonzalez M.A., Jencyk J., Jurga S., Mielcarek J., Wąsicki J. "On the molecular Dynamics In long-acting calcium channel blocker lacidipine: solid-state NMR, neutron scattering and periodic DFT study". **RSC Advances**, 2016, vol. 6, p. 66617-66629.
90. Zhernenkov M., Bolmatov D., Soloviov D., Zhernenkov K., Toperverg B.P., Cunsolo A., Bosak A. & Cai Yo.Q. "Revealing the mechanism of passive transport in lipid bilayers via phonon-mediated nanometre-scale density fluctuations". **Nature Communications**, 2016, vol. 7, p. 1-9.

3. PUBLICATIONS

Applied studies (texture, stresses, geological materials)

91. Бокучава Г.Д., Петров П., Папушкин И.В., "Применение нейтронной стресс-дифрактометрии для исследования остаточных напряжений и микродеформаций в образцах-свидетелях корпуса реактора, восстановленных методами лучевой сварки". **Поверхность. Рентгеновские, синхротронные и нейтронные исследования**, 2016, № 11, с. 22-33. (Bokuchava G.D., Petrov P., Papushkin I.V., "Application of Neutron Stress Diffractometry for Studies of Residual Stresses and Microstrains in Reactor Pressure Vessel Surveillance Specimens Reconstituted by Beam Welding Methods". **Journal of Surface Investigation. X-ray, Synchrotron and Neutron Techniques**, 2016, vol.10, Issue 6, p. 1143-1153.
92. Зель И.Ю., Иванкина Т.И., Левин Д.М., Локаичек Т. "Лучевые скорости Р-волн и обратная задача акустики применительно к анизотропным средам". **Кристаллография**, 2016, том 61, № 4, с. 601–607.
93. Зель И.Ю., Иванкина Т.И., Локаичек Т., Керн Х., Левин Д.М. "О причинах сейсмической анизотропии горных пород: экспериментально-теоретическое исследование на образцах биотитовых гнейсов". **Геофизические исследования**, 2016, том.17, № 3, с.70-87. DOI: 10.21455/gr2016.3-6.
94. Bokuchava G.D. "Materials microstructure characterization using high resolution time-of-flight neutron diffraction". **Romanian Journal of Physics**, 2016, vol. 61, №. 5-6, p. 903-925.
95. Bokuchava G.D., Papushkin I.V., Tamonov A.V., Kruglov A.A. "Residual stress measurements by neutron diffraction at the IBR-2 pulsed reactor". **Romanian Journal of Physics**, 2016, vol. 61, №. 3-4, p. 491-505.
96. Dului O. G., Ivankina T.I., Herman E., Ricman C., Tiseanu I. "Orientation distribution function of biotite platelets based on optical, thin sections and μ -CT image analysis in an Outokumpu (Finland) biotite gneiss: Comparison with neutron diffraction texture analysis". **Russian Journal of Earth Sciences**, September 2016, vol. 16(3), ES3003. DOI: 10.2205/2016ES000573.
97. Keppler R., Stipp M., Behrmann J.H., Ullemeyer K. & Heidelbach F. "Deformation inside a paleosubduction channel – Insights from microstructures and crystallographic preferred orientations of eclogites and metasediments from the Tauern Window". **Journal of Applied Geology**, 2016, vol. 82, p. 60-79. Austria. DOI: 10.1016/j.jsg.2015.11.006.
98. Lychagina T. & Nikolayev D. "Quantitative comparison of the measured crystallographic textures". **Journal of Applied Crystallography**, 2016, vol. 49 (4), p. 1290-1299.
99. Vilhelm J., Ivankina T., Lokajicek T., Rudajev V. "Comparison of laboratory and field measurements of P and S wave velocities of a peridotite rock". **International Journal of Rock Mechanics and Mining Sciences**, 2016, vol. 88, p. 235–241.

Instruments and Methods

100. Балагуров А.М., Бескровный А.И., Журавлев В.В., Миронова Г.М., Бобриков И.А., Неов Д., Шеверев С.Г. "Дифрактометр для исследований переходных процессов в реальном времени на импульсном источнике нейтронов ИБР-2" **Поверхность**, 2016, вып. 6, стр. 3-16. (Balagurov A.M., Beskrovny A.I., Zhuravlev V.V., Mironova G.M., Bobrikov I.A., Neov D., Sheverev S.G. "Neutron Diffractometer for Real-Time Studies of Transient Processes at the IBR-2 Pulsed Reactor". **Journal of Surface Investigation "X-ray, Synchrotron and Neutron Techniques"**, 2016, vol.10, No. 3, p. 467–479.)
101. Боднарчук В.И., Садилов С.В., Манюшин С.А., Ерхан Р., Авдеев М.В., Ярадайкин С.П. "Геометрический фактор в методе спин эхо малоуглового рассеяния нейтронов с использованием линейно возрастающих во времени магнитных полей". **Поверхность. Рентгеновские, синхротронные и нейтронные исследования**, 2016, № 11, с. 7-11.
102. Кожевников С.В., Жакетов В.Д., Петренко А.В., Булавин М.В., Верхоглядов А.Е., Куликов С.А., Шабалин Е.П. "Использование криогенного замедлителя на нейтронном рефлектометре РЕМУР". **Поверхность** 2016, вып. 16 стр. 5-14.
103. Кожевников С.В., Игнатович В.К., Петренко А.В., Раду Ф. "Нейтронные резонансы в плоских волноводах". **ЖЭТФ**, 2016, вып. 150, DOI: 10.7868/S0044451016110000.
104. Козленко Д.П., Кичанов С.Е., Лукин Е.В., Руткаускас А.В., Белушкин А.В., Бокучава Г.Д., Савенко Б.Н. "Экспериментальная установка для исследований с помощью методов нейтронной радиографии и томографии на реакторе ИБР-2". **Письма в ЭЧАЯ**, 2016, т. 13, № 3, с.550-557. (Kozlenko D.P., Kichanov S.E., Lukin E.V., Rutkauskas A.V., Belushkin A.V., Bokuchava G.D., Savenko B.N. "Neutron radiography and tomography facility at IBR-2 reactor". **PEPAN Letters**, 2016, vol. 13, № 3, p. 346-351.)
105. Никитенко Ю.В., Игнатович В.К., Кожевников С.В., Петренко А.В. "Двухзеркальный спин-волновой интерферометр нейтронов". **Поверхность**, 2016, №10, стр. 5-13.
106. Никитенко Ю.В. ЭСпин-эхо спектрометр нейтронов скользящей геометрии". **Поверхность**, 2016, №2, стр. 1-9.
107. Balasoiu M., Kuklin A.I. "Magnetic Scattering Determination from SANS Contrast Variation Experiments at IBR-2 Reactor". **Romanian Journal of Physics**, 2016, vol. 61(3-4), p. 473-482.
108. Kozhevnikov S.V., Ott F., Radu F. "Neutron methods for the direct determination of the magnetic induction in thick films". **Journal of Magnetism and Magnetic Materials**, 2016, vol. 402, p. 83-93.
109. Kozhevnikov S.V., Khaydukov Yu.N., Keller T., Ott F., Radu F. "Polarized neutron channeling for the investigations of weakly magnetic thin films". **Письма в ЖЭТФ**, 2016, vol. 103, p. 38-43.
110. Zlokazov V.B., Bobrikov I.A., Balagurov A.M. "Mathematical methods for the analysis of polycrystal phase evolutions". **The European Physical Journal**, 2016, v. 108, p. 2049. EPJ Web of Conferences, 2016, vol. 108, p. 02049 (pp.1-6).

Articles about the organized conferences

111. Gorshkova Yu.E., Kozlenko D.P., "CMR@IBR-2 - International Conference "Condensed Matter Research at the IBR-2" in FLNP JINR", Dubna", **Neutron News**, 2016, vol. 27(1), pp. 18-20. DOI: 10.1080/10448632.2016.1125734.
112. Kučerka N., Balasoju M. & Kuklin A.I. III International Conference on Small Angle Neutron Scattering Dedicated to the 80th Anniversary of Yu. M. Ostanevich. **Neutron News**, 2016, 27:4, 14-16.

Patents

113. Никитенко Ю.В. Способ измерения спектра переданного импульса нейтронов. Патент на изобретение №2593431 от 12 июля 2016г.

SECTOR OF RAMAN SPECTROSCOPY

114. Arzumanyan G.M., Doroshkevich N.V., Mamatkulov K.Z., Shashkov S.N., Zinovev E.V., Vlasov A., Round E. and Gordeliy V.I. "Highly Sensitive Coherent anti-Stokes Raman Scattering Imaging of Protein Crystals". **JACS**, 2016, vol. 138(41), p. 13457-13460.
115. Arzumanyan G.M., Kuznetsov E.A., Zhilin A.A., Dymshits O.S., Shemchuk D.V., Alekseeva I.P., Mudryi A.V., Zhivulko V.D., Borodavchenko O.V. "Photoluminescence of transparent glass-ceramics based on ZnO nanocrystals and co-doped with Eu³⁺, Yb³⁺ ions". **J. Optical Materials**, DOI information: 10.1016/j.optmat.2016.10.054
116. Girel K., Yantsevich E., Arzumanyan G., Doroshkevich N. and Bandarenka H. "Detection of DNA molecules by SERS spectroscopy with silvered porous silicon as an active substrate". **Physica Status Solidi A**, 2016, vol. 1–5, DOI: 10.1002/pssa.201600432
117. Othman H.A., Arzumanyan G.M., Moncke D. "The influence of different alkaline earth oxides on the structural and optical properties of undoped, Ce-doped, Sm-doped, and Sm/Ce co-doped lithium aluminophosphate glasses". **J. Optical Materials**, <http://dx.doi.org/10.1016/j.optmat.2016.10.051>
118. Arzumanyan G.M., Mamatkulov K.Z., Brozhek A.D., Fabelinsky V.I., Kozlov D.N., Orlov S.N., Polivanov Y.N., Shcherbakov I.A., Smirnov V.V., Vereschagin K.A., Lagarkov A.N., Ryzhikov I.A., Sarychev A.K., Budashov I.A., Kurochkin I.N. "Surface Enhanced CARS from Gold Nanoparticle-Immobilized Molecules at Cerium Dioxide/Aluminium Film". Technical Digest (Nanophotonics and Plasmonics) of International Conference on Coherent and Nonlinear Optics (ICONO)&Conference on Lasers, Applications, and Technologies (LAT) - **ICONO/LAT** 2016, 26–30 September, 2016, p. 88-89, Minsk, Belarus.
119. Канюков Е.Ю., Белоногов Е.К., Якимчук Д.В., Козловский А.Л., Кадыржанов К.К., Арзуманян Г.М., Демьянов С.Е. "Особенности формирования медного осадка в порах диоксида кремния". **Известия НАН Беларуси, серия физико-технических наук**, 2016, №3, стр. 11-15.

DEPARTMENT OF IBR-2 SPECTROMETERS COMPLEX

120. Ananiev V., Beliakov A., Bulavin M., Verkhoglyadov A., Kulagin E., Kulikov S., Mukhin K., Shabalin E. and Loktaev K. "Pelletized cold moderator of the IBR-2 reactor: current status and future development". **Journal of Physics: Conference Series**, September 2016, vol. 746(1):012031, pp.1-6.
121. Булавин М.В., Васин Р.Н., Куликов С.А., Локаичек Т., Левин Д.М. "Использование комбинированного замедлителя на реакторе ИБР-2: преимущества для нейтронографического текстурного анализа горных пород". **Поверхность. Рентгеновские, синхротронные и нейтронные исследования**, 2016, № 5, с. 1-10.
122. Кожевников С.В., Жакетов В.Д., Петренко А.В., Верхоглядов А.Е., Куликов С.А., Шабалин Е.П., Булавин М.В. "Использование криогенного замедлителя на нейтронном рефлектометре РЕМУР". **Поверхность. Рентгеновские, синхротронные и нейтронные исследования**, 2016, №1, с. 5-14. (Kozhevnikov S. V. et al. "Application of a cryogenic moderator in the REMUR neutron reflectometer". **Journal of surface investigation X-ray, synchrotron, and neutron techniques**, 2016, vol. 10, № 1, p. 1–9.)
123. Belyakov A.A., Bulavin M.V., Verkhoglyadov A.E., Skuratov V.A., Smelyansky I.A., Kulikov S.A., Kustov A.A., Mukhin K.A., Lyubimtsev A.A., Sirotin A.P., Shirokov V.K and Petukhova T.B., Possibility of loading the chamber of the "central" pelletized cold moderator for IBR-2 reactor beams 1, 4–6, and 9, **Physics of particles and nuclei letters**. – 2016. – Vol. 13, №6. – pp. 774-781.
124. Manoshin S.A., Belushkin A.V., Ioffe A.I. "Development of the methods for simulating the neutron spectrometers and neutron-scattering experiments". **Physics of Particles and Nuclei**, 2016, vol. 47, № 4, p. 667–680.
125. Белушкин А.В., Маношин С.А., Рихвицкий В.С. "Анализ применимости модифицированного кинематического приближения для описания незеркального отражения нейтронов от поверхности микро- и наноструктурированных объектов". **Кристаллография**, 2016, том 61, № 5, с. 736–744. (Belushkin A.V., Manoshin S.A., Rikhvitskiy V.S. "Analysis of the Applicability of the Modified Kinematic Approximation to Describe the Off-Specular Neutron

3. PUBLICATIONS

- Scattering from the Surface of Micro- and Nanostructured Objects". **Crystallography Reports**, 2016, vol. 61, Issue 5, p. 760–767.)
126. Belushkin A.V., Manoshin S.A. "Some peculiarities for grazing incidence neutron diffraction from 3D near-surface nanostructures", Submitted to **Journal of Applied Crystallography**, 2016.
 127. Dobrin I., Chernikov A., Kulikov S., Buzdavin A., Culicov O., Morega A., Nedelcu A., Morega M., Popovici I. and Dobrin A. "A 4 T HTS Magnetic Field Generator, Conduction Cooled, for Neutron Physics Spectrometry", **IEEE TRANSACTIONS ON APPLIED SUPERCONDUCTIVITY**, 2016, VOL. 26, NO. 3. <http://ieeexplore.ieee.org/document/7387718/>
 128. Balagurov A.M., Beskrovnyy A.I., Zhuravlev V.V., Mironova G.M., Bobrikov I.A., Neov D., Sheverev S.G. "Neutron diffractometer for real-time studies of transient processes at the IBR-2 pulsed reactor". **Journal of Surface Investigation X-ray Synchrotron and Neutron Techniques**, May 2016, vol. 10, Issue 3, p. 467-479
 129. Куликов С.А., Приходько В.И. "Новое поколение систем сбора и накопления данных комплекса спектрометров реактора ИБР-2". **Физика элементарных частиц и атомного ядра**, 2016, том 47, вып. 4, стр. 1288-1302.
 130. Kulikov S.A., Prikhodko V.I. "New generation of data acquisition and data storage systems of the IBR-2 reactor spectrometers complex". **Physics of Particles and Nuclei**, 07/2016, vol. 47(4), p. 702-710.
 131. Кирилов А.С. "Новые версии программ юстировки и визуализации спектров для рефлектометров ИБР-2". **Письма в ЭЧАЯ**. 2016, Т.13, № 1(199), с. 208-21.
 132. Levchanovskiy F., Murashkevich S. "De-Li-DAQ-2D – a new data acquisition system for position-sensitive neutron detectors with delay-line readout". **Physics of Particles and Nuclei Letters**, 2016, vol. 13, № 5, p. 591–594.
 133. Цулаиа М.И., Саламатин И.М., Саламатин К.М., Беликов Д.Б., Мареев Ю.Д., Сиротин А.П. "Модернизация установки Колхида для исследования взаимодействия поляризованных нейтронов с поляризованными ядрами". **Сообщение ОИЯИ**, 2016, P13-2016-23, Дубна.

NUCLEAR PHYSICS DEPARTMENT

Experimental investigations

134. Adam J., Chilap V.V., Furman V.I. et al., "Study of secondary neutron interactions with ^{232}Th , ^{129}I , and ^{127}I nuclei with the uranium assembly "QUINTA" at 2, 4, and 8 GeV deuteron beams of the JINR Nuclotron accelerator", **Applied Radiation and Isotopes** 107 (2016) 225–233.
135. Artiushenko M.Yu., Baldin A.A., Berlev A.I. et al., "Comparison of neutron-physical characteristics of uranium target of assembly "QUINTA" irradiated by relativistic deuterons and ^{12}C nuclei", **VANT** 2016. №3(103)
136. Данилян Г.В., Копач Ю.Н., Новицкий В.В. и др. "О РОТ-эффектах в тройном и бинарном делении ядер ^{233}U и ^{235}U поляризованными холодными нейтронами", **Proc. International Seminar on Interaction of Neutrons with Nuclei - ISINN24**, May 23-27, 2016, Dubna, Russia.
137. Achakovskiy O.I., Belyshev S.S., Dzhilavyan L.Z., Pokotilovski Yu.N. "Cross sections of the reactions $^{14}\text{N}(\gamma, 2n)^{12}\text{N}$, $^{14}\text{N}(\gamma, 2p)^{12}\text{B}$, $^{13}\text{C}(\gamma, p)^{12}\text{B}$ ". **Izvestija RAN**, 2016, vol. 80, №5, p. 633-640; **Bulletin of the Russian Academy of Science**, 2016, vol. 80, №5, p. 572-578.
138. Barbagallo M., Musummaro A., Consentino L. et al., "The $^7\text{Be}(n, \alpha)^4\text{He}$ reaction and the Cosmological Lithium Problem: measurement of the cross section in a wide energy range at n_TOF (CERN)", **Physical Review Letters** 117:152701 (2016)
139. Belyshev S.S., Dzhilavyan L.Z., Pokotilovski Yu.N. "Emission of quanta, electrons, positrons from characteristic targets at decays of ^{12}N and ^{12}B , produced in these targets". **Izvestija RAN**, 2016, vol. 80 №5, p. 627-632; **Bulletin of the Russian Acad of Science**, 2016, vol. 80 №5, p. 566-571.
140. Bystritsky V.M., Grozdanov D.N., Zontikov A.O., Kopach Yu.N., Rogov Yu.N., Ruskov I.N., Sadovsky A.B., Skoy V.R., Barmakov Yu.N., Bogolyubov E.P., Ryzhkov V.I., Yurkov D.I. "Angular distribution of 4.43-MeV γ -rays produced in inelastic scattering of 14.1-MeV neutrons by ^{12}C nuclei". **Physics of Particles and Nuclei Letters**, 2016, vol. 13/4, p. 504, doi: 10.1134/S154747711604004X. (Быстрицкий В.М. и др. **Письма в ЭЧАЯ**, 2016, том 13, вып. 4).
141. Bystritsky V.M., Grozdanov D.N., Kopatch Yu.N., Ruskov I.N., Skoy V.R., Zontikov A.O. and Ivanov I.Zh. "Response of a hexagonal NaI(Tl) scintillation probe in the attenuated neutron radiation of 14.1 MeV neutron generator ING-27" **23rd International Seminar on Interaction of Neutrons with Nuclei (ISINN-23)**, May 25-29, 2015, Dubna, Russia.
142. Frank A.I. "Interaction of neutrons with birefringent medium moving with an acceleration". **Journal of Physics: Conference Series**, 2016, volume 711, p. 012016.
143. Frank A.I., Kulin G.V., Bushuev V.A. "Non-stationary transformation of neutron energy by a moving grating". **Journal of Physics: Conference Series**, 2016, vol. 746, p. 012053.
144. Frank A.I., Kustov D.V., Kulin G.V., Goryunov S.V., Roshchupkin D.V., Irzhak D.V. "Experiment proposed for the observation of UCN interaction with matter moving with giant acceleration". **Journal of Physics: Conference Series**, 2016, vol. 746, p. 012054.
145. Gledenov Yu. M., Zhang G., Sedysheva M.V., Wang Z., Khuukhenkhuu G., Krupa L., Fan X., Zhang L., Bai H., Chen J. "Cross Sections $^{56}\text{Fe}(n, \alpha)^{53}\text{Cr}$ and $^{54}\text{Fe}(n, \alpha)^{51}\text{Cr}$ Reactions in the MeV Region". In: **Proc. of the 23 International Seminar on Interaction of Neutron with Nuclei (ISINN-23)**, 2016, E3-2016-12, p. 334-337, Dubna.
146. Gledenov Yu.M., Sedysheva M.V., Zhang G., Wang Z., Fan X., Zhang L., Bai H., Chen J., Krupa L., Khuukhenkhuu G. "Cross Sections $^{144}\text{Sm}(n, \alpha)^{141}\text{Nd}$ Reaction at 4.0, 5.0 and 6.0 MeV". In: **Proc. of the 23 International Seminar on**

- Interaction of Neutron with Nuclei (ISINN-23)**, Dubna, 2016, E3-2016-12, pp. 338-345.
147. Gledenov Yu.M., Krupa L., Sansarbayer E., Chuprakov I.A. "Spectrometer of Charged Particles on the EG-5 FLNP JINR". In: **Proc. of the 23 International Seminar on Interaction of Neutron with Nuclei (ISINN-23)**, 2016, E3-2016-12, p. 189-196, Dubna.
 148. Gook A., Geerts W., Hamsch F.-J., Oberstedt S., Zeynalov Sh. "A position-sensitive twin ionization chamber for fission fragment and prompt neutron correlation experiments". **Nuclear Instruments and Methods in Physics**, 2016, A830, p. 366-374.
 149. Grozdanov D.N., Zontikov A.O., Bystritsky V.M., Kopatch Yu.N., Ruskov I.N., Skoy V.R. "Optimization of "Romashka" setup for investigation of (n, n' γ)-reactions with tagged neutrons method". **23rd International Seminar on Interaction of Neutrons with Nuclei (ISINN-23)**, May 25-29, 2015, Dubna, Russia, 346-353.
 150. Gundorin N. A., Zeinalov Sh. S., Kopach Yu. N., Popov A. B., and Furman V. I., "Investigations of Fission Characteristics and Correlation Effects", **Phys. of Part. and Nuclei**, 2016, Vol. 47, No. 4, pp. 681-701.
 151. Günsing F., Aberle O., Andrzejewski J. et al., "Nuclear data activities at the n TOF facility at CERN", **Eur. Phys. J. Plus** (2016) 131: 371 DOI: 10.1140/epjp/i/2016-16371-4
 152. Khushvaktov J., Adam J., Baldin A.A. et al., "Interactions of secondary particles with thorium samples in the setup QUINTA irradiated with 6 GeV deuterons", **Nuclear Instruments and Methods in Physics Research B** 381 (2016) 84-89
 153. Khuukhenkhoo G., Gledenov Yu.M., Zhang G., Sedysheva M.V., Odsuren M., Zolbadral Ts., Munkhsaikhan J., Sansarbayer E. "Analysis of Fast Neutron Induced (n, α) Reaction Cross Sections and Angular Distributions for Medium Mass Nuclei". In: **Proc. of the 23 International Seminar on Interaction of Neutron with Nuclei (ISINN-23)**, 2016, E3-2016-12, p. 353-360, Dubna.
 154. Khuukhenkhoo G., Odsuren M., Gledenov Y.M., et al. "Statistical model analysis of (n, α) cross sections for 4.0-6.5 MeV neutrons". **13th International Symposium on Origin of Matter and Evolution of Galaxies (OMEG 2015)**, EPJ Web of Conferences, 2016, vol. 109, article number 05004.
 155. Kopatch Yu.N., Bystritsky V.M., Grozdanov D.N., Zontikov A.O., Ruskov I.N., Skoy V.R., Rogov Yu.N., Sadovsky A.B., Barmakov Yu.N., Bogolyubov E.P., Ryzhkov V.I., Yurkov D.I. "ANGULAR CORRELATION OF GAMMA-RAYS IN HE INELASTIC SCATTERING OF 14.1 MEV NEUTRONS ON CARBON". **23rd International Seminar on Interaction of Neutrons with Nuclei (ISINN-23)**, May 25-29, 2015, Dubna, Russia.
 156. Kulin G.V., Frank A.I., Goryunov S.V., Geltenbort P., Jentschel M., Bushuev V.A., Lauss B., Schmidt-Wellenburg Ph., Panzarella A. and Fuchs Y. "Spectroscopy of ultracold neutrons diffraction by a moving grating". **Physical Review A**, 2016, vol. 93, p. 033606.
 157. Kulin G.V., Frank A.I., Goryunov S.V., Geltenbort P., Jentschel M., Bushuev V.A., Lauss B., Schmidt-Wellenburg Ph., Panzarella A., Fuchs Y. "Time-of-flight Fourier Spectrometry with UCN". **Journal of Physics: Conference Series**, 2016, vol. 746, p. 012021
 158. Kulin G.V., Frank A.I., Goryunov S.V., Kustov D.V., Geltenbort P., Jentschel M., Lauss B., Schmidt-Wellenburg Ph. "Time-of-flight Fourier UCN spectrometer". **Nuclear Instruments and Methods in Physics Research Section A**, 2016, vol. 819, p.67-72.
 159. Lychagin E.V., Mutyukhlyayev V.F., Muzichka A.Yu., Nekhaev G.V., Nesvizhevsky V.V., Onegin V.S., Sharapov E.I., Strelkov A.V. "UCN sources at external beams of thermal neutrons. An example of PIK reactor". **Nuclear Instruments and Methods in Physics Research Section A**, 2016, vol. 823, p. 47-55.
 160. Lychagin E.V., Mityukhlyayev V.A., Muzychka A.Yu., Nekhaev G.V., Nesvizhevsky V.V., Onegin M.S., Sharapov E.I. and Strelkov A.V. "UCN sources at external beams of thermal neutrons. Estimation of the source intensity at PIK reactor". **Neutron Spectroscopy, Nuclear Structure, Related Topics; ISINN-23** May 25-29, 2015, Dubna, **JINR Report E3-2016-12**, p.15-31.
 161. Mitsyna L.V., Popov A.B. "Remarks on the modern status of the neutron charge radius problem". In: **ISINN-23**, May 25-29, 2015, Dubna, **JINR Report E3-2016-12**, p.151-158.
 162. Morris C.L., Adamek E.R., Broussard L.J. et al. (30 authors, including Sharapov E.I.). "A new method for measuring the neutron life time using in situ neutron detector". **Report LA-UR-16-27352 (2016)**, Los Alamos National Laboratory, Los Alamos, arXiv:1610.04560.
 163. Odsuren M., Kato K., Khuukhenkhoo G., Gledenov Yu.M., Sansarbayer E. "Resonance States of the Alpha-Alpha System". In: **Proc. of the 23 International Seminar on Interaction of Neutron with Nuclei (ISINN-23)**, 2016, E3-2016-12, p. 202-207, Dubna.
 164. Oprea C., Oprea A. "Neutron Induced Capture and Fission Processes on 238U nucleus". **European Physical Journal Web of Conferences: EDP Science**, 2016, vol. 111, p. 11002.
 165. Paradelo C., Calviani M., Tarrío D. et al., "High-accuracy determination of the 238U/235U fission cross section ratio up to ≈ 1 GeV at n_TOF at CERN", **Phys. Rev. C** 91, 024602
 166. Pokotilovski Yu.N. "Effect of oxide films and structural inhomogeneities on transmission of ultracold neutrons through foils." **The European Physical Journal Applied Physics**, 2016, vol. 73 (2), p. 20302.
 167. Sukhovoij A.M., Mitsyna L.V. and Jovancevich N. "Overall Picture of the Cascade Gamma Decay of Neutron Resonances within a Modified Practical Model". **Physics of Atomic Nuclei**, 2016, vol. 79, p. 313-235. (Сухоной А.М., Мицына Л.В., Йованчевич Н. "Картина процесса каскадного гамма-распада нейтронного резонанса в современной практической модели", **Ядерная Физика**, 2016, вып. 79б стр. 207-219).
 168. Vu D.C., Sukhovoij A.M., Mitsyna L.V., Zeinalov Sh.S., Jovancevic N., Knezevic D., Krmar M., Dragic A. "Representation of the Radiative Strength Functions in the Practical Model of Cascade Gamma Decay". **Preprint of JINR**, 2016, E3-2016-43, Dubna, submitted to "Physics of Atomic Nuclei".

3. PUBLICATIONS

169. Wei W., Broussard L.J., Morris C.L. et al. (32 authors, including Sharapov E.I.). "Position-sensitive detector of ultracold neutrons with imaging camera and its implications to spectroscopy". **Nuclear Instruments and Methods in Physics Research A**, 2016, vol. 830, p. 36-45.
170. Zakharov M.A., Kulin G.V., Frank A.I., Goryunov S.V., Kustov D.V. "A new approach to the experiment intended to test the weak equivalence principle for the neutron". **Journal of Physics: Conference Series**, 2016, vol. 746, p. 012050.
171. Бушуев В.А., Франк А.И. "Влияние пространственной когерентности нейтронного пучка на дифракцию на движущейся фазовой решетке". **Труды XX Международного симпозиума «Нанофизика и нанозлектроника»**, 2016, том 1, с. 356-358.
172. Бушуев В.А., Франк А.И., Кулин Г.В. "Динамическая дифракция нейтронов на движущейся решетке". **ЖЭТФ**, 2016, том 149, стр. 41-52. (Bushuev V.A., Frank A.I. and Kulin G.V. "Dynamic theory of neutron diffraction from a moving grating". **JETP**, 2016, vol. 122, p. 32-42).
173. Гундорин Н.А., Зейналов Ш.С., Копач Ю.Н., Попов А.Б., Фурман В.И. "Исследования характеристик и корреляционных эффектов в делении". **Физика элементарных частиц и атомного ядра**, 2016, том 47, вып. 4, 1248-1287.
174. Кожевников С.В., Игнатович В.К., Петренко А.В., Раду Ф. "Нейтронные резонансы в плоских волноводах". **ЖЭТФ**, 2016, том 150, № 6, стр. 1094-1101.
175. Лычагин Е.В., Козленко Д.П., Седышев П.В., Швецов В.Н. "Нейтронная физика в ОИЯИ — 60 лет Лаборатории нейтронной физики им. И.М. Франка", **УФН**, 2016, вып. 186:3, стр. 265–274.
176. Франк А.И., Бушуев В.А., Кулин В.Г. "Нестационарное преобразование энергии нейтронов при дифракции на движущейся решетке". **Труды XX Международного симпозиума «Нанофизика и нанозлектроника»**, 2016, том 1, стр.419-420.
177. Франк А.И. "Ультрахолодные нейтроны и взаимодействие волн с движущимся веществом". **ЭЧАЯ**, 2016, том 47, вып. 4, стр.1192-1227. (Frank A.I. "Ultracold Neutrons and the Interaction of Waves with Moving Matter". **Physics of Particles and Nuclei**, 2016, vol. 47, № 4, p. 647–666).
178. Ignatovich V.K. "Single Measurement Bell's Inequality with Detection Efficiencies". **Physics Journal, Изд: American Institute of Science**, 2016, vol. 2, № 1, p. 1-5.
179. Ignatovich V.K. "Singular Bound States and Cold Nuclear Fusion". **Physics Journal, Изд: American Institute of Science**, 2016, vol. 2, № 1, pp. 6-10.
180. Ignatovich V.K., Utsuro M. "Change of neutron energy at reflection from and transmission through a matter layer". **SCIREA Journal of Physics, Изд: Science Research Association a global academic organization**, 2016, vol.1, № 1, pp. 41-51.
181. Ignatovich V. "Proposal of an Experiment to Investigate Properties of the Neutron Wave-Packet". **SCIREA Journal of Physics, Изд: Science Research Association a global academic organization**, 2016, vol.1, № 1, p. 11-22.
182. Никитенко Ю.В., Игнатович В.К., Кожевников С.В., Петренко А.В. "Двухзеркальный нейтронный спин-интерферометр". **Поверхность. Рентгеновские, синхротронные и нейтронные исследования**, 2016, № 10, стр. 5-13. (Nikitenko Yu.V., Ignatovich V.K., Kozhevnikov S.V. and Petrenko A.V. "Two-Mirror Spin-Wave Neutron Interferometer". **Journal of Surface Investigation. X-ray, Synchrotron and Neutron Techniques**, 2016, vol.10, №5, p. 992-1000).
183. Balalykin N.I., Huran J., Nozdryn M.A., Feshchenko A.A., Kobzev A.P., Arbet J. "Transmission photocathodes based on stainless steel mesh and quartz glass coated with N-doped ALC thin films prepared by reactive magnetron sputtering". **Journal of Physics: Conference Series**, 2016, vol. 700, p. 012050.
184. Huran J., Hrubcin L., Bohacek P., Borzakov S.B., Skuratov V.A., Kobzev A.P., Kleinova A., Sasinkova V. "The effect of Xe ion and neutron irradiation on the properties of SiC and SiC(N) films prepared by PECVD technology". **Radiation @ Application**, April 2016, vol.1, issue 1, p. 14-19.
185. Kulik M., Kolodynska D., Kobzev A.P., Komarov F.F., Hubicki Z., Pyszniak K. "Chemical composition of native oxides on noble gases implanted GaAs". **Thin Solid Films**, 2016, vol. 616, p. 55-61.
186. Allajbeu S., Qarri F., Marku E., Bektashi L., Ibro V., Frontasyeva M.V., Stafilov T., Lazo P.V.. "Contamination scale on atmospheric deposition for assessing air quality in Albania evaluated from most toxic heavy metal and moss biomonitring". **Air Quality, Atmosphere & Health**. DOI:10.1007/s11869-016-0453-9.
187. Allajbeu Sh., Yushin N.S., Qarri F., Dului O.G., Lazo P., Frontasyeva M. V.. "Atmospheric depositions of rare earth elements in Albania studied by the moss biomonitring technique, neutron activation analysis and GIS technology". **Environmental Science and Pollution Research**. No. 23, 2016, p. 14087-14101. DOI 10.1007/s11356-016-6509-4.
188. Aleksiyenak Y.V., Leonchik S.V., Ignatenko O.V., Komar V.A., Konovalova A.V., Frontasyeva M. V. "Neutron activation analysis and electron microscopy in the investigation of crystallization processes and characteristics of diamonds in the C-Mn-Ni-Fe systems". **Journal of Radioanalytical and Nuclear Chemistry**, July 2016, Vol. 309, No. 1, pp. 267-271.
189. Badawy W., Chepurchenko O.Ye., Samman H. El, Frontasyeva M.V.. "Assessment of industrial contamination of agricultural soil adjacent to Sadat city, Egypt". **Ecological Chemistry and Engineering**, S, Vol. 23, No. 2, 2016, p. 297-310. DOI: 10.1515/eces-2016-0021.

190. Culicov O.A., Dului O.G., Zinicovscaia I.. "Study of elemental grouping in moss-bags as a function of height and location of the exposure site", **Romanian Reports in Physics**, Vol. 68, 2016, p. 736–745.
191. Culicov O.A., Zinicovscaia I., Dului O.G. "Active Sphagnum girgensohnii Russow Moss Biomonitoring of an Industrial Site in Romania: Temporal Variation in the Elemental Content". **Bulletin of Environmental Contamination and Toxicology**, Vol. 96, 2016, p. 650-656.
192. Ene A., Frontasyeva M. V., Cantaragiu A., Pintilie V., Pascu E., Soimu D., Chiriac E., Coguteac V., Buliga A., Tobol M., "Nuclear and X-ray methods used in environmental and material science", **Annals of the University Dunarea de Jos of Galati, Fascicle II - Mathematics, Physics, Theoretical Mechanics**, Year VIII (XXXIX), No.1, 2016, p.86-91.
193. Fiałkiewicz-Kozieł B., Smieja-Król B., Frontasyeva M., Stowiński M., Marcisz K., Lapshina E., Gilbert D., Buttler A., Jassev V. E. J., Kaliszan K., Laggoun-Défarage F., Kołaczek P., Lamentowicz M.. "Anthropogenic- and natural sources of dust in peatland during the Anthropocene". **NATURE Scientific Reports** Nr 6, Article number: 38731 (2016);doi:10.1038/srep38731
194. Gorbunov A.V., Ermolaev B.V., Lyapunov S.M., Okina O.I., Pavlov S.S., Frontasyeva M.V.. "Estimation of mercury intake from consumption of fish and seafood in Russia". **Food and Nutrition Sciences**, No. 7, 2016, p. 516-523.
195. Gorelova S.V., Frontasyeva M.V., Volkova E.V., Vergel K.N., Babicheva D.E.. "Trace element accumulating ability of different moss species used to study atmospheric deposition of heavy metals in Central Russia: Tula Region case study". **International Journal of Biology and Biomedical Engineering**, Vol. 10, 2016, p. 273-285. ISSN: 1998-4510.
196. Gorelova S.V., Babicheva D. E., Frontasyeva M. V., Vergel K. N., Volkova E. V.. "Atmospheric Deposition of Trace Elements in Central Russia: Tula Region Case Study. Comparison of Different Moss Species for Biomonitoring". **Environmental Science**, 1, 220-229. ID: 73703-145
197. Goryainova Z., Vuković G., Aničić Urošević M., Vergel K., Ostrovnyaya T., Frontasyeva M., Zechmeister H.. "Assessment of vertical element distribution in street canyons using the moss Sphagnum girgensohnii: A case study in Belgrade and Moscow cities". **Atmospheric Pollution Research**, Volume 7, Issue 4, July 2016, Pages 690–697
198. Keränen A., Leiviskä T., Zinicovscaia I., Frontasyeva M.V., Hormi O., Tanskanen J.. "Quaternized pine sawdust in the treatment of mining wastewater". **Environmental Technology**. 2016; 37(11):1390-7. doi: 10.1080/09593330.2015.1116611.
199. Xuesong Li, Frontasyeva M.V., Hristozova G., Nekhoroshkov P. S., Zinicovscaia I., Yushin N., Vasilev A., Chepurchenko O.. "Neutron activation analysis of elemental content of edible and medicinal plant iron stick yam". **Proc. of the 23 International Seminar on Interaction of Neutron with Nuclei (ISINN-23)**, May 25-29, 2015, Dubna, Russia, 411-419.
200. Ososkov G., Frontasyeva M., Uzhinskiy A., Kutovskiy N., Rummyantsev B., Nechaevsky A., Trofimov V., Vergel K.. "Data Management of the Environmental Monitoring Network: UNECE ICP Vegetation Case". **Proceedings of XVIII International Conference «Data Analytics and Management in Data Intensive Domains» DAMDID/RCDL'2016** (October 11-14, Ershovo, Moscow, Russia). ISBN 978-5-94588-206-5, Moscow: FRC IM RAS Publ., 2016. pp. 309-314.
201. Pavlov S.S., Dmitriev A.Yu., Frontasyeva M.V.. "Automation system for neutron activation analysis at the reactor IBR-2, Frank Laboratory of Neutron Physics, Joint Institute for Nuclear Research, Dubna, Russia". **Journal of Radioanalytical and Nuclear Chemistry**, May 2016, Vol. 309, No. 1, pp. 27-38. <http://link.springer.com/article/10.1007/s10967-016-4864-8>
202. Rummyantsev I.V., Dunaev A.M., Ostrovnyaya T.M., Frontasyeva M.V., Grinevich V.I.. "Evaluation of soil quality soil in the Ivanovo region". **Ecology of Urban Areas**. No. 2, 2016, p. 5-13. (In Russian). И.В. Румянцев, А.М. Дунаев, Т.М. Островная, М.В. Фронтасьева, В.И. Гриневич. Оценка качества почвенного покрова на территории Ивановской области. Проблемы региональной экологии. № 2, 2016, с. 5-13.
203. Schröder W., Nickel S., Schönrock S., et al. "Spatially valid data of atmospheric deposition of heavy metals and nitrogen derived by moss surveys for pollution risk assessments of ecosystems". **Environmental Science and Pollution Research**, 23 (11), 10457–10476 (2016); ISSN 0944-1344, DOI 10.1007/s11356-016-6577-5, 2016.
204. Zinicovscaia I., Hramco C., Dului O.G., Vergel K.N., Culicov O.A., Frontasyeva M.V., Duca G.. "Air pollution study in the Republic of Moldova using moss biomonitoring technique. **Bulletin of Environmental Contamination and Toxicology**. DOI: 10.1007/s00128-016-1989-y.
205. Zinicovscaia I., Safonov A., Ttregubova V., Ilin V., Cepoi L., Chiriac T., Rudi L., Frontasyeva M.V. . "Uptake of metals from single and multi-component systems by arthrospira (Spirulina) platensis biomass". **Ecological Chemistry and Engineering**. S, 2016, v.23, p. 401-412.
206. Zinicovscaia I., Cepoi L., Chiriac T., Rudi L., Culicov O.A., Frontasyeva M.V., Pavlov S.S., Kirkesali E.I., Gundorina S.F., Mitina T., Akshintsev A., Rodlovskaya E.. "Spirulina platensis as biosorbent of chromium and nickel from wastewaters". **Desalination and Water Treatment**, 2016, v.57, p.11103-11110. <http://DOI:10.1080/19443994.2015.1042061>
207. Zinicovscaia I., Chiriac T., Cepoi L., Rudi L., Culicov O., Frontasyeva M., Rudic V.. "Selenium intake and assessment of the biochemical changes in arthrospira (Spirulina) platensis biomass during the synthesis of selenium nanoparticles". **Canadian Journal of Microbiology**. 2016, doi: 10.1139/cjm-2016-0339

3. PUBLICATIONS

Books, Chapters in Books

208. Frontasyeva M. V., Steinnes E. and H. Harmens. Monitoring long-term and large-scale deposition of air pollutants based on moss analysis. Chapter in a book "Biomonitoring of Air Pollution Using Mosses and Lichens: Passive and Active Approach – State of the Art and Perspectives", Edts. M. Aničić Urošević, G. Vuković, M. Tomašević, Nova Science Publishers, New-York, USA, 2016.
209. Lazo P.V., Allajbeu S., Qarri F., Marku E., Bekteshi L., Ibro V., Frontasyeva M.V., Stafilov T.. Trace metals distribution on atmospheric deposition in Albania evaluated by moss biomonitoring, ICP/AES and ENAA analysis. Chapter of the Book: The Mediterranean Region, ISBN 978-953-51-5503-4, Editor Borna Fuerst-Bjeliš, University of Zagreb, Croatia. Submitted in 2016.
210. Mankovská B., Izakovičová Z., Oszlányi J., Frontasyeva M.V.. Temporal and spatial trends (1990-2010) of heavy metal accumulation in mosses in Slovakia. Chapter in a book "Biological Diversity and Conservation". Edt. Prof. Dr. Ersin YÜCEL ISSN 1308-5301 Print; ISSN 1308-8084 Online, Turkey, 2016, pp. 5.
211. Harmens H., Mills G., Hayes F., Sharps K., Frontasyeva M., et al., AIR POLLUTION AND VEGETATION - ICP VEGETATION, ANNUAL REPORT 2015/2016, H. Harmens, G. Mills, F. Hayes, K. Sharps, M. Frontasyeva, (Eds.), ICP Vegetation Programme Coordination Centre, Centre for Ecology and Hydrology, Environment Centre Wales, Bangor, Gwynedd, UK, Moss Survey Coordination Centre, Frank Laboratory of Neutron Physics, Joint Institute for Nuclear Research, Dubna, Moscow Region, Russian Federation, September 2016; ISBN: 978-1-906698-58-4..

4. PRIZES AND AWARDS

MISCELLANEOUS

- In 2015, the International Academy of Authors of Scientific Discoveries and Inventions (IAASDI) awarded **Vladislav Luschikov** the Roentgen Medal for outstanding scientific achievements. Unfortunately, Vladislav Ivanovich passed away shortly before being awarded the Roentgen Medal. At the beginning of 2016, IAASDI representatives visited Dubna and presented the medal and diploma to his son Igor.



- On September 15, 2016, FLNP Chief Researcher **Alexander Frank** was awarded the honorary title "Honored scientist of the Moscow Region."



AYSS AND FLNP FELLOWSHIPS

In 2016, within the framework of the competition of the Association of Young Scientists and Specialists of JINR, the scholarships were awarded to:

- grant for young PhD researchers

A.I. Ivankov
A.V. Nagornyi
T.V. Tropin

- grant for young researchers

C. Colmon
N.M. Belozerova
K.N. Vergel
D.N. Grozdanov
I.V. Gapon
C. Hramco

- grant for young specialists

I.A. Markovnikov
K. Nazarov
N.A. Kovalenko
V.V. Shvetsov
K.I. Mikhailov

- grant for young workers

D.A. Motchev

Since 2002, in FLNP a scholarship named after Academician of the USSR Academy of Sciences and first Director of the Laboratory of Neutron Physics **I.M. Frank** has been established in order to stimulate scientific and methodical research of young scientists.

In 2016 **I.M. Frank scholarships** were awarded to:

- In Neutron Nuclear Physics: **I. Zinicovscaia**
- In Condensed Matter Physics: **I. A. Bobrikov, E.V. Lukin**
- In Methodical Investigations: **S.V. Goryunov, I.A. Morkovnikov**
- In Development of basic facilities: **K.V. Udovichenko**

Since 2006, a scholarship has been founded to immortalize the memory of outstanding scientist, Corresponding Member of the USSR Academy of Sciences **F.L. Shapiro**. The scholarship is awarded annually to young FLNP employees in the following research directions: UCN physics; polarized neutrons; neutron spectroscopy.

In 2016 **F.L. Shapiro scholarships** were awarded to:

- In «Neutron Spectroscopy» **D.N. Grozdanov, O.V. Tomchuk and N.V. Bazhazhina**

5. EVENTS

FLNP SEMINARS

- **I. Medhat** (Spectroscopy Department, National Research Center, Egypt) “*Spectroscopic Analyses of River Nile Sediment*” (27.01.2016)
- **Ch. Schanzer** (Swiss Neutronics, Switzerland) “*State-of-the-art neutron optics by Swiss Neutronics and their application*” (11.05.2016)



E.P. Shabalin

- **E.P. Shabalin, G.G. Komyshev, A.D. Rogov** (FLNP, JINR) “*High-flux pulsed neptunium reactor for beam investigations*” (12.05.2016)
- **V.K. Ignatovich, V.I. Bodnarchuk** (FLNP, JINR), “*О длине когерентности нейтрона*” (19.05.2016)
- **Yu.N. Peptyolyshev** (FLNP, JINR). “*Cascade booster-breeder – new possibilities for a high-flux neutron source*” (15.06.2016)
- **R. Wieczorek** (Faculty of Chemistry, Wroclaw University, Poland) “*The metal-peptide interactions, structural impact*” (20.07.2016)
- **M.V. Vener** (Dmitry Mendeleev University of Chemical Technology of Russia, Moscow, Russia) “*Toward a unified description of intermolecular (noncovalent) interactions in molecular crystals. Solid-state DFT computations*” (20.07.2016)
- **A.I. Frank** (FLNP, JINR) “*Same topical problems of neutron optics*” (29.09.2016)
- **R.B. Hoover** (Astrobiology Laboratory, Athens State Univ., Athens, Alabama USA, Buckingham Centre for Astrobiology, Univ. of Buckingham, Buckingham, UK) “*Perspectives in astrobiology: life in the cosmos*” (06.10.2016)
- **seminar dedicated to the 80th anniversary of E.P. Shabalin** (FLNP JINR) (17.10.2016)
- **J.R. Granada** (Neutron Physics Department and Instituto Balseiro, Centro Atomico Bariloche, CNEA, Argentina and CONICET, Argentina) “*New Neutron Scattering Kernels for Liquid Hydrogen and Deuterium*” (20.10.2016)



M.V. Frontasyeva

CONFERENCES AND MEETINGS

- **The 24th International Seminar on Interaction of Neutrons with Nuclei: Fundamental Interactions & Neutrons, Nuclear Structure, Ultracold Neutrons, Related Topics (ISINN-24)** took place in Dubna in the JINR International Conference Hall from May 24 to May 27. The Seminar is organized every year at the end of May by the Frank Laboratory of Neutron Physics. This year it was dedicated to the 60th anniversary of JINR.

The Seminar was attended by about 70 researchers from different JINR laboratories, about 30 scientists from Russia and CIS, as well as around 30 representatives from a wide variety of countries including Bulgaria, Belgium, Vietnam, Germany, Egypt, Italy, China, Poland, Romania, France, USA and South Africa. During the four working days the participants presented a total of 50 oral and 50 poster reports on the themes of the Seminar. The scientific program included sessions traditional for ISINN: fundamental interactions and UCN physics, physics of nuclear fission, nuclear analytical techniques in biology and ecology, nuclear reactions with fast neutrons,

nuclear structure, methodological aspects of experiments with neutrons, accelerator-driven subcritical systems. The section devoted to the review of the available neutron sources, sources currently under construction and those that are planned, as well as to the research programs for them became a distinctive feature of this Seminar.

As before, ISINN remains a platform where participants can present their as-yet-unpublished and sometimes preliminary results, where in an informal and enjoyable atmosphere

in the breaks between sessions and during the traditional picnic one has a chance to discuss one's work with colleagues, get advice, and establish new scientific contacts and cooperation.

The presentations of ISINN-24 and materials of the previous seminars are available at the web page: hppt:\visinn.jinr.ru.



ISINN-24, Dubna, Russia

- **III International Conference on Small Angle Neutron Scattering (YuMO2016)** took place at the Frank Laboratory of Neutron Physics (FLNP) on June 6-9, 2016. The meeting was dedicated to the 80th anniversary of *Yuriy Mechislavovich Ostanevich* (1936–1992), who has made a determinative and crucial contribution to the construction of spectrometers at the pulsed reactor IBR-2.



YuMO 2016, Dubna, Russia

He contributed in particular, to the development of time-of-flight SANS technique, and the selection of advanced scientific areas for its application. His leadership and outstanding scientific achievements in SANS studies of polyelectrolytes, small molecules, fractals, metallic glasses, macromolecules, polymers, etc., were recognized by a number of awards including the State Prize of the Russian Federation in 2000. The small-angle neutron scattering (SANS) instrument at the IBR-2 reactor is called YuMO in his honour.

5. EVENTS

The YuMO2016 conference focused on providing opportunities to discuss various possibilities of exploiting the SANS technique in many aspects of condensed matter research. The FLNP had an opportunity to welcome more than 110 participants from 14 different countries and 3 continents comprising Europe, North America and Australia. The scientific program was filled with 43 oral presentations extending over 930 minutes, while more than 60 posters were presented during the poster sessions and breaks.

- **Workshop on small-angle neutron scattering MURomets 2016** was held in Gatchina on September 28-30, 2016. The exhibitions stand of Frank Laboratory of Neutron Physics provide the Conference participants with an opportunity to become acquainted with the operation and plans of development for the neutron sources in JINR. The presentation was primarily focused on the implementation of the user policy at the IBR-2 pulsed reactor and presentation of facilities dedicated for small angle and reflectometry investigations.
- **The 29th Task Force Meeting of the ICP Vegetation** organized by The Frank Laboratory of Neutron Physics, Dubna, Russia together with the ICP Vegetation Programme Coordination Centre Centre for Ecology & Hydrology Bangor, UK - was held in Dubna from 29 February until 5 March 2016 (UNECE ICP Vegetation Meeting – International Cooperative Programme in the frames of the United Nation Economic Commission for Europe Convention on Long-Range Transboundary Air Pollution). The meeting was dedicated to the 60th anniversary of JINR. The program of the meeting was divided to the two sections: Ozone and Heavy Metals. In the frame of this sections lectures covered such topics as: Ozone flux-effect relationships for vegetation;



29th Task Force Meeting of UNECE ICP Vegetation, Dubna, Russia

Identifying and mapping ozone-sensitive communities of (semi-)natural vegetation, impacts of ozone on biodiversity; current status of heavy metals in mosses survey 2015/2016, including participation of Eastern European Countries and countries in Asia; mosses as biomonitors of heavy metal, nitrogen, persistent organic pollutants (POPs) and radionuclide pollution.

A meeting from this series was held in JINR in 2007 (The 20th TFM of UNECE ICP Vegetation). The FLNP sector of neutron activation analysis and applied research has been taking part the Commission's activities on biomonitoring of atmospheric deposition using mosses as biomonitors and nuclear analytical methods for over 20 years. Coordination of the moss programme was transferred from UK to the Joint Institute for Nuclear Research in 2014.

- On 20.10.and 8-9.12. 2016 two **meetings of TANGRA project** organized by JINR and LLC "Diamant" were held in FLNP JINR. More than 25 scientists from Azerbaijan, Bulgaria, Croatia, India, Italy, Kazakhstan, Moldova, Russia, Serbia and Thailand took part in the meetings.

The two-day meeting working programs included:

- Visit of the JINR FNLP neutron-producing facilities: IBR-2, IREN, EG-5 and TANGRA;
- Presentations on nuclear physics with neutrons: theory, experiment, applications;
- Brain-ring: ideas & experience exchange;
- Presentation of the "COST" project: present status and proposal for improving;
- Plans for further collaboration & cooperation.

EDUCATIONAL PROGRAM

- The FLNP successfully collaborates with the JINR University Centre in the organization of **summer practical work for students** from JINR Member States (Belarus, Czech Republic, Poland, Romania, Slovakia,) and Associated Members (Egypt, South Africa).

Lectures and excursions to the FLNP facilities were organized for **teachers of physics** from Russia and JINR Member States.



Summer practice, 2016, Dubna, Russia

- The **Student Training Course: «Advanced Materials Investigation by Means of Neutron Scattering Methods»** organized by the Joint Institute for Nuclear Research together with the West University of Timisoara and University Ovidius from Constanta (Romania) took place in JINR from August 27 to September 4, 2016. The program of the course, which included 9 lectures delivered by FLNP specialists and 4 practical works, covered such topics as neutron diffraction on pulsed sources, neutron scattering in Earth sciences, structural aspects of functional properties

5. EVENTS

forming in materials by means of neutron studies, introduction to texture analysis, determination of nanoparticle structure parameters using small-angle scattering, studies of perspective biophysical membranes by neutron optics, introduction to inelastic neutron scattering, small-angle neutron scattering investigations of ferrofluids and magnetic elastomers, basics of diffraction data refinement, experimental work with the MAUD program. The participants also visited the IBR-2 reactor and a number of neutron scattering instruments.

Among the participants were students and professors from the West University of Timisoara and Ovidius University from Constanta, Romania, several students from Moscow Physics and Engineering Institute, Moscow State University, Dubna University.



AMIMNSM, 2016, Dubna, Russia

- **The VII International School for Young Scientists and Students “Instruments and Methods of Experimental Nuclear Physics. Electronics and Automatics of Experimental Facilities”** was held on November 7-11, 2016 in Dubna. The School was organized by the Frank Laboratory of Neutron Physics with the support of the JINR Directorate. Seventy nine attendees from the JINR Member States (Belarus, Kazakhstan, Russia, Ukraine) took part in the School. School members arrived from 11 cities. The most representative group of participants came from Dubna, Obninsk, Yekaterinburg, Astana, Moscow and Almaty. Among them were students, PhD students and junior researchers.



VII IMENP 2016, Dubna, Russia

The topics of the School include neutron sources, neutron detectors, spectrometers, sample environment systems, detector electronics and data acquisition and electronics, automation of experiments on spectrometers, information technologies. Leading scientists and specialists from JINR have read 13 lectures and have conducted eight different laboratory works (8 hours each) in the framework of these lectures. During the School young scientists and students visited the IBR-2 reactor and IREN and got acquainted with the operation of the IBR-2 Spectrometers' complex.

VISITS AT OUR FACILITIES

- I. Medhat, Spectroscopy Department, National Research Center, Egypt (27.01.2016)
- Members of the Commission of the JINR Plenipotentiary Representative of the Polish Republic (17.02.2016)
- F. Carsughi, Heinz Maier-Leibnitz Zentrum (MLZ), Germany (24.02.2016)
- J. Kulda, Institut Laue-Langevin, France (21.04.2016)
- Ch.Schanzer, Swiss Neutronics, Switzerland (11.05.2016)
- Group of foreign journalists from Great Britain and Germany ("New Scientist", "Gizmag", "Physics World", "WeltTrends", "VDI Nachrichten", "The Independent" , German Radio) (16.06.2016)
- Members of the PAC for Nuclear Physics (23.06.2016)
- Chao-Ming Fu, Director of the Department of Science and Technology of the representative office of the Taipei-Moscow Coordination Commission on Economic and Cultural Cooperation under the Ministry of Science and Technology of Taiwan (01.07.2016)
- R. Wieczorek, Wroclaw University, Poland (17-22.07.2016)
- M.V. Vener, Dmitry Mendeleev University of Chemical Technology of Russia, Moscow, Russia (20.07.2016)
- Delegation of the Korean Institute of Industrial Technology-KITECH (06.10.2016)
- R.B. Hoover, Athens State University, USA (06.10.2016)
- J.R. Granada, Centro Atomico Bariloche, CNEA, Argentina (20.10.2016)



STRUCTURE OF LABORATORY AND SCIENTIFIC DEPARTMENTS

6. ORGANIZATION

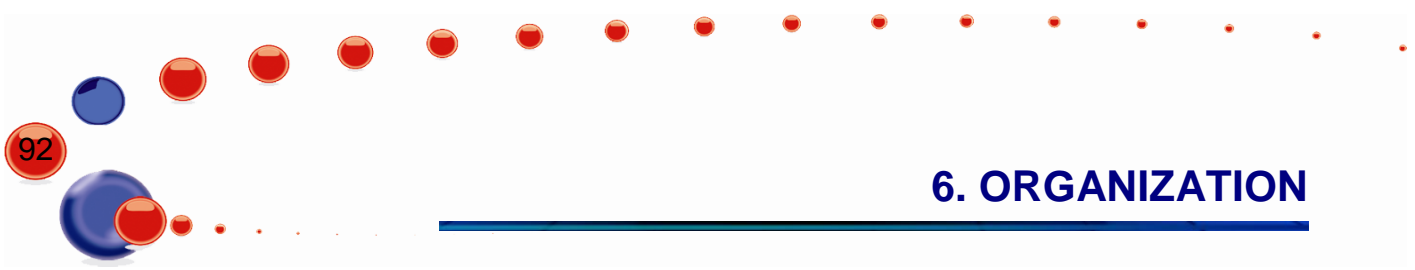
Directorate:	
Director	<i>V.N. Shvetsov</i>
Deputy Director	<i>O.A. Culicov</i>
Deputy Director	<i>E.V. Lychagin</i>
Deputy Director	<i>N. Kucerka</i>
Deputy Director	<i>S.V. Kozenkov</i>
Chief engineer:	<i>A.V. Vinogradov</i>
Scientific Secretary	<i>D.M. Chudoba</i>
Laboratory Scientific Leader	<i>V.L. Aksenov</i>
Advisor to Directorate	<i>V.D. Ananiev</i>
Advisor to Directorate	<i>L.B. Pikelner</i>

Reactor and Technical Departments	Head
IBR-2 reactor	Chief engineer: <i>A.V. Dolgikh</i>
Mechanical maintenance division	<i>A.A. Belyakov</i>
Electrical engineering department	<i>V.A. Trepalin</i>
Design bureau	<i>A.A. Kustov</i>
Experimental workshops	<i>A.N. Kuznetsov</i>

Scientific Departments	Head
The Division of Condensed Matter Research and Developments	<i>A.V. Belushkin</i>
Nuclear physics department	<i>V.N. Shvetsov</i>
Sector of Raman Spectroscopy	<i>G.M. Arzumanyan</i>

Administrative Services
Secretariat
Finances
Personnel

Scientific Secretary Group
Secretariat
Translation
Graphics



6. ORGANIZATION

DIVISION OF CONDENSED MATTER RESEARCH AND DEVELOPMENTS

DEPARTMENT OF NEUTRON INVESTIGATION OF CONDENSED MATTER

Sub-Division	Title	Head
Head of the Department		
<i>D.P. Kozlenko</i>		
Sector 1: Neutron Diffraction. Head: <i>G D. Bokuchava</i>		
Group No.1	HRFD	<i>A.M. Balagurov</i>
Group No.2	DN-2	<i>A.I. Beskrovnyi</i>
Group No.3	DN-12	<i>B.N. Savenko</i>
Group No.4	SKAT /Epsilon	<i>Ch. Scheffzük</i>
Sector 2: Neutron Optics. Head: <i>M. V. Avdeev</i>		
Group No.1	REMUR	<i>Yu.V. Nikitenko</i>
Group No.2	REFLEX	<i>V.I. Bodnarchuk</i>
Group No.3	GRAINS	<i>V.I. Petrenko</i>
Small angle scattering group		<i>A.I. Kuklin</i>
Inelastic neutron scattering group		<i>D. Chudoba</i>

DEPARTMENT OF IBR-2 SPECTROMETERS COMPLEX

Sub-Division	Title	Head
Head of the Department		
<i>S.A. Kulikov</i>		
Group No.1	Detectors	<i>A.V. Churakov</i>
Group No.2	Electronics	<i>A.A. Bogdzel</i>
Group No.3	Information technologies	<i>A.S. Kirilov</i>
Group No.4	Sample environment and choppers	<i>A.P. Sirotin</i>
Group No.5	Cryogenic investigations	<i>A.N. Chernikov</i>
Group No.6	Cold moderators	<i>M.V. Bulavin</i>

SECTOR OF RAMAN SPECTROSCOPY

Sub-Division	Title	Head
Head of the Sector		
<i>G.M. Arzumanyan</i>		
Group of biomolecular spectroscopy		
Group of luminescence and structural analysis		

6. ORGANIZATION

NUCLEAR PHYSICS DIVISION

Sub-Division	Title	Head
Sector 1.	Investigations of neutron-nuclear interactions	<i>Y.N. Kopatch</i>
Sector 2.	Investigation of neutron fundamental properties.	<i>E.V. Lychagin</i>
Sector 3.	Neutron Activation Analysis and Applied Research:	<i>M.V. Frontasyeva</i>
IREN facility		<i>V.G. Pytaev</i>

PERSONNEL

Theme	Departments	People
-1104-	Nuclear Physics Division	122
	The Division of Condensed Matter Research and Developments	
-1121-	Department of neutron investigation of condensed matter	95
-1122-	Department of IBR-2 spectrometers complex	48
-1111-	Sector of Raman Spectroscopy	8
-1105-	IBR-2 reactor	46
	Mechanical and Technical Department	47
	Electric and Technical Department	30
	Central Experimental Workshops	36
	Nuclear Safety Group	6
	Design Bureau	5
	FLNP infrastructure:	
	Directorate	10
	Services and Management Department	24
	Scientific Secretary Group	5
	Supplies Group	4
Total		486

PERSONNEL FROM THE JINR MEMBER STATES (BESIDES THE RF) at December 31, 2016 (work stages longer than 4 months)

Country	People	of which young specialists (≤ 35 years)
Azerbaijan	9	8
Armenia	1	1
Belarus	1	1
Bulgaria	8	4
Czech Republic	2	2

6. ORGANIZATION

Georgia	2	1
Germany	1	
Kazakhstan	19	19
Moldova	1	1
Mongolia	9	9
Poland	9	2
Romania	9	3
Slovakia	2	1
Ukraine	14	11
Uzbekistan	1	1
Vietnam	4	4
TOTAL	92	70

Other 8 employes from Mongolia, Slovakia Poland and Czech Republic performed work stages of three months in FLNP.

OUR PhD STUDENTS

In 2016 28 PhD students from 10 countries conducted their experimental research at the FLNP facilities.

Name	Country	PhD student of
Alekseenok Yu.V.	Belarus	International Sakharov Environmental University
Hristozova G.	Bulgaria	Paisii Hilendarski University
Vasiliev A.	Bulgaria	Sofia University
Sanizlo A.	Hungary	Obuda University
Bagdaulet M.	Kazakhstan	Al-Farabi Kazakh National University
Muhametuli B.	Kazakhstan	Al-Farabi Kazakh National University
Hramco C.	Moldova	University of the Academy of Science of Moldova
Nyamsuren B.	Mongolia	National University of Mongolia
Luczynska K.	Poland	Institute of Nuclear Chemistry and Technology
Belozeroва N.M.	Russia	JINR University centre
Zhaketov V.D.	Russia	JINR University centre
Rumyantsev I.	Russia	Ivanov State University
Rutkauskas A.V.	Russia	JINR University centre
Rizhikov Yu.L.	Russia	Moscow Institute of Physics and Technology
Vlasov A.B.	Russia	Moscow Institute of Physics and Technology

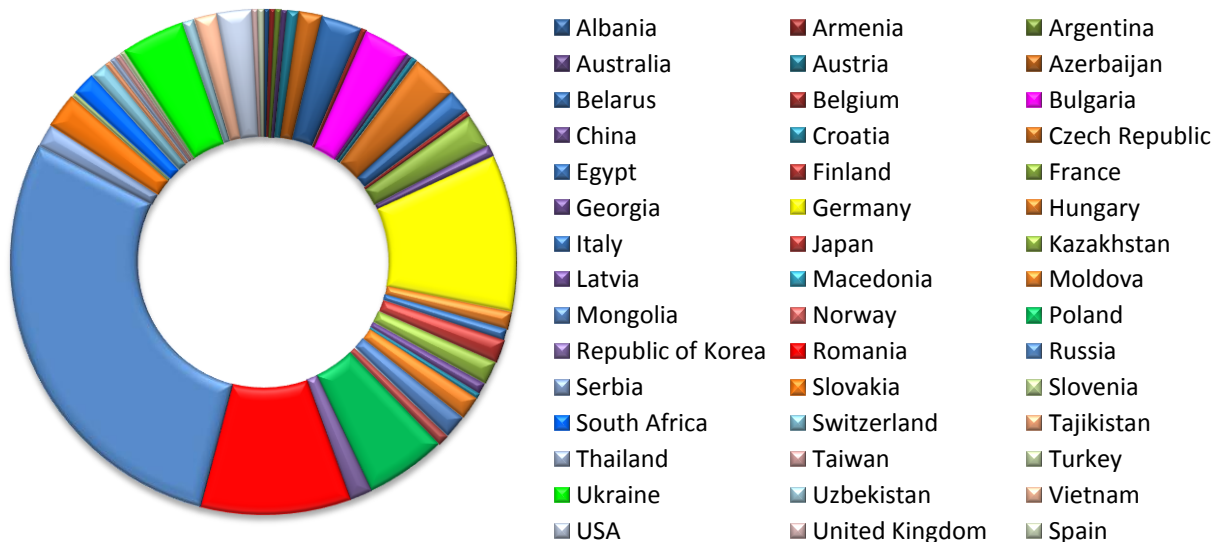
6. ORGANIZATION

Zinovev E.V.	Russia	Moscow Institute of Physics and Technology
Husenov M.A.	Russia	Moscow State University of Technology „STANKIN“
Suminkov S.V.	Russia	Moscow State University
Khalansky D.A.	Russia	Dubna International University for nature, Society and Man
Zelenyak T.Y.	Russia	Dubna International University for nature, Society and Man
Vergel K. N.	Russia	Dubna International University for nature, Society and Man / FLNP JINR
Kravtsova A.V.	Russia	A.O. Kovalevsky Institute of biology of the Southern Seas
Nekhoroshkov P.S.	Russia	A.O. Kovalevsky Institute of biology of the Southern Seas
Gapon I.V.	Ukraine	National University of Kyiv
Nagornaya T.V.	Ukraine	National University of Kyiv
Samoylenko S.A.	Ukraine	National University of Kyiv
Husenov M.A.	Republic of Tajikistan/Russia	S.U. Umarov Physical-Technical Institute of Academy of Sciences of the Republic of Tajikistan/ Moscow State University of Technology „STANKIN“
Rakhmonov H.R	Republic of Tajikistan/Russia	S.U. Umarov Physical-Technical Institute of Academy of Sciences of the Republic of Tajikistan/ National Research Nuclear University MEPhI

In 2016, 3 PhD theses were defended using the experimental material obtained in FLNP.

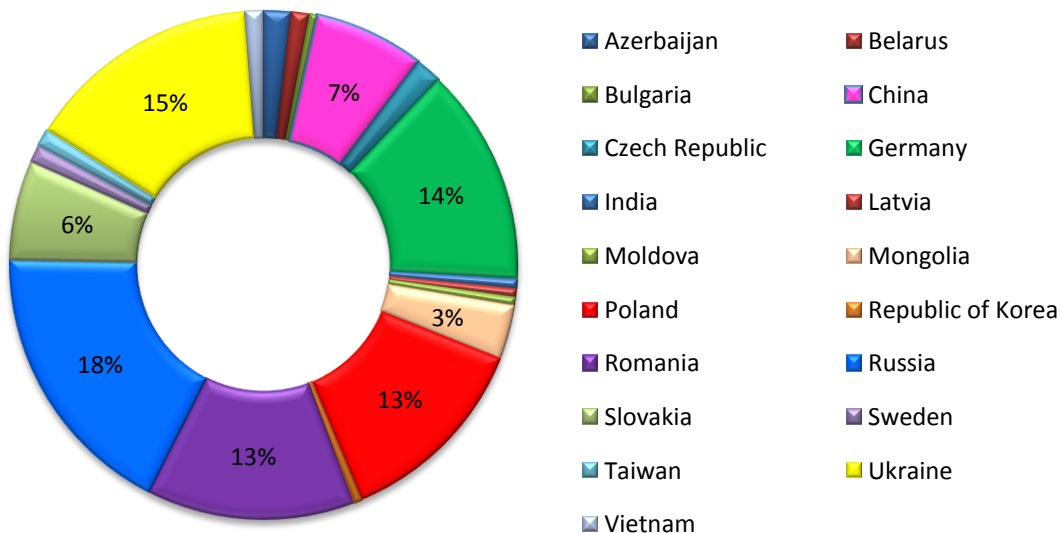
INTERNATIONAL COOPERATION

In 2016 the Frank Laboratory of Neutron Physics collaborated with 270 institutions from 45 countries.



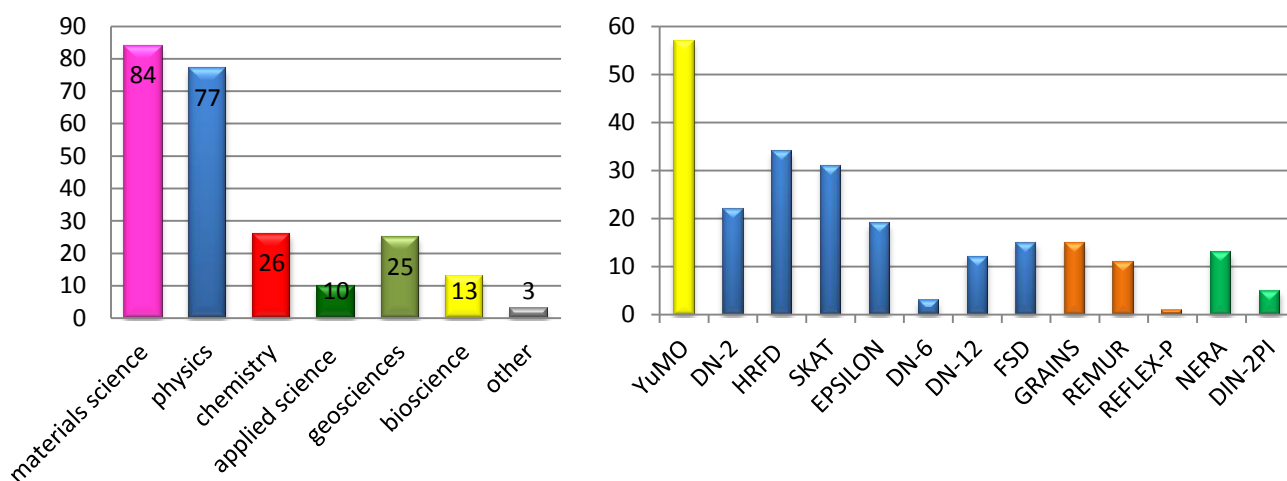
USER INTERACTION

In 2016 were two calls for proposals for experiments at the IBR-2 reactor (01 September – 15 October 2013; Call-II: 01 March – 15 April 2014). A total of 238 proposals for conducting experiments were received from 19 different countries. The received proposals covered the broad spectrum of neutron research in physics, materials science, chemistry, geosciences, biology and applied sciences. 208 received proposals were admitted for realization.



7. INTERNATIONAL COOPERATION AND USER INTERACTION

Proposal distribution by science (left) and by facilities (right).



List of Visitors from the Member States or Associated Members of JINR in 2016

Country	Nr of visitors
Azerbaijan	3
Armenia	2
Belarus	7
Bulgaria	7
Czech Republic	2
Egypt	6
Germany	22
Kazakhstan	2
Moldova	2
Mongolia	7
Poland	26
Romania	10
Serbia	5
Slovakia	8
Ukraine	14
RSA	2
Vietnam	2

List of Visitors from the not Member States or Associated Members of JINR in 2016

Country	Nr of visitors
Argentina	1
China	7
Croatia	2
Republic of Korea	7
Sweden	6
Taiwan	1
Tajikistan	1
USA	5

8. FLNP AND MASS-MEDIA

In the year 2016 Frank Laboratory of Neutron Physics was at center of interest of mass media in Russia and abroad

Dubna Channel
January 2016



Postępy Fizyki Jądrowej
59 Z.2 2016

Dubna
March 2016



Neutron News

ISSN: 1044-8632 (Print) 1931-7382 (Online) journal homepage: <http://www.lanp.ornl.gov/flnp/np2>

III International Conference on Small Angle Neutron Scattering Dedicated to the 80th Anniversary of Yu. M. Ostenevich

Norbert Kučerka, Maria Batasou & Alexander I. Kuklin

To cite this article: Norbert Kučerka, Maria Batasou & Alexander I. Kuklin (2016) III International Conference on Small Angle Neutron Scattering Dedicated to the 80th Anniversary of Yu. M. Ostenevich, Neutron News, 27, 4, 14-16, DOI: 10.1080/10448632.2016.1233010

To link to this article: <http://dx.doi.org/10.1080/10448632.2016.1233010>

Neutron News
27 No 4 2016

Physics-Uspekhi

Neutron physics at the JINR: 60 years of the I M Frank Laboratory of Neutron Physics

E V Lyagin, D P Kuzlerko, V V Seleznev and V N Shvetsov

© 2016 Uspekhi Fizicheskikh Nauk and P N Lebedev Physics Institute of the Russian Academy of Sciences

Abstract

26 March 2016 marked 60 years since the Joint Institute for Nuclear Research was founded in 1956 and within which the Laboratory of Neutron Physics was established. Already four years later, in 1960, the world's first pulsed fast reactor (known by its Russian acronym as IRR) operating in the periodic mode was put into operation, followed in 1984 by IRR-2. The research achievements over the last decade are summarized, the state-of-the-art laboratory hardware is discussed, and the prospects for the future are reviewed.

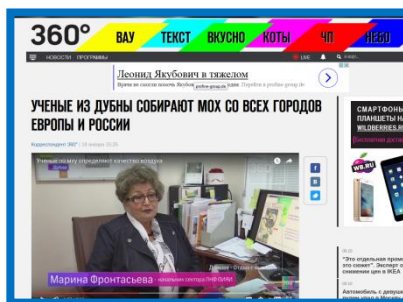
Physics-Uspekhi
59 (3) 2016

PhysicsWorld
29 No5 2016

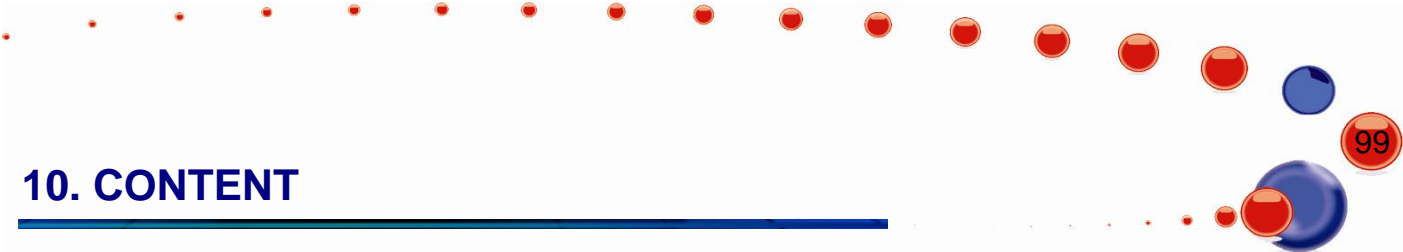
FLNP

Intense resonance neutron source (IREN) at the Laboratory of Neutron Physics - Joint Institute for Nuclear Research

The IREN facility is an intense resonance neutron source being built at the Frank Laboratory of Neutron Physics of the Joint Institute for Nuclear Research (JINR) in Dubna, Russia. It is a unique facility for the study of the neutron resonance region of the cross-sections of the nuclei of the elements of the periodic table of the elements. The facility is designed to provide a neutron flux of up to 10¹⁶ neutrons/cm² at a resonance energy of 10 eV. The facility is designed to provide a neutron flux of up to 10¹⁶ neutrons/cm² at a resonance energy of 10 eV. The facility is designed to provide a neutron flux of up to 10¹⁶ neutrons/cm² at a resonance energy of 10 eV.



360° TV
December 2016



10. CONTENT

PREFACE

1. SCIENTIFIC RESEARCH	3
• CONDENSED MATTER PHYSICS	3
• MULTIMODAL PLATFORM FOR RAMAN AND NONLINEAR OPTICAL MICROSCOPY AND MICROSPECTROSCOPY FOR CONDENSED MATTER STUDIES	30
• NEUTRON NUCLEAR PHYSICS	37
• NOVEL DEVELOPMENT AND CONSTRUCTION OF EQUIPMENT FOR THE IBR-2 SPECTROMETERS COMPLEX	62
2. NEUTRON SOURCES	71
3. PUBLICATIONS	73
4. PRIZES AND AWARDS	84
5. EVENTS	85
6. ORGANIZATION	91
7. INTERNATIONAL COOPERATION AND USER INTERACTION	96
8. FLNP AND MASS-MEDIA	98